ORNL-5356

An Experimental Study of Heat Transfer Enhancement for Ammonia Condensing on Vertical Fluted Tubes

S. K. Combs

OAK RIDGE NATIONAL LABORATORY
OPERATED BY UNION CARBIDE CORPORATION · FOR THE DEPARTMENT OF ENERGY

Printed in the United States of America. Available from
National Technical Information Service
U.S. Department of Commerce
5285 Port Royal Road, Springfield, Virginia 22161
Price: Printed Copy $7.25; Microfiche $3.00

ORNL-5356
Dist. Category UC-93

Contract No. W-7405-eng-26

Engineering Technology Division

AN EXPERIMENTAL STUDY OF HEAT TRANSFER ENHANCEMENT FOR AMMONIA CONDENSING ON VERTICAL FLUTED TUBES

S. K. Combs

Date Published: January 1978

OAK RIDGE NATIONAL LABORATORY
Oak Ridge, Tennessee 37830
operated by
UNION CARBIDE CORPORATION
for the
DEPARTMENT OF ENERGY

CONTENTS

LIST OF FIGURES

TABLE PAGE

LIST OF TABLES

LIST OF SYMBOLS

a_o	y-intercept on the Wilson plot representing the composite resistance of the condensing side and wall, Eq. (5-11)
a_1	slope of the line on the Wilson plot
A	heat transfer surface area of test tube
A_c	cross-sectional flow area of the annulus in the test section
c_p	specific heat
D	tube diameter
D_H	hydraulic diameter of the annulus in the test section
D_r	diameter of rod inserted through center of test section
F	volume flow rate
g	local gravitational acceleration
G	mass flux
h	average or mean individual heat transfer coefficient
h_{fg}	latent heat of vaporization
h^*	composite condensing heat transfer coefficient including both vapor side and wall
H	standard nondimensional heat transfer coefficient (average or mean)
k	thermal conductivity
L	tube length
$\dot{m}$	mass flow rate
P	pressure
P_t	outside perimeter of tube
Q	heat load
Q/A	heat flux
r	radius

R resistance to heat flow

$R_{\Delta T*}$ ratio of condensing temperature differences [ΔT* (smooth tube)/ ΔT* (fluted tube)] at equal heat load

R_{h*} ratio of condensing coefficients [h* (fluted tube)/h* (smooth tube)] at equal heat flux

R_Q ratio of heat loads [Q (fluted tube)/Q (smooth tube)] at equal condensing temperature difference

Re Reynolds number

T temperature

ΔT temperature difference

$\overline{\Delta T}$ mean temperature difference between the condensing vapor and coolant

ΔT^* composite condensing temperature difference including both vapor side and wall

U overall condensing heat transfer coefficient

v water velocity

Greek Symbols

Γ Condensate mass flow rate at bottom of tube per unit length of periphery

Δ finite difference

μ absolute viscosity

ρ mass density

σ surface tension

Subscripts

avg average

b bulk

c	ammonia condensate
f	film
fi	inside fouling
fo	outside fouling
i	inside
in	inlet
o	outside
out	outlet
sat	saturation
v	vapor; vapor (condensing) side
w	water; water side
wall	wall; surface

ABSTRACT

Experiments were run to determine heat transfer performance of single vertical tubes with ammonia condensing on the outside. The four test tubes (aluminum) were of 1-in. nominal diameter and 4-ft length with 0 (smooth), 24, 48, and 60 external flutes. Test parameter ranges were as follows:

Condensing temperature:	69°F to 109°F
Condensing pressure:	127 psia to 245 psia
Heat load:	1700 Btu/hr to 17,000 Btu/hr
Heat flux:	1600 Btu/hr·ft^2 to 16,000 Btu/hr·ft^2

The condensing heat transfer coefficients are reported as composite coefficients that include the resistance of both the condensing side and the tube wall. The composite condensing coefficients ranged from 720 to 9600 Btu/hr·ft^2·°F. All parameters were based on total condensing surface area. The data show that, for a given heat flux, a fluted tube can increase condensing coefficients by up to 7.2 times smooth tube values.

The condensing temperature difference (composite) varied from 0.3 to 23°F in the experiments; and the data show that, for a given condensing temperature difference, a fluted tube can accommodate heat loads up to 5.4 times the smooth tube values. Alternatively, for a given heat load, a smooth tube requires condensing temperature differences up to 9.7 times the fluted tube values.

Tests were also run to evaluate the effect of tube length on the heat transfer performance of fluted tubes; however, no appreciable effect was detectable in going from an "effective" condensing length of 4 ft to 2 ft.

CHAPTER I

INTRODUCTION

The present energy crisis has generated increased interest in exploitation of alternative energy sources. Thus, such renewable resources as geothermal, solar, and ocean thermal are being considered for widespread development. Each of these resources is characterized within the scope of current technology by a relatively low source temperature (concentrating collectors being developed could provide a high-temperature solar source). Thermodynamic considerations show that only a fraction of heat at low temperature can be converted to net work. Thus, the heat exchangers in a conversion system utilizing a secondary fluid will be large and constitute a major part of the total system capital cost. Any significant increase in the thermal performance of the heat exchangers (condensers and evaporators) could result in a substantial capital cost reduction of a power conversion plant and favorably affect the overall feasibility of developing the resource.

One method for increasing the thermal performance of heat exchangers is enhancement of the heat transfer coefficient through use of modified heat transfer surfaces. Studies at the Oak Ridge National Laboratory[1] in the period 1964 to 1972 considered the thermal performance of evaporator-condenser tubes modified in various ways to augment condensation and evaporation or boiling coefficients. This work was done for the Office of Saline Water and concentrated on water and brines for application to desalination plants. The results from the program were very encouraging, reporting overall coefficients up to seven times larger for augmented surfaces than those obtained with conventional smooth tubes.

In a manner similar to this earlier work, the present study examined the potential for improving the heat transfer performance of condensers for conditions corresponding to an ocean thermal energy conversion (OTEC) plant. Two groups (Lockheed Missiles and Space Company, Inc.,[2] and TRW Systems Group[3]) established separate baseline designs for OTEC power plants in 1975. More recently (1976), Bell[4] presented a brief survey of the key elements in the design of the plants, including critical features controlling the design of the heat exchangers. A typical plant concept (the baseline system configuration of TRW) is depicted in Fig. 1-1.

Specifically, the enhancement of heat transfer coefficients for ammonia condensing on vertical tubes was investigated in this study. Ammonia was chosen since this is the prime candidate for the working fluid in an OTEC plant. Other potential fluids include propane and a halogenated hydrocarbon (Freon) type refrigerant, R-12/31. However, ammonia has superior heat transfer characteristics and thermodynamic properties; it is also inexpensive and readily available. Both Lockheed and TRW selected ammonia for their baseline heat exchanger designs (see Refs. 2, 3, and 4 for discussion and comparison of working fluids).

The need for these studies rests in large part on the sparseness of the condensing experimental data for fluids other than water. The experimental study undertaken included the determination of average heat transfer coefficients for ammonia condensing both on smooth tubes and on fluted tubes of various geometries. The emphasis on fluted tubes stemmed from

ORNL Dwg. 77-18183

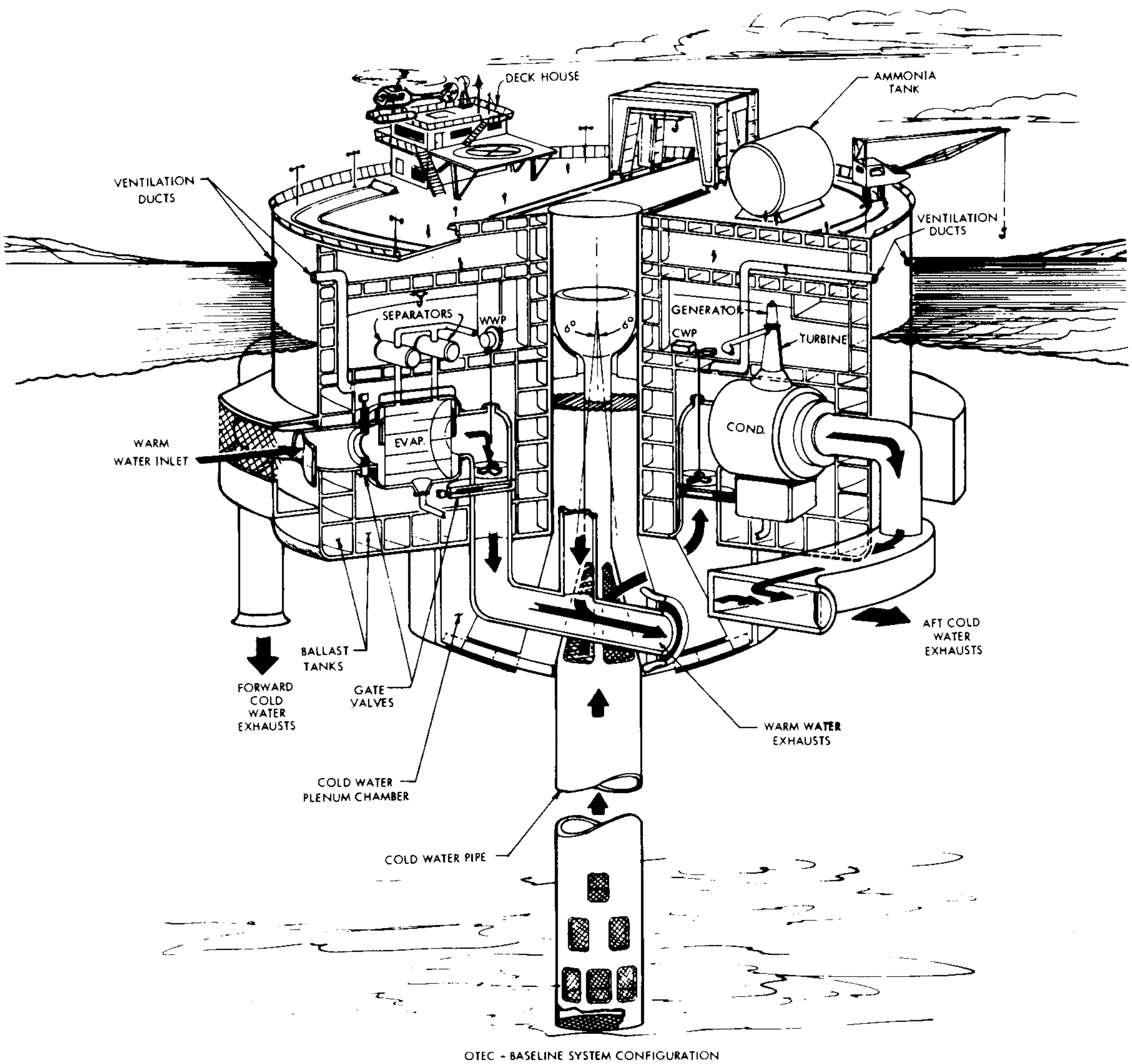

Fig. 1-1. Conceptual baseline design for an OTEC plant (TRW Systems Group).

the performance efficacy identified in water studies, such as that of Alexander and Hoffman.[1] The principle of operation (condensation mode) for the fluted tube is pictorially shown in Fig. 1-2. The condensate film is subjected to surface tension forces acting to push it from the crests into the troughs. This results in the major portion of the crest having a very thin film of condensate which greatly reduces the resistance to

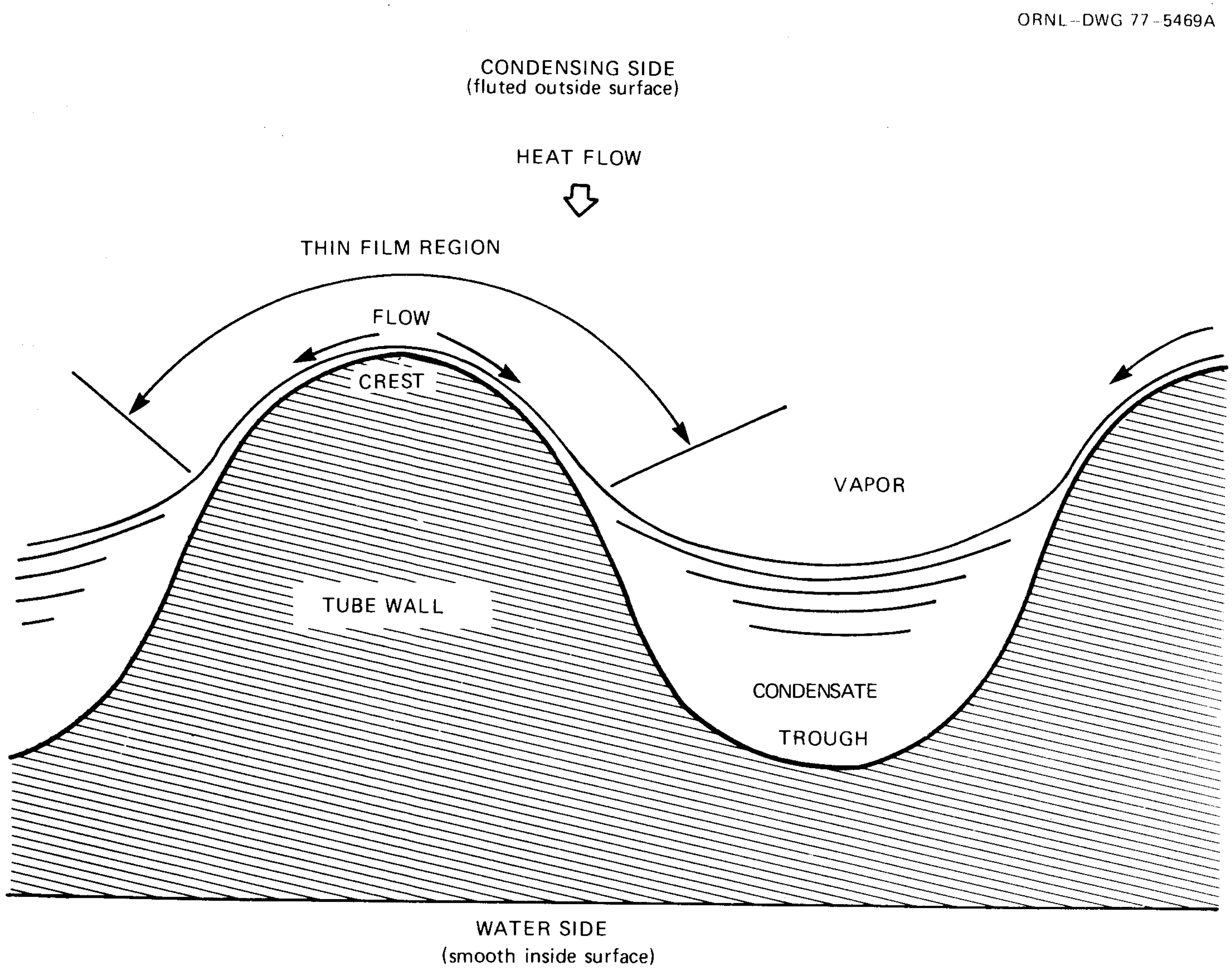

Fig. 1-2. Fluted tube principle of operation (condensation mode) — surface tension forces acting to push condensate from crests into troughs.

heat flow through the crest area. The condensate in the troughs is channeled off by gravity with the heat flow through this area somewhat less. The net effect is an improvement in heat transfer performance of fluted tubes over conventional smooth tubes.

CHAPTER II

BACKGROUND

In 1916, Nusselt[5] derived the theoretical relations for predicting heat transfer coefficients for film condensation of pure vapors on tubes and plates. Subsequently, extensive work was carried out in the general area of film condensation by other investigators; their efforts included many modifications to Nusselt's analysis. Thus, for film condensation on the outside of vertical surfaces in laminar flow, McAdams[6] developed a semiempirical relationship for predicting the heat transfer coefficients in which Nusslet's theoretical equation was multiplied by a constant. This recommmended equation by McAdams was based on a comparison of Nusselt's predicted coefficients with experimental data; the experimental data averaged at least 20% above Nusselt's theoretical prediction. Kutateladze[7] presented a semiempirical equation for predicting film condensation coefficients for laminar flow on vertical surfaces that purports to account specifically for the effect of ripples (irregularities in the liquid-vapor interface) on heat transfer. For film condensation where the flow is turbulent, McAdams[6] recommended the correlation of Kirkbride.[8]

More recently, investigators have focused their attention on the potential for augmenting film condensation heat transfer. In most film-type condensing situations, the major resistance to heat transfer lies in the liquid film that forms on the cooled surface as the vapor condenses. Therefore, condensation heat transfer enhancement depends primarily on methods for reducing the effective thickness (or resistance) of this liquid film. Modified surfaces, such as fluted tubes, have proved successful in reducing the resistance of the liquid film.

The first study of fluted enhanced surfaces was by Gregorig[9] (1954), who showed analytically and experimentally that fluting the tube surface can significantly augment film condensation heat transfer; thus, by fluting the outside surface of a vertical tube, Gregorig obtained increases of 200 to 800% in the average film condensation coefficient for condensing steam. The observed enhancement was attributed to surface tension forces (see Fig. 1-2) acting to push the condensate from the convex surfaces (crests) into the concave channels (troughs) down which it drains by gravity. This results in thinning of the liquid film on the crests, greatly reducing the resistance to heat flow through the crest area. The resistance to heat flow is increased somewhat in the troughs through the thickening of the film by addition of the fluid from the crests. The overall effect is an improvement in the average condensing film coefficient; however, the magnitude of the augmentation depends on the trade off between improvement in the crest area heat transfer and the degradation in trough area heat transfer.

Gregorig's idea stemmed from the fact that the pressure of the fluid inside a curved interface will be greater than the pressure of the fluid outside the interface by an amount given by Laplace's formula (see Ref. 10):

$$P_1 - P_2 = \sigma(1/r_1 + 1/r_2) ,$$

where $(P_1 - P_2)$ is the surface pressure difference, r_1 and r_2 are the principal radii of curvature of the interface, and σ is the surface tension. Thus, if a vertical condensing surface is not smooth, but instead contains corrugations or ridges (flutes) and troughs running vertically on the surface, condensate forming on the crests will be at a slightly higher pressure than surrounding vapor, while liquid in the troughs will be slightly below the pressure of the vapor. This difference in pressure is what forces the liquid off the crests into the troughs resulting in thin film regions as illustrated in Fig. 1-2.

Other investigators have confirmed Gregorig's findings. The study of fluted tubes by Carnavos[11] reported film condensing coefficients 4.5 to 7 times greater than those obtained for a comparable smooth tube at a given heat flux. The work of Alexander and Hoffman[1] with modified surfaces indicated significant increases in the overall heat transfer coefficients (6 to 7 times larger than those of smooth tubes); no direct measurement of condensing-side coefficients was made in this study. Thomas[12,13] achieved considerable enhancement of film condensation by modifying vertical condenser tubes in two ways: (1) loosely attached small longitudinal wires, and (2) loosely clamped longitudinal fins. With the wires, Thomas was able to increase the condensing film heat transfer coefficient as much as a factor of 4.5 over a smooth tube; while with the fins, enhancement factors greater than 9 were reported.

All of the work previously mentioned was with condensing steam and, in general, most of the work on film condensation has been done with steam. Little experimental data are reported for fluids other than water, and even less for such fluids condensing on enhanced surfaces. Thus, for the past several years, the Oak Ridge National Laboratory[14,15] has been involved in an experimental program to obtain film heat transfer coefficients for fluorocarbons condensing on both smooth and fluted vertical surfaces. Kratz et al.[16] studied ammonia condensing on smooth tubes in several types of condensers, but reported only overall coefficients.

This present study evaluated the performance of fluted tubes for augmenting ammonia condensing film heat transfer coefficients and includes extensive experimental condensing data for ammonia on both smooth and fluted vertical tubes.

CHAPTER III

DESCRIPTION OF EQUIPMENT

Equipment used in this investigation is shown schematically in Fig. 3-1. The system was designed for a heat load of 5 kW and consisted of three circuits — an ammonia loop, a primary cooling loop, and a secondary cooling loop. The ammonia loop was designed for a maximum operating pressure and temperature of 250 psia and 110°F. The test section, a single-tube vertical condenser, was built to accommodate tubes of 1- or 2-in.-nominal diameter and 4 ft in length. The system was manually controlled, and the heat load was set by the power input to the boiler. The ammonia loop was constructed of stainless steel to minimize compatibility problems. View ports on the test section permitted visual observation of the condensing surface with the aid of a light at suitable locations. Water served as the coolant in both the primary and secondary cooling loops. The primary coolant removed the heat from the tube in the test section; and in turn, the heat was transferred to the secondary coolant.

General Flow Description

Flow directions in the system are indicated by arrows in Fig. 3-1. Typically, the ammonia was vaporized in the boiler and passed through an entrainment separator before entering the condensing test section. The vapor entered the top of the test section, and the liquid (collected in the separator) returned to the boiler. The vapor condensed on the outer surface of the test tube in the test section and formed a falling film of liquid. The liquid condensate exited at the bottom of the test section,

ORNL-DWG 77-12422

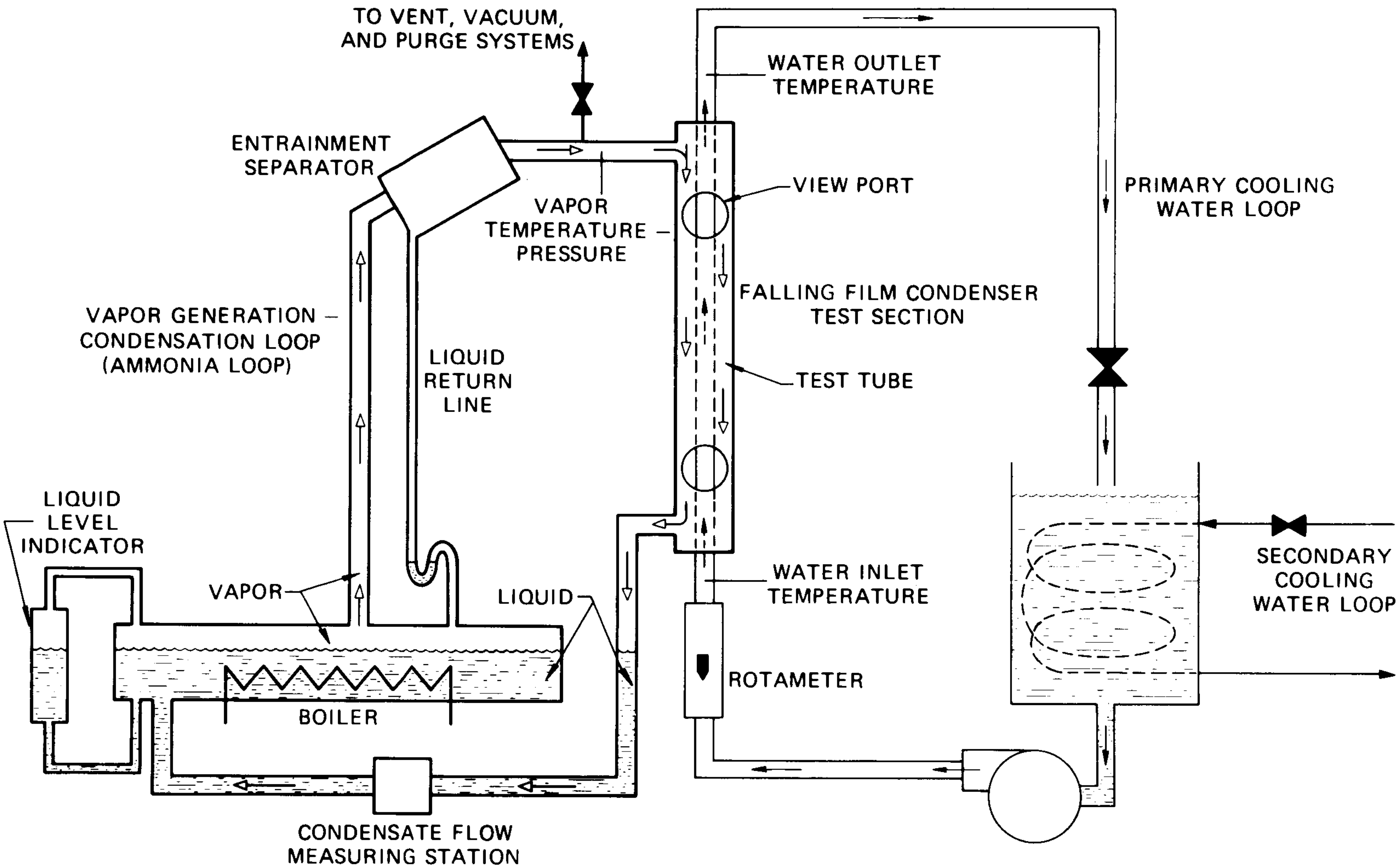

Fig. 3-1. Schematic diagram of experimental apparatus.

passed through a condensate measuring station, and returned to the bottom of the boiler to complete the closed loop. A pump was not needed for the circulation of the ammonia since the liquid head in the test-section side of the loop furnished the driving force required for flow through the condensate measuring station.

In the primary cooling loop, a centrifugal pump transferred demineralized water from a storage tank to the bottom of the test section and upward through the test tube. The primary cooling flow was measured by rotameters upstream of the test section and controlled by a hand valve located downstream of the test section. From the top of the test section, the water returned to the storage tank to complete the closed loop.

The secondary cooling loop removed the heat load from the system by transferring the heat from the primary cooling water to plant process water. Primary cooling water recirculating through the storage tank dumped heat to secondary cooling water which passed through a cooling coil in the tank and then discharged to the drain. The flow rate of the secondary coolant was regulated by a hand valve located downstream of the cooling coil.

Figure 3-2 pictures the system in overall view, while Figs. 3-3 and 3-4 give more detail of individual sections. These photographs do not show the insulation that was installed prior to experimental operation to minimize heat losses.

Boiler

The boiler body (Fig. 3-2) was fabricated from a 4-ft length of 6-in. Schedule 40 stainless steel pipe. Twelve tubular heaters of 4-ft active

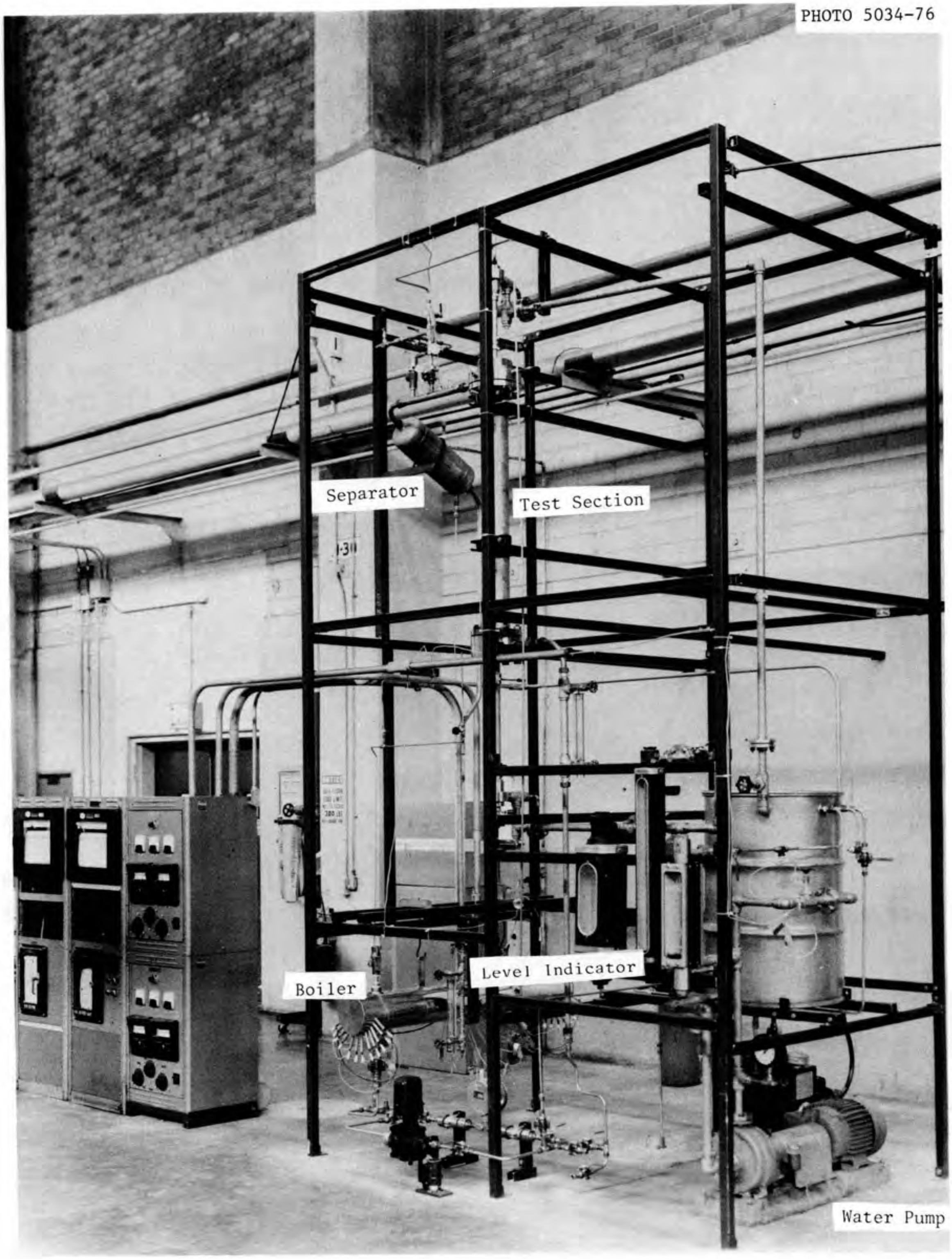

Fig. 3-2. Test facility.

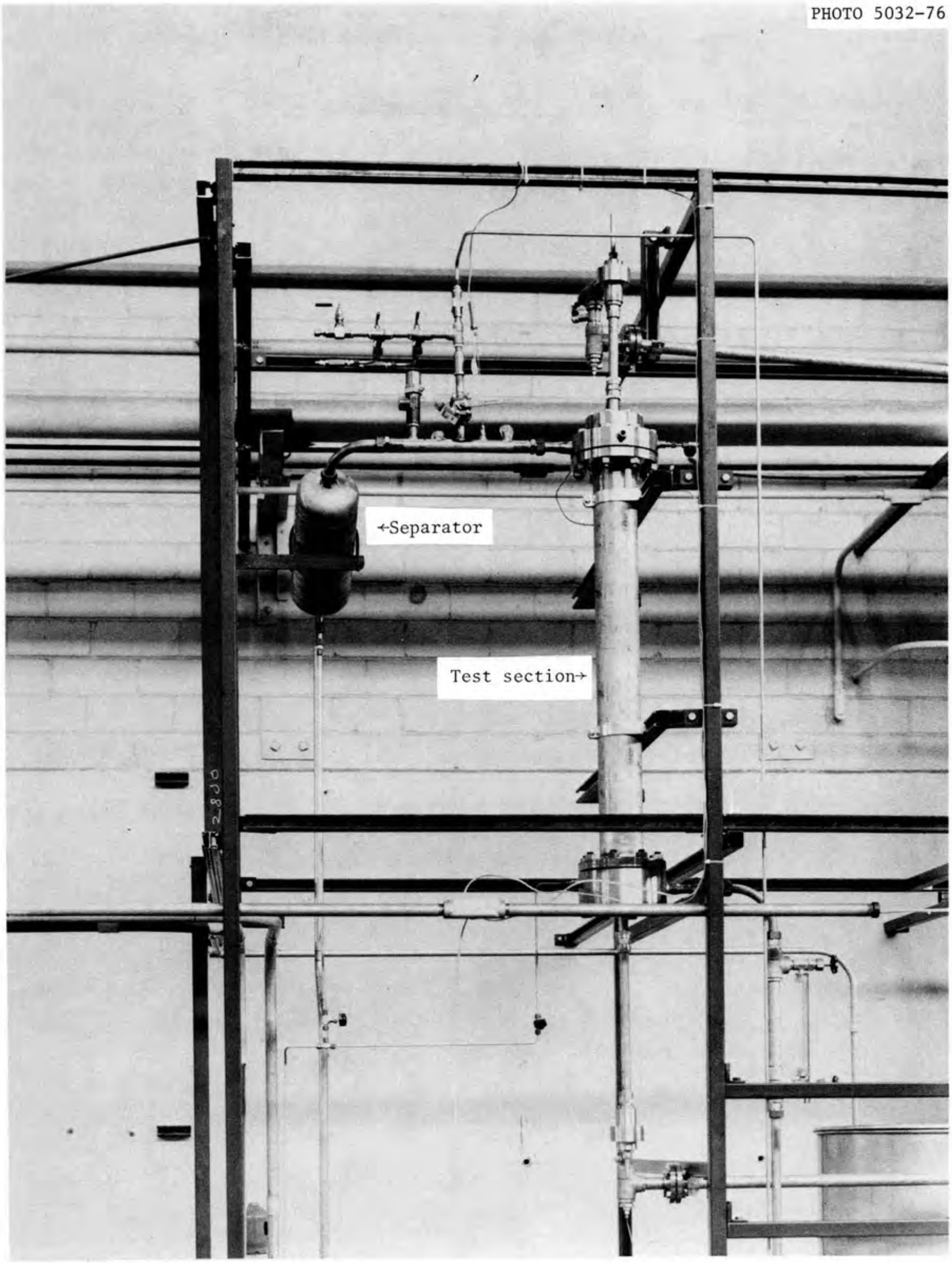

Fig. 3-3. Close-up view of test section and separator.

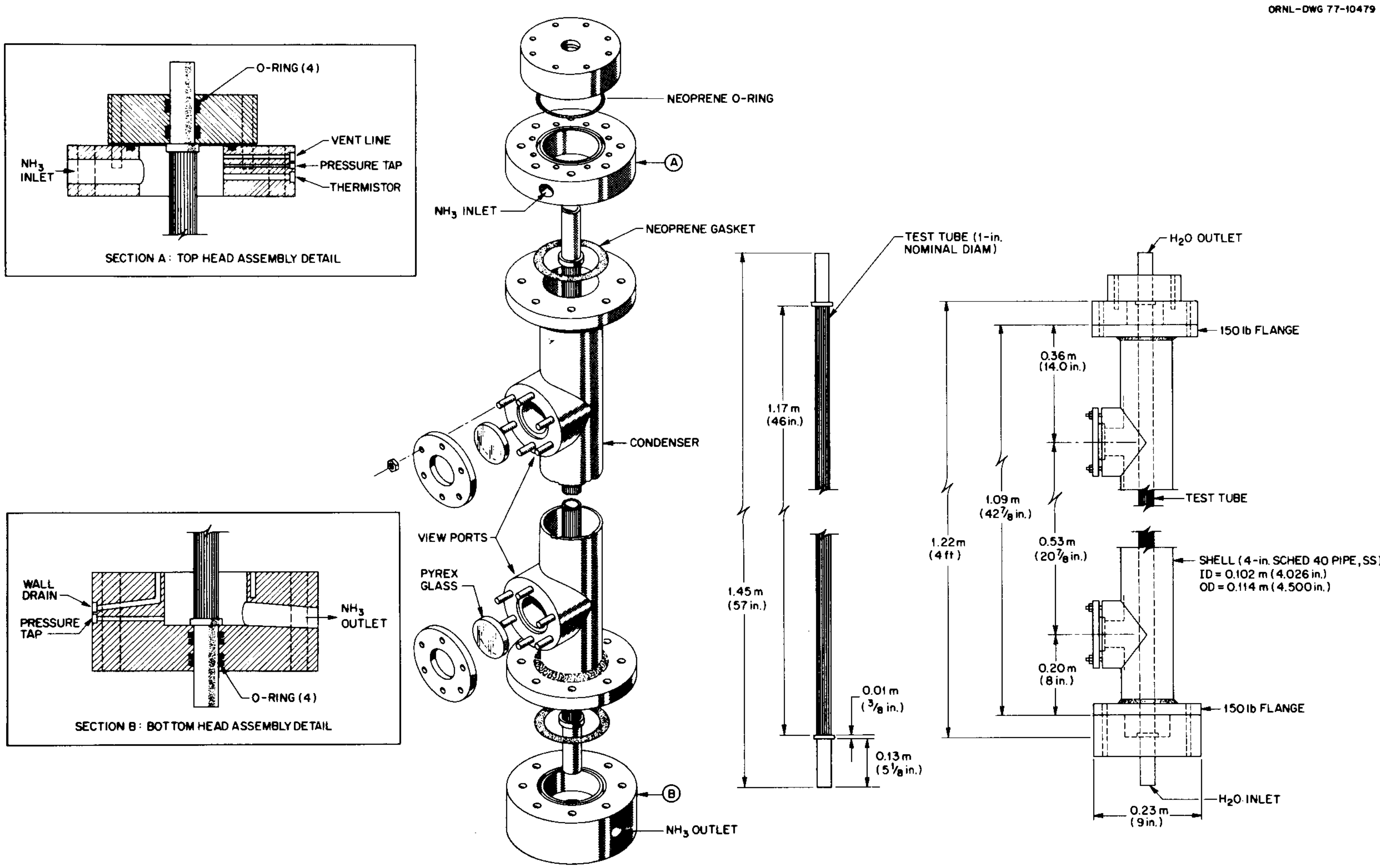

Fig. 3-4. Details of the test section.

heated length were strapped to the bottom section of the pipe for electrical resistance heating. A sight glass (Fig. 3-2) was connected to the boiler to provide liquid level monitoring capability. The top section of the boiler was equipped with a baffle made of stainless steel metal to aid in reducing liquid entrainment. The boiler held ~3 gal of liquid when half-filled for standard operation.

Entrainment Separator

The separator (Fig. 3-3) was constructed from a 1-ft length of 6-in. Schedule 40 stainless steel pipe. Separation of entrained liquid from the vapors was accomplished by two stainless steel mesh demistors (Otto H. York Company, 6-in. diameter by 6 in. thick) located in the body of the separator. The separator was mounted in the ammonia loop at a 30° angle to the horizontal with liquid exiting at the lowest point in the separator and vapor at the highest. Liquid returned to the boiler through a vertical drainage line.

Condensing Test Section

Shell and heads

The shell (Fig. 3-3) of the test section was fabricated from 4-in. Schedule 40 stainless steel pipe. Figure 3-4 is a detailed sketch of the test section including an assembly diagram. The outside (condensing) surface of the experimental test tube could be viewed at locations near the top and bottom of the test tube through two windows (Fig. 3-4). The photographs (Figs. 3-2 and 3-3) were taken before the view ports were added to the shell. Two heads (which were mated to the shell by 4-in., 150-lb stainless steel flanges) were fabricated from stainless steel bar stock and were designed to facilitate tube installation and removal. The top head consisted of two sections, the lower and upper sections. The lower section bolted directly to the top flange and contained a radial 1-in.-diam hole for the vapor entrance. The upper section containing four 1-in.-diam O-ring seals for sealing a 1-in.-OD test tube was bolted to the lower section of the top head. The bottom head consisted of only one section containing four 1-in.-diam O-ring seals and a radial 1-in.-diam hole for exit of condensate from the test tube. Provision was made in the bottom head to collect separately the condensate forming on the inside of the shell, and this condensate was returned to the boiler downstream of the condensate measuring station. The total condensing length in the test section was 4 ft.

Tube installation

The heads on the test section (Fig. 3-4) were designed to seal around a smooth 1-in.-OD tube; therefore, experimental test tubes (other than smooth 1-in.-OD) were prepared for testing by aluminum welding a 1-in.-OD sleeve to each end of a 4-ft length of test tube. One end of a prepared test tube is shown in Fig. 3-5 to illustrate this sleeve connection. For installation, the upper section of the top head (Fig. 3-4) was removed and the test tube was inserted downward into the test section until the bottom sleeve slid through the four O-ring seals in the bottom head. The upper section of the top head was then slid over the top sleeve and bolted to the lower section to complete the shell-side sealing operation. Next, the required connections were made to the primary cooling loop.

PHOTO 4506-75

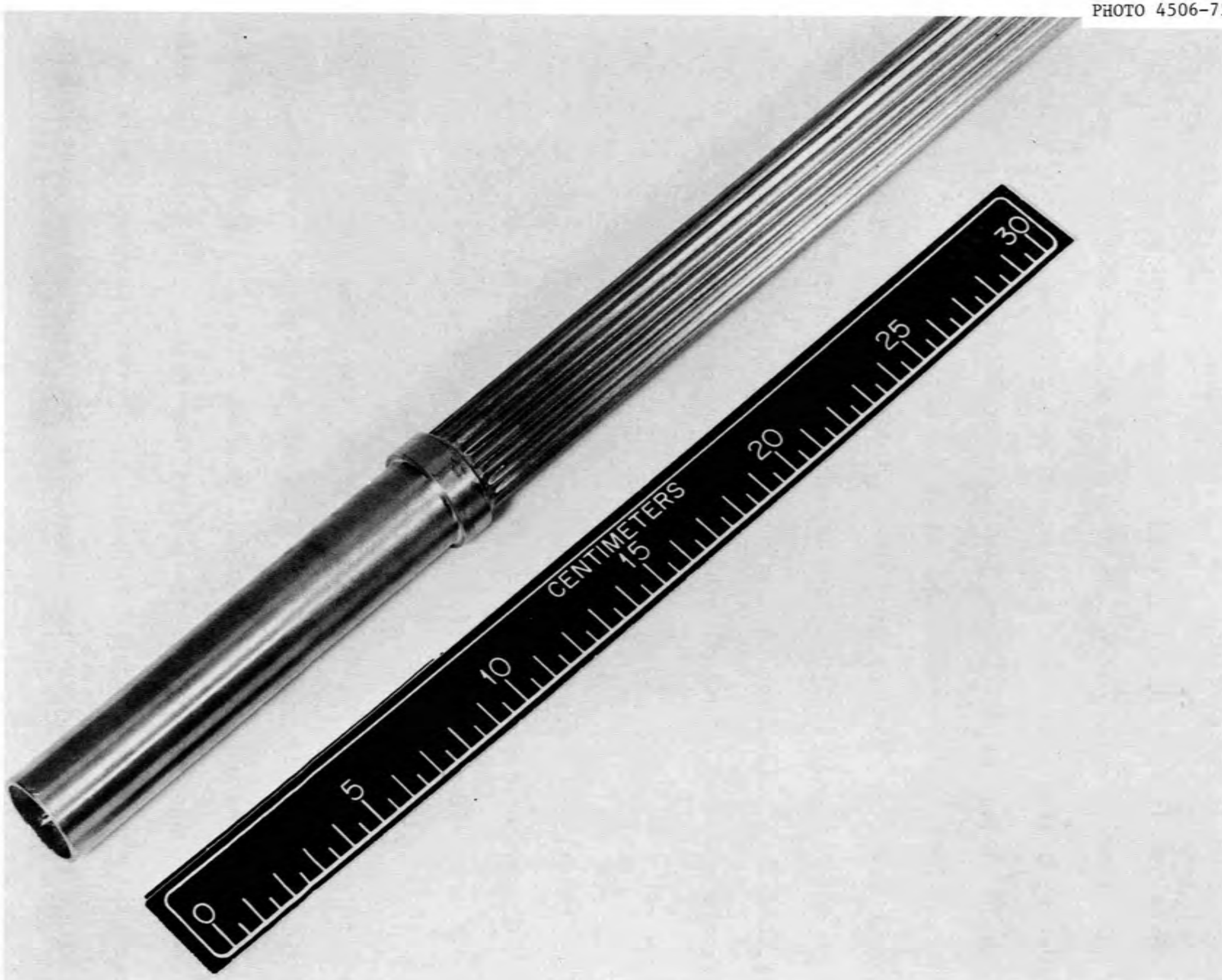

Fig. 3-5. Sleeve connection for a sample test tube.

A stainless steel rod of 0.50-in. outside diameter was installed through the center of the test section (inside the test tube) in order to decrease the hydraulic diameter and increase the velocity for a given primary cooling volume flow. Both of these variations tended to increase the heat transfer coefficients on the water side; and, as a result, improved the accuracy of the Wilson-plot technique[17] used to interpret the experimental data. For example, with a smooth 0.87-in.-ID tube (designated Tube A in the following section), insertion of the 0.50-in.-OD rod decreased the hydraulic diameter by 57% and increased the velocity by 49%.

Test Tubes

The performance of four tubes (1-in.-nominal diameter) was examined in this investigation. Letter designations (as noted in Table 3-1) are used to identify the tubes. Detailed descriptions of the tubes are given in Table 3-1, and enlarged photographs of tube samples are presented in Figs. 3-6 and 3-7. All tubes were aluminum and, with the exception of Tube A, were fluted; Tube A had a smooth surface. As shown in Table 3-1, Tubes F and G had rounded flutes (corrugations), while Tube E had square flutes (square ridges). All tubes except Tube G had a smooth inside surface; the inside surface of Tube G contained some irregularities (scratches) apparently created during the extrusion process.

Tube E was selected from an assortment of tubes remaining from previous heat transfer studies at the Oak Ridge National Laboratory by Alexander and Hoffman.[1] Tubes F and G were fortuitous findings, being commonly sold as standard shower curtain rods, in that the number of flutes fell conveniently in multiples of 12 between Tubes A and E. Tube F

Table 3-1. Characteristics of tubes

Cross section	Tube designation	Inside diameter		Outside perimeter		Outside surface area		Number of flutes
		cm	(in.)	cm	(in.)	m^2	(ft^2)	
	A	2.21	(0.87)	7.98	(3.14)	0.0974	(1.05)	—
	E	2.21	(0.87)	12.70	(5.00)	0.1490	(1.60)	60
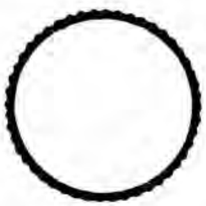	F	2.29	(0.90)	8.26	(3.25)	0.0964	(1.04)	48
	G	2.54	(1.00)	9.75	(3.84)	0.1143	(1.23)	24

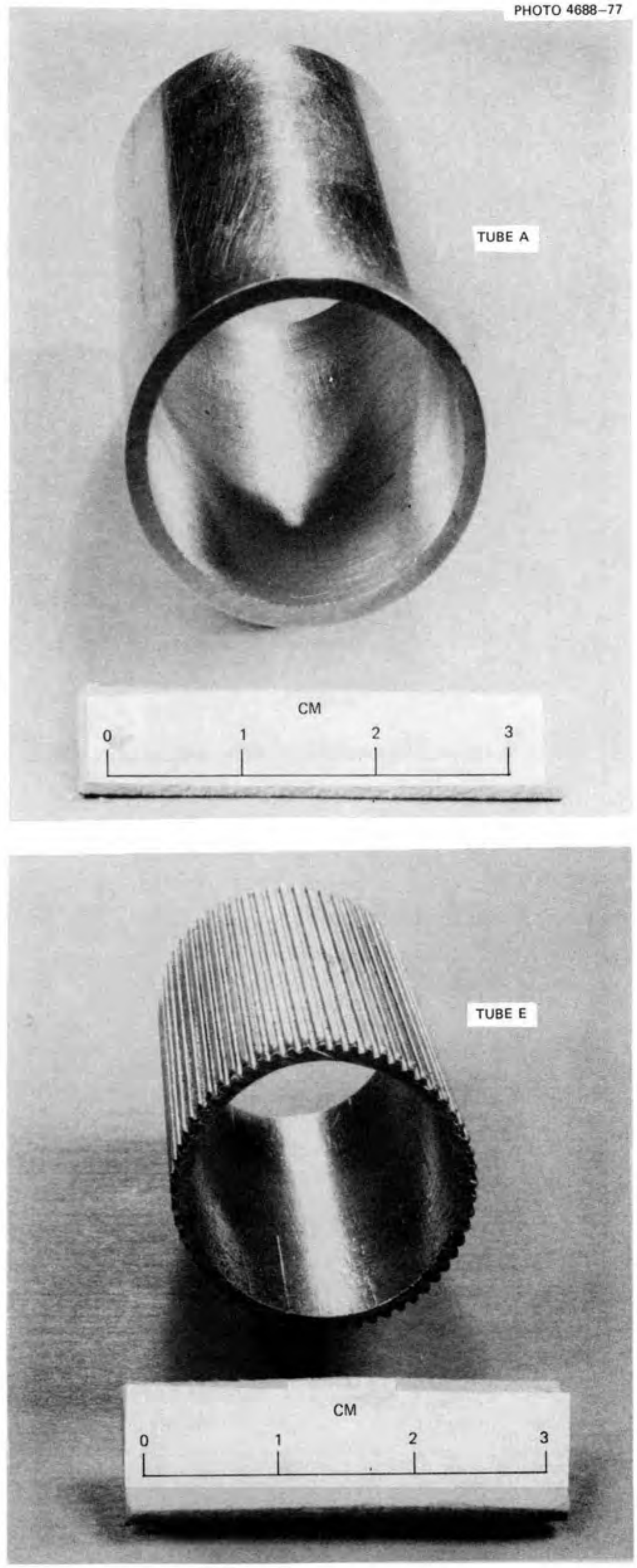

Fig. 3-6. Photographs of tube samples — Tubes A and E.

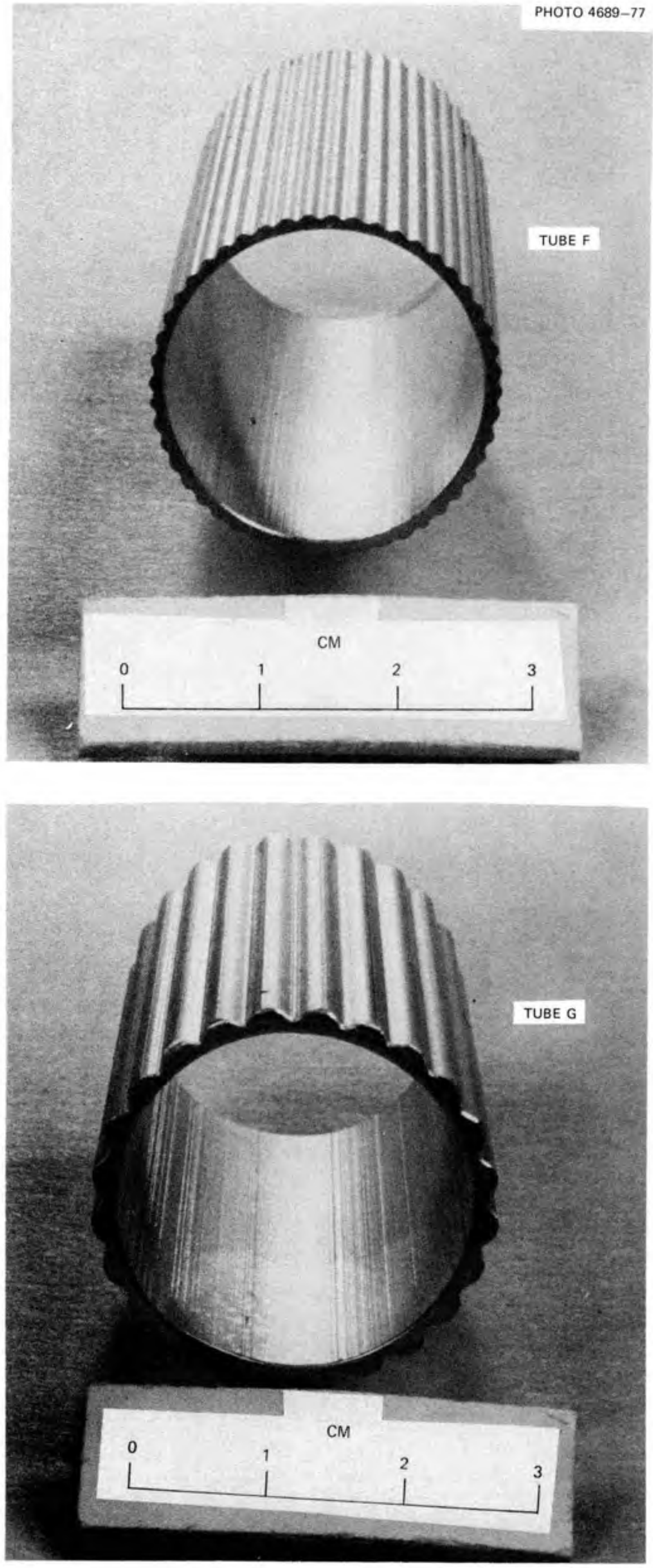

Fig. 3-7. Photographs of tube samples — Tubes F and G.

is distributed by the Macklanburg Duncan Company, and Tube G is distributed by Kirsch under the designation Part No. BF100-54.

The outside surface areas of the fluted tubes were calculated from estimates of the tube perimeters (Table 3-1) and the measured lengths after preparation for testing. For Tubes F and G, the perimeters were obtained as the length of a thin tape fitted tightly in the corrugations of the outside surface of the tube. The small size and shape of the ridges of Tube E made it difficult to use the same technique; and therefore, the perimeter of Tube E was estimated as the product of the number of ridges and the measured perimeter of a typical ridge element.

The active length of smooth Tube A was 48 in., while for the fluted tubes the effective length was 46 in. About 1 in. at each end of the fluted test tubes was taken up by sleeve and installation clearances.

A duplicate of Tube F (designated as Tube F-1) was also tested with a neoprene skirt attached at the midpoint of the condensing length; these tests were conducted to obtain some indication of the effect of tube length on the condensing heat transfer performance of fluted tubes. The midsection area of this tube showing the skirt configuration is pictured in Fig. 3-8.

Storage Tank and Pump

The storage tank (Fig. 3-2, p. 13) was fabricated from a 55-gal stainless steel drum. This tank served as a storage volume for the primary cooling water, while also providing the necessary liquid head for the centrifugal pump. A coil of copper tubing (100 ft long X 0.5-in.-OD) located within the drum provided for heat exchange to the secondary

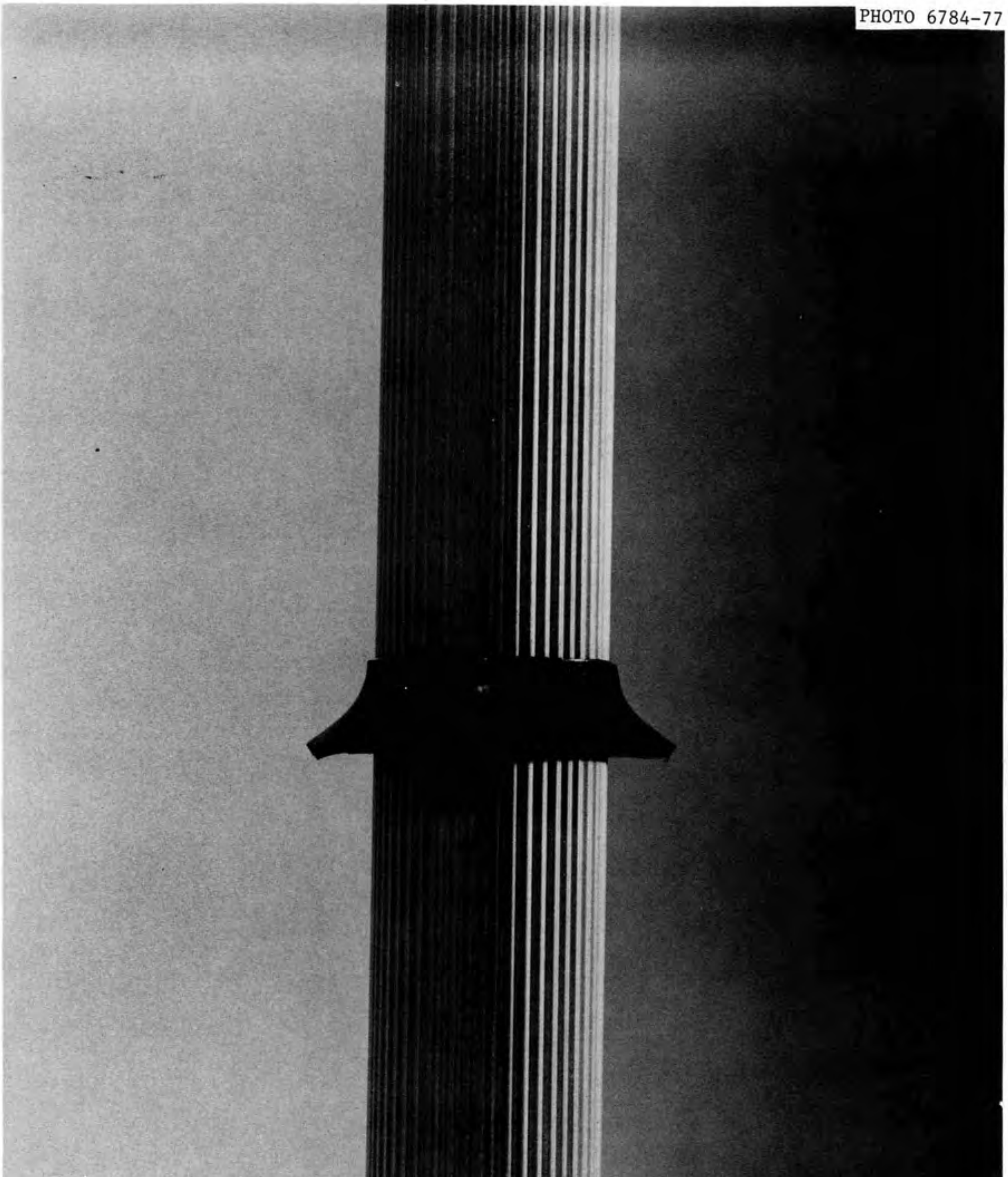

Fig. 3-8. Midsection view of Tube F-1 (Tube F with a neoprene skirt attached at the midpoint of the condensing length).

cooling water; plant process water was circulated through this secondary loop. Circulation of the primary cooling water was by means of a centrifugal pump (Goulds Pumps, Model 3196 ST); this pump (Fig. 3-2, p. 13) was rated at 30 gpm at 170 ft of head and was driven by a 7.5-hp motor. Adequate circulation of the process water through the cooling coils was furnished by the line pressure.

Vent and Vacuum Systems

A port for venting the shell of the condenser was provided at the top of the test section. A vacuum pump, connected to the loop at several locations, permitted evacuation of isolated sections of the loop. A cold trap was located between the loop and the vacuum pump to prevent ammonia from contaminating the oil of the vacuum pump; liquid nitrogen was used in the cold trap.

Seals and Gaskets

The ammonia loop was equipped for the most part with neoprene gaskets and seals. However, Teflon was used for several applications. No compatibility problems were encountered between the ammonia and the seals and gaskets during experimental operation.

CHAPTER IV

PROCEDURES AND INSTRUMENTATION

This experimental study was undertaken to determine heat transfer coefficients for ammonia condensing on the outside of vertical tubes. Water, circulating at relatively high velocities inside the tubes, served as the heat sink. The Wilson-plot technique[17] was then used to isolate the condensing coefficients. The necessary heat rates and temperature differences were calculated from experimental data taken during steady-state operations (see Appendix A for sample calculations). Accurate temperature measurements were critical, since it was sometimes necessary to measure very small temperature differences (~0.2°F) to within ±0.04°F to obtain reliable heat balances. Further, small condensate flows (as low as 0.01 gpm) had to be measured accurately for good interpretation of the experimental data. The operating procedures and instrumentation are described in detail in the following sections.

Operating Procedures

Filling

Before filling operations began, the ammonia loop was evacuated (~28 in. Hg) by the vacuum pump. Once evacuation was complete, ammonia was introduced as a vapor at the top of the loop. Primary cooling water flowing in the test tube caused the ammonia to condense. From the test section, the liquid ammonia then flowed to the boiler. The liquid level in the boiler was monitored visually by the liquid level indicator. When the boiler was half filled with liquid, the vessel supplying the ammonia was valved off; and the system was ready to operate.

Removal of noncondensable gases

One difficulty encountered during operation of the system arose from the presence of noncondensable gases (primarily air). Noncondensable gases impose an added resistance to the transfer of heat by blanketing the cooling surface. The working fluid vapor must then diffuse through the gas, causing a decrease in vapor partial pressure toward the liquid-vapor interface. The effect is to lower the interface saturation temperature below the temperature of the main vapor-gas mixture. Thus, a significant decrease in condensing film coefficient can result from the presence of noncondensable gases; this is discussed further by McAdams[6] and Kern.[18]

Two techniques were employed in this study to remove noncondensable gases from the system. One method was frequent venting at the top of the test section to remove the noncondensable gases before and during operation. In some cases, the noncondensable gases were swept into the test section by the vapor flow. The second technique developed for removing noncondensable gases took advantage of the noncondensable gases collecting in the test section. In this procedure, the heat rate to the boiler was set near the maximum design value, thus creating a high vapor flow that caused most noncondensable gases to be swept into the test section. At this point, the boiler was valved off from the condensing test section; and a vacuum was pulled on the test section removing all fluids (including noncondensable gases) from the test section. This technique was very effective in removing noncondensable gases from the system.

The normal operating procedure included both frequent venting and noncondensable sweeping. Noncondensable gas removal was particularly necessary when a test tube was changed or when unusual operating problems were encountered. A higher than normal difference in temperature between the vapor at the top and the condensate at the bottom of the ammonia loop was a good indication of the presence of noncondensable gases.

Steady-state operation

The heat rate to the boiler was controlled by a stack of six Variacs. Each Variac regulated the voltage to two tubular heaters, and any combination of the six Variacs could be used to obtain desired experimental heat rates. After setting the heat rate to the boiler, the primary cooling flow rate was adjusted by the valve downstream of the test section. Since the inlet temperature of the secondary cooling water was fixed by the plant process water conditions, the flow rate of the secondary cooling water was used to control the temperature of the primary cooling water. This, in turn, controlled the vapor temperature in the test section. Temperatures and pressures throughout the system were monitored to determine when steady-state conditions existed; steady state was assumed when there was no significant change in temperatures (±0.1 to 0.2°F) throughout the system over a five- to ten-minute span.

Once a steady state was achieved, the experimental data were recorded. The information recorded included the vapor temperature and pressure in both the condenser and boiler, the flow rate and temperature of the condensate, the inlet and outlet temperatures and flow rates of the primary and secondary coolants, and the voltage and current to each pair of heater rods. These experimental data were then used to calculate heat transfer rates and temperature differences in the system and to check pressure-temperature values against saturation data in the literature (see Appendix A for examples).

After all the data were recorded for a given steady-state situation, the flow rate of the primary cooling water was changed and the flow rate of the secondary cooling water adjusted (range of 0 to 4 gpm) until the system reached a new steady state. When this steady state was reached, the experimental data were again recorded. The same procedure was followed until data were collected for at least three coolant flow rates at the same boiler heat rate. In the experiments, the primary cooling flow rates ranged from 3.0 to 34.0 gpm. The heat rate to the boiler was then changed, and the entire procedure was repeated at the new heat rate.

Instrumentation

Voltage and current

The voltage across each pair of tubular heaters was measured by voltmeters, and the current through each pair of heaters was measured by ammeters. The voltage and current information was used to control and monitor the power input to the boiler.

Pressure

The pressures in the boiler and the condenser were measured with gauges (main instrument was a U.S. Gauge, Dial No. 33006) capable of spanning the range of 0 to 300 psig. The ammonia loop was also equipped with a compound gauge for reading low pressures and subatmospheric pressures.

Temperature

The system was equipped with chromel-alumel thermocouples that were read with a potentiometer to obtain the temperatures used in the data analysis and recorded continuously on two multipoint recorders to obtain a permanent record. Thermocouples were located in the liquid and vapor of the boiler, in the vapor feed to the test section, in the inlet and outlet of both cooling water loops, near the condensate measuring station, and on each heater. The recorded thermocouple data were used in deciding when the system reached a steady state.

Both a quartz thermometer and a thermistor were located in the vapor feed to the test section and in the inlet and outlet of the primary cooling water. In addition, a quartz thermometer was located near the condensate measuring station. The information from the quartz thermometers (Hewlett Packard, Model 2801A) and the thermistors (Thermometrics, Part No. S-10-4-wire) was used for data reduction because of the greater accuracy attributed to these instruments. However, the experimental data from the three sets of temperature measuring instruments were checked against each other to increase the confidence in the temperature measurements.

Flow rate

The condensate flow in the ammonia loop was measured by two instruments: an integral orifice meter and a turbine flow transducer. These two instruments were located in parallel with piping permitting the routing of the flow through either device. An integral flow orifice assembly was used to adapt a pneumatic d/p cell transmitter (Foxboro Model 15A) for the measurement of low flow rates. With the integral orifice meter, it was necessary to change orifice plates (bores of 0.0595, 0.0810, 0.0995, and 0.159 in.) for various flow ranges. A turbine flow transducer (Flow Technology, Model FTM-NX3-LJS) equipped with a range extending amplifier (Flow Technology, Model LFA-300AX) facilitated operation. The range extending amplifier made it possible to cover the full range of interest (0.01 to 0.2 gpm) with only one instrument. Measurements from the turbine flow transducer were used in reducing the data with the integral orifice meter results used as a check. The two values always agreed to within a few percent.

The primary cooling water flow was measured by one of two rotameters in parallel upstream of the test section. The rotameters were capable of covering the operating range of 3.0 to 34.0 gpm. The larger rotameter was used to measure primary coolant flows greater than 10 gpm, while the smaller rotameter measured primary coolant flows below 10 gpm. The information from these two rotameters was utilized in the data reduction (see Appendix A, Table A-1).

The secondary cooling water was measured by a small rotameter upstream of the cooling coil. The rotameter was used for monitoring secondary coolant flows that ranged from 0 to 4.0 gpm.

CHAPTER V

ANALYSIS

Overall Condensing Coefficients

The heat transfer rate in the condenser can be written:

$$Q = UA\overline{\Delta T} \ , \tag{5-1}$$

where U is the overall heat transfer coefficient, $\overline{\Delta T}$ is the mean temperature difference between the condensing vapor and the primary cooling water, and A is surface area of the test tube. The heat transfer rate can be computed from either the condensate mass flow rate ($\dot{m}_c$) or from the product of mass flow rate ($\dot{m}_w$) and temperature rise (ΔT_w) of the primary cooling water; thus,

$$Q = \dot{m}_c \, h_{fg} \tag{5-2}$$

and

$$Q = \dot{m}_w \, c_{pw} \, \Delta T_w \ , \tag{5-3}$$

where h_{fg} is the latent heat of ammonia, and c_{pw} is the heat capacity of water. In this analysis, all physical property data for ammonia were taken from ASHRAE handbooks,[19-21] where ammonia is designated as Refrigerant 717.

The arithmetic mean difference is used for $\overline{\Delta T}$, since in most cases the temperature difference across the water was relatively small. Therefore, assuming saturated vapor:

$$\overline{\Delta T} = T_v - (T_{w,in} + T_{w,out})/2 \ , \tag{5-4}$$

where T_v is the ammonia vapor temperature and the second term on the right is the average of the inlet water temperature ($T_{w,in}$) and the outlet water temperature ($T_{w,out}$).

The overall coefficient can be computed from Eq. (5-1) using either Eq. (5-2) or Eq. (5-3) to calculate Q. Defining an overall coefficient (U_o) based on the outside surface area (A_o) and rearranging Eq. (5-1):

$$U_o = \frac{Q}{A_o \overline{\Delta T}} . \qquad (5\text{-}5)$$

The next step in the analysis is the evaluation of individual condensing-side coefficients from the overall coefficients.

Individual Condensing-Side Coefficients

Wall-temperature measurement

Individual coefficients of heat transfer between fluids and surfaces can be determined from direct measurements of surface temperatures. However, as pointed out by McAdams,[6] there are many problems that arise in correctly obtaining surface temperatures. This is especially true with fluted tubes due to the more complex geometry and the associated varying temperature distribution in the wall. The problem is complicated even more for such fluids as water and ammonia where the condensing coefficients are rather high and the corresponding temperature differences are relatively small. Thus, in many experiments, wall temperatures were not measured. Wall temperature measurements were also not attempted in this investigation; instead, methods of evaluating individual coefficients from the measured overall coefficients were employed. These alternative methods are discussed below.

Wilson plot

A technique introduced by Wilson[17] in 1915 was used as the primary method of analysis in this study; this is a graphical method of interpreting overall coefficients of heat transfer in surface condensers such that individual condensing-side coefficients can be evaluated. Beatty et al.[22] determined film coefficients for various fluids condensing on the outside of finned tubes by a modification of the method proposed by Wilson. In this analysis, the Wilson-plot method was applied as originally presented by Wilson. The following treatment presents the method and describes the application to the experimental data in this study.

The overall resistance to heat flow ($\Sigma R = 1/U$) in a condenser is equal to the sum of the individual resistances; thus,

$$1/U = R_v + R_{fo} + R_{wall} + R_{fi} + R_w \,, \tag{5-6}$$

where R_v is the resistance on the vapor (condensing) side, R_{wall} that of the wall, R_w that on the water side, and R_{fo} and R_{fi} account for any fouling on the outside and inside surfaces of the tube, respectively. Introducing individual average heat transfer coefficients (h), neglecting any fouling, and correcting for differences in area, the overall coefficient based on the outside surface area is represented by:

$$\frac{1}{U_o} = \frac{1}{h_v} + R_{wall} + \frac{A_o}{h_w\,A_i} \,, \tag{5-7}$$

where A_i is the inside surface area of the tube, h_v is the vapor-side heat transfer coefficient based on the outside tube area, and h_w is the water-side heat transfer coefficient based on the inside tube area. For a smooth tube, the wall resistance based on the outside tube area is given by:

$$R_{wall} = r_o \ln (r_o/r_i)/k \ , \tag{5-8}$$

where r_o and r_i are the outside and inside radii of the tube, respectively, and k is the thermal conductivity of the tube wall.

Neglecting the effects of changes in water temperature, the water-side resistance ($1/h_w$) can be taken as a function of the water velocity (v). For turbulent flow of water, this can be expressed as

$$1/h_w \propto 1/v^{0.8},$$

and thus, Eq. (5-7) can be rewritten:

$$\frac{1}{U_o} = \frac{1}{h_v} + R_{wall} + a_1 \ v^{-0.8} \ . \tag{5-9}$$

If, following Wilson, the sum of the first two resistances ($1/h_v + R_{wall}$) is taken as approximately constant, Eq. (5-9) becomes:

$$\frac{1}{U_o} = a_o + a_1 \ v^{-0.8} \ . \tag{5-10}$$

In this form, a plot of $1/U_o$ vs $1/v^{0.8}$ on ordinary rectangular coordinates should give a straight line from which the constants a_o and a_1 can be determined. Thus, the constant a_o is given by the y-intercept on the Wilson plot and corresponds to the sum of the first two resistances (vapor side plus wall) in Eq. (5-9):

$$a_o = \frac{1}{h_v} + R_{wall} \ . \tag{5-11}$$

The constant a_1 is the slope of the straight line on the Wilson plot.

For a smooth tube, Eq. (5-8) can be used to calculate a wall resistance, and h_v can be computed from Eq. (5-11). However, for fluted tubes, it is very difficult to estimate the contribution of the wall due to the more complicated wall geometry and heat distribution. Accordingly, the coefficients for the fluted tubes are reported as a composite condensing coefficient (h^*) that includes both the vapor-side resistance and the wall resistance:

$$h^* = \frac{1}{(1/h_v) + R_{wall}} \qquad (5\text{-}12)$$

or

$$h^* = \frac{1}{a_o} \,. \qquad (5\text{-}13)$$

The corresponding composite condensing temperature difference is given by:

$$\Delta T^* = \frac{Q}{h^* \, A_o} \,, \qquad (5\text{-}14)$$

and represents the temperature difference between the vapor and the inside wall of the test tube.

The Wilson plot is based on a constant resistance to heat flow on the vapor side, if one assumes that the wall resistance does not vary significantly with the temperature for a series of runs. The correctness of this assumption relative to these experiments is considered as follows. According to the theoretical relation of Nusselt[5] for smooth tubes, the resistance (thus, the mean heat transfer coefficient) on the vapor side depends on both the temperature difference and the temperature of the condensate film and is given by:

$$h_v = 0.943 \left[\frac{k_f^3 \, \rho_f^2 \, g \, h_{fg}}{L \, \mu_f \, \Delta T_f}\right]^{1/4} \,, \qquad (5\text{-}15)$$

where k, ρ, h_{fg}, and μ are fluid properties (f refers to film temperature), L is the tube length, g is the local gravitational acceleration, and ΔT_f is the mean temperature difference across the film. An alternate form of Eq. (5-15) is:

$$h_v = 0.925 \left[\frac{k_f^3 \rho_f^2 g P_t}{\mu_f \dot{m}_c}\right]^{1/3} , \qquad (5\text{-}16)$$

where P_t is the outside perimeter of the tube and $\dot{m}_c$ is the mass flow rate of condensate exiting at the bottom of the tube. This form results from the application of the relationship:

$$h_v P_t L \Delta T_f = \dot{m}_c h_{fg} ,$$

where each side of the expression represents the heat transferred from the condensing vapor to the water. By solving for ΔT_f and substituting in Eq. (5-15), the alternate form [Eq. (5-16)] is obtained in which the mass flow rate of the condensate ($\dot{m}_c$) is a measured quantity.

In the experiments, the same heat load was maintained for a series of runs with varying water-side velocities; thus, the mass flow rate ($\dot{m}_c$) in Eq. (5-16) was essentially held constant (see Appendix D for tabulation of $\dot{m}_c$). This implies that ΔT_f in Eq. (5-15) was also constant for a series of runs. Therefore, the heat transfer coefficient is dependent mainly on the fluid properties in Eqs. (5-15) and (5-16) which vary with the film temperature. However, over small ranges in temperature, the fluid properties will not vary significantly. Thus, for a series of runs, no appreciable error should be introduced by assuming that the sum of the first two resistances ($1/h_v + R_{wall}$) in Eq. (5-7) is indeed constant.

The assumption of no fouling is probably valid, since the tubes were run for only short periods of time (two to four weeks) during which the experimental overall coefficients did not degrade.

The temperature of the condensate was not measured at the point of exit from the test tube but was measured instead somewhat downstream at the condensate measuring station (see Fig. 3-1, p. 11). Therefore, there was no way of directly determining the amount of subcooling of the condensate film; however, the temperature difference between the vapor (T_v) in the test section and the condensate (T_c) at the measuring station indicated that the amount of subcooling was probably insignificant (see Appendix D for a tabulation of the experimental values of T_v and T_c).

The analyses outlined by Rohsenow and Choi[23] for the influence of fluid film turbulence and vapor shear stress on the condensate flow indicated negligible effect on the ammonia condensation results. The maximum vapor velocity in the test section during the experiments was less than 0.2 ft/sec.

Water-side correlations

An alternative scheme was employed for a rough check of the Wilson-plot results. Heat transfer correlations for fully developed turbulent flow in round tubes were used to estimate the water-side heat transfer coefficients. Three of the more widely accepted correlations are the following:

McAdams[6]

$$\frac{hD}{k_b} = 0.023\left(\frac{GD}{\mu_b}\right)^{0.8}\left(\frac{\mu c_p}{k}\right)_b^{0.4} \qquad (5\text{-}17)$$

Colburn[24]

$$\frac{h}{c_{pb}G}\left(\frac{\mu_f\, c_{pb}}{k_b}\right)^{2/3} = \frac{0.023}{(GD/\mu_b)^{0.2}} \qquad (5\text{-}18)$$

Sieder and Tate[25]

$$\frac{h}{c_{pb}G}\left(\frac{\mu c_p}{k}\right)_b^{2/3}\left(\frac{\mu_{wall}}{\mu_b}\right)^{0.14} = \frac{0.027}{(GD/\mu_b)^{0.2}} \qquad (5\text{-}19)$$

The subscripts refer to the temperature at which the particular fluid property is evaluated; wall refers to wall temperature, b to bulk temperature, and f to the "film temperature" defined by $1/2(T_{wall} + T_b)$. Since wall temperatures were not measured in this investigation, all water properties were evaluated at the bulk or mixed-mean temperature. The hydraulic diameter for the annulus was used wherever tube diameter was required.

Substituting the h predicted by one of the three correlations above for h_w in Eq. (5-7) and solving for the composite condensing coefficient yield:

$$h^* = \frac{1}{(1/U_o) - (A_o/h_w A_i)} \; . \qquad (5.20)$$

For a smooth tube, the wall resistance can be calculated from Eq. (5-8); and the average vapor-side coefficient (h_v) can be evaluated by the use of Eq. (5-12).

In principle, the composite coefficient can be calculated for each condensing run from the overall coefficient, water velocity, and water properties; therefore, one could evaluate a composite coefficient for each water velocity used in the Wilson plot. However, the composite coefficient in Eq. (5-20) is very sensitive to the water-side coefficient, especially at low water velocities (low water-side coefficients). At best, the water-side correlations allow for a rough check of the Wilson-plot results; at low water velocities, Eq. (5-20) is too sensitive to h_w

for a meaningful comparison. In Appendix C, Eqs. (5-17), (5-18), and (5-19) have been evaluated for the highest water velocity in each series of runs (Wilson plot), and the results are compared with the Wilson-plot results. This comparison is discussed further in Chapter VI for both the smooth and the fluted data.

Detailed sample calculations are presented in Appendix A.

CHAPTER VI

RESULTS AND DISCUSSION

Condensing experiments conducted in this investigation (501 runs which yielded 92 heat transfer data points) are documented in Appendix D (Tables D-1 through D-5), where the experimental data are tabulated along with the overall condensing coefficients. Heat balance checks are also listed in Appendix D; over 98% of the checks were better than ±10% and over 80% were better than ±5%. Results from the Wilson plots (sample plots are shown in Appendix A) are presented in Fig. 6-1, where h^* (the

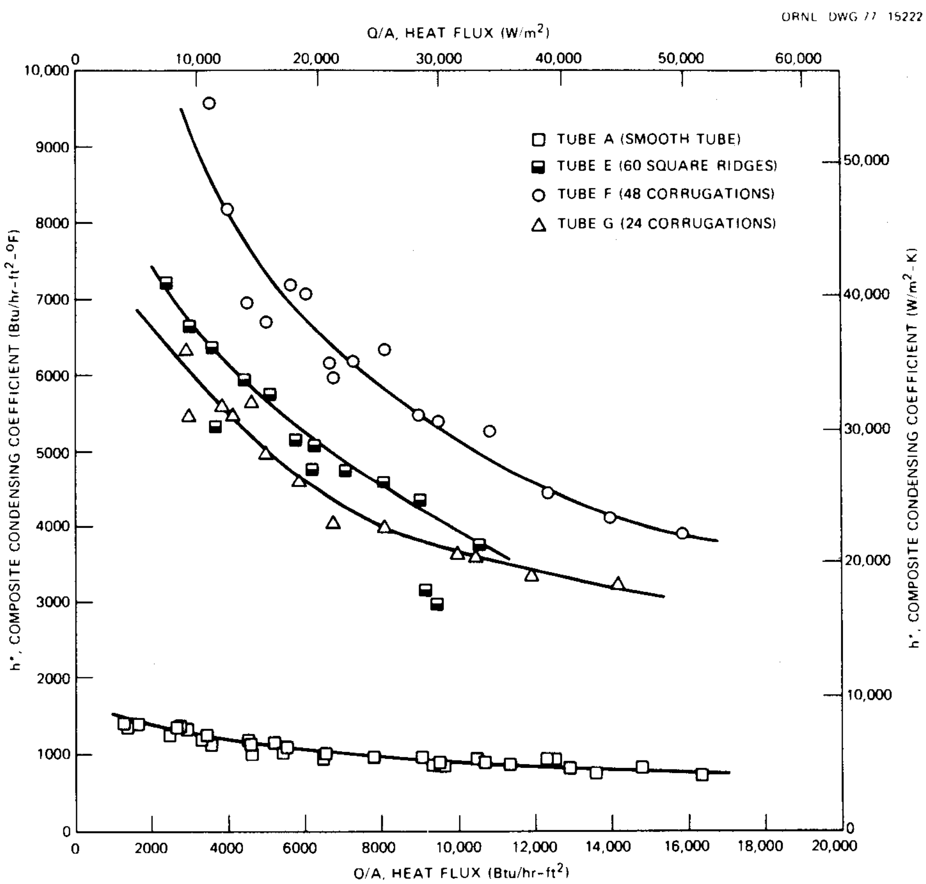

Fig. 6-1. Composite condensing heat transfer coefficients for ammonia.

composite condensing coefficient) is given as a function of the heat flux (Q/A); it should be noted that the heat transfer area used in obtaining both h^* and Q/A is the total outside tube surface area. Wilson-plot results are tabulated in Appendix B (Tables B-1 through B-5) and are compared with results from water-side correlations in Appendix C (Tables C-1 through C-3). Parameter ranges for the experiments were as presented in Table 6-1.

Smooth Tube

Tube A (smooth) data are presented in Fig. 6-2 in nondimensional form. The ordinate is the standard nondimensional heat transfer coefficient (mean or average coefficient):

$$H = h_V/(k^3\rho^2 g/\mu^2)^{1/3} \ . \tag{6-1}$$

In this case, the wall resistance has been eliminated from the composite coefficient by the use of Eq. (5-8). The abscissa is the liquid film Reynolds number:

$$Re = 4\Gamma/\mu \ , \tag{6-2}$$

where Γ is the condensate mass flow rate at bottom of tube per unit length of periphery. All fluid properties (k, ρ, and μ) were evaluated at the equivalent film temperature as suggested by McAdams.[6] The method for obtaining the equivalent film temperature is illustrated in Appendix A under "Nondimensional Quantities."

As illustrated in Fig. 6-2, the smooth-tube data lie considerably above the Nusselt[5] (analytical) prediction; however, the semiempirical correlation of McAdams[6] is in good agreement with the smooth-tube data. A correlation by Zazuli,[7] which purports to account for ripple effects in the condensate film, seems to be slightly higher than the experimental

Table 6-1. Parameter ranges for condensing tests

Parameter	Units		Test tube A	E	F	F-1	G
Condensing temperature	K	→	293–316	296–314	298–315	301–315	302–316
	(°F)	→	(69–109)	(73–105)	(77–107)	(82–108)	(83–109)
Condensing pressure	MPa	→	0.88–1.7	0.95–1.6	1.0–1.6	1.1–1.6	1.1–1.7
	(psia)	→	(127–242)	(138–227)	(146–236)	(160–240)	(163–245)
Composite condensing temperature difference	K	→	0.7–12.6	0.2–1.8	0.2–2.2	0.2–1.9	0.3–2.5
	(°F)	→	(1.2–22.7)	(0.3–3.2)	(0.4–4.0)	(0.4–3.5)	(0.5–4.4)
Heat load	W	→	500–5000	1000–5000	1000–4800	1050–4500	1000–5100
	(Btu/hr)	→	(1700–17,000)	(3500–17,000)	(3500–16,000)	(3600–15,000)	(3500–17,000)
Heat flux	W/m^2	→	5200–52,000	7000–33,000	11,000–50,000	11,000–48,000	8800–45,000
	$(Btu/hr\cdot ft^2)$	→	(1600–16,000)	(2200–11,000)	(3400–15,000)	(3500–15,000)	(2800–14,000)
Composite condensing heat transfer coefficient	$W/m^2\cdot K$	→	4100–7900	17,000–41,000	22,000–54,000	24,000–48,000	18,000–36,000
	$(Btu/hr\cdot ft^2\cdot °F)$	→	(720–1400)	(3000–7200)	(3900–9600)	(4200–8500)	(3200–6300)

ORNL-DWG 77-15227

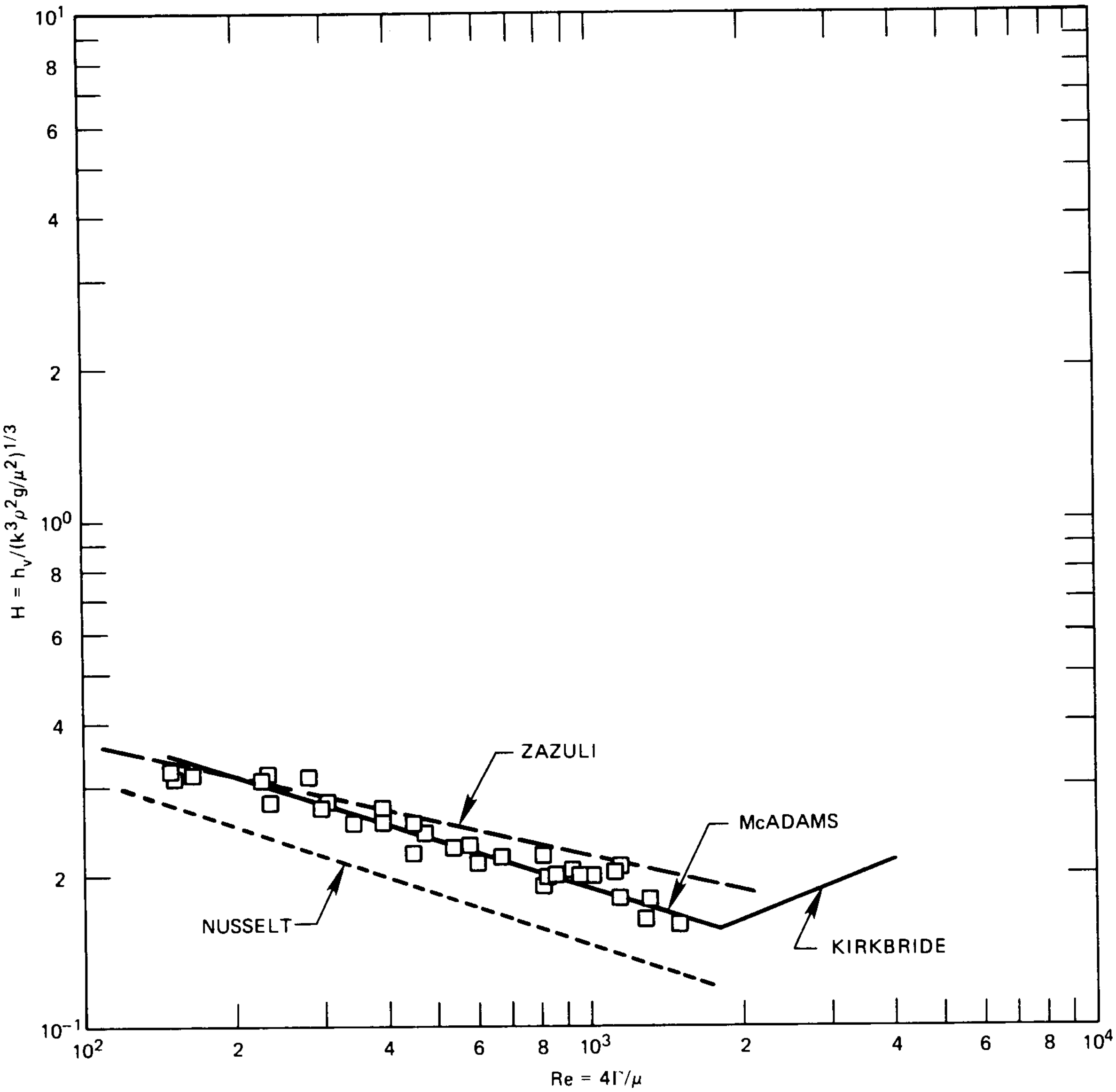

Fig. 6-2. Vertical smooth-tube (A) condensation data for ammonia — standard nondimensional coordinates.

data on the average. In general, however, it can be claimed that the smooth-tube data are in good agreement with standard correlations.

The smooth-tube data for ammonia are plotted in Fig. 6-3 along with similar data taken previously at Oak Ridge National Laboratory[15] for

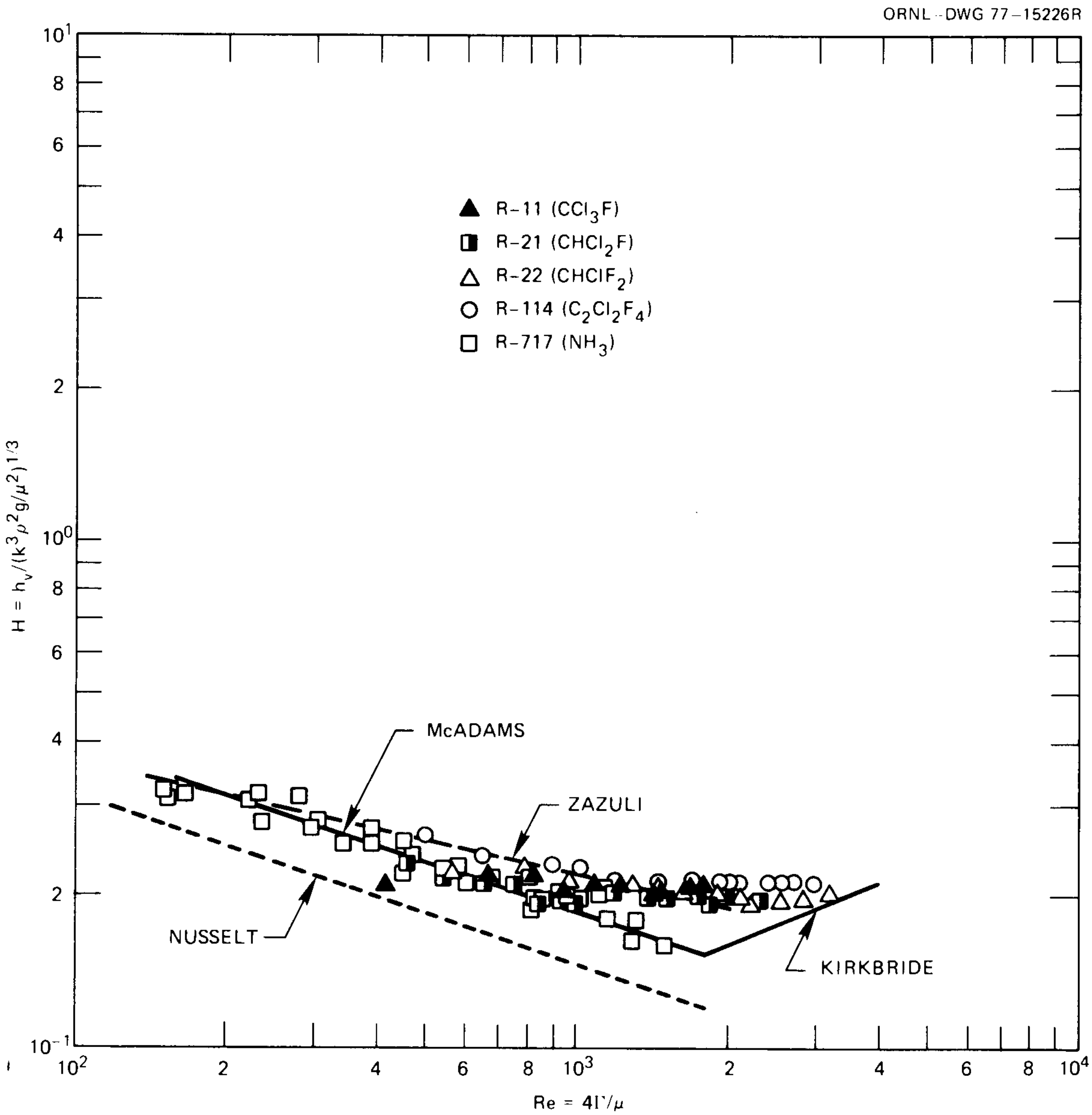

Fig. 6-3. Comparison of vertical smooth-tube (A) condensation data for ammonia to similar data for fluorocarbons — standard nondimensional coordinates.

fluorocarbons condensing on smooth tubes. The data from all fluids, including ammonia, are seen to group in a rather tight band despite the rather wide spread in individual fluid properties (see Table 6-2); this suggests that the nondimensional groups account adequately for the governing mechanisms of heat transfer. As seen in Fig. 6-3, the data for

Table 6-2. Comparison of fluid properties at 38°C (100°F)

Property[a]	Units		Refrigerant number (Formula)					
			11 (CCl_3F)	21 ($CHCl_2F$)	22 ($CHClF_2$)	114 ($C_2Cl_2F_4$)	717 (NH_3)	718[b] (H_2O)
Saturation pressure, P_{sat}	Pa	→	1.618×10^5	2.761×10^5	1.452×10^6	3.161×10^5	1.461×10^6	6550
	(psia)	→	(23.46)	(40.04)	(210.6)	(45.85)	(211.9)	(0.950)
Thermal conductivity, k	W/m·K	→	0.0839	0.0974	0.0815	0.0613	0.452	0.628
	(Btu/hr·ft·°F)	→	(0.0485)	(0.0563)	(0.0471)	(0.0354)	(0.261)	(0.363)
Viscosity, μ	Pa·s	→	3.70×10^{-4}	2.84×10^{-4}	1.84×10^{-4}	2.9×10^{-4}	1.23×10^{-4}	6.53×10^{-4}
	(lb_m/hr·ft)	→	(0.894)	(0.686)	(0.0444)	(0.71)	(0.298)	(1.58)
Density, ρ	kg/m^3	→	1445	1335	1141	1416	583.1	993.2
	(lb_m/ft^3)	→	(90.21)	(83.36)	(71.23)	(88.40)	(36.40)	(62.00)
Latent heat of vaporization, h_{fg}	J/kg	→	1.749×10^5	2.211×10^5	1.693×10^5	1.230×10^5	1.110×10^6	2.410×10^6
	(Btu/lb_m)	→	(75.24)	(95.12)	(72.84)	(52.91)	(477.8)	(1037)
Heat capacity, c_p	J/kg·K	→	895	1090	1310	1040	4845	4175
	(Btu/lb_m·°F)	→	(0.214)	(0.260)	(0.313)	(0.249)	(1.158)	(0.998)
Surface tension, σ	N/m	→	0.0167	0.0163	0.00645	0.0105	0.0175	0.0699
	(lb_f/ft)	→	(1.14×10^{-3})	(1.12×10^{-3})	(4.42×10^{-4})	(7.20×10^{-4})	(1.20×10^{-3})	(4.79×10^{-3})

[a]The properties k, μ, ρ, and c_p are for the liquid.

[b]Shown for comparison.

ammonia (squares) span the Reynolds number range of 150 to 1500 and do not enter the laminar-turbulent transition as do the data for the fluorocarbons (Re = 400 to ~3000).

Results from the Wilson plots for the smooth tube are compared with the results using water-side correlations (McAdams,[6] Colburn,[24] and Sieder and Tate[25]) in Eq. (5.20). The composite condensing coefficients (h^*) from Eq. (5.20) were in good agreement (−11.4 to +6.9%) with the corresponding Wilson-plot coefficients; this comparison is presented in detail in Table C-1 of Appendix C. The results were not very sensitive to the correlation used for predicting water-side coefficients; thus, the comparison ranged from −10 to 0% with the McAdams correlation, from −6.4 to +6.9% with Colburn, and from −11.4 to 0% with Sieder and Tate. The agreement between the two methods is very good, since ±10 to ±30% is usually considered an acceptable range for predicted heat transfer coefficients.

Fluted Tube

Heat transfer data for the three fluted tubes (E, F, and G) are presented along with smooth-tube (A) data in dimensional form in Fig. 6-1. More scatter is observed in the fluted-tube data than was found with the smooth-tube data; this difference results from the problems of measuring the lower temperature differences associated with the higher coefficients for the fluted tubes. The coefficients are reported as composite coefficients because of the difficulty in accounting for the wall resistance of the fluted tubes; therefore, it is not convenient to put the coefficients in nondimensional form as was done for the smooth tube. The wall resistance of the smooth tube can be evaluated (see Appendix A) and is only about 10% of the composite resistance; but for the fluted tubes, the wall resistance is a much greater percentage since the coefficients are significantly higher. Thus, reporting composite coefficients circumvents the problem of evaluating the wall resistance. In practice, designers can work easily with the composite coefficient.

The curves drawn through the experimental data in this chapter provide only a means for visual comparison and a basis for estimating enhancement ratios; no analytical curve fitting was employed. The data for Tube A in Fig. 6-1 (p. 42) show that for a smooth tube heat transfer coefficients decrease only slightly with increasing heat flux in the test range. In contrast, the data for the fluted tubes indicate heat transfer coefficients that are not only considerably higher than those achieved with Tube A but also decrease rapidly with increasing heat flux. Tube E data are slightly above Tube G data at the lower heat fluxes but approach Tube G values at higher heat fluxes (~11,000 to 12,000 Btu/hr·ft^2). Heat transfer coefficients for Tube F are higher than those for Tube E over the full heat flux range of these experiments. While Tubes E and G have significantly greater condensing area (see Table 3-1, p. 20) than Tubes A and F, this effect is essentially accounted for since the ordinate and abscissa bases are on total area bases. Therefore, some additional effect must account for the observed performance improvement. Such results are consistent with those of previous investigators (working primarily with water) who attributed their findings to surface tension drainage effects on contoured surfaces (see Refs. 1, 9, 11–15). Alternatively, the condensing coefficient and heat flux can be based on the area determined from the nominal outside (rubber band) tube circumference in which case an improvement in the heat transfer coefficient due to the extra area would also show up.

A comparison of the data for the fluted tubes in Fig. 6-1 suggests that the heat transfer coefficients are a function of the shape of the flute as well as the size and number of flutes. Thus, the coefficients for Tube E (60 square ridges) are lower than those for Tube F (48 corrugations) and comparable to the coefficients for Tube G (24 corrugations). This suggests that the corrugations or rounded flutes on Tubes F and G are more efficient than square ridges, since fewer flutes are required to achieve better or similar performance. It is observed that the performance of the fluted tubes is similar to that found with fluorocarbons (see Refs. 14 and 15) where data were substantially above that of a smooth tube; however, the magnitude of the coefficients is much greater for ammonia ($\sim$5 to 10 times for a smooth tube) and is attributed to superior fluid properties of ammonia (see Table 6-2).

Figure 6-4 uses an enhancement ratio [R_{h*} = h* (fluted tube)/h* (smooth tube)] to provide another form of comparison between fluted-tube and smooth-tube coefficients. The ratio is plotted as a function of heat flux. For Tube F, the enhancement ratio (R_{h*}) ranged from 5.0 at high heat flux to over 7.0 at low heat flux; for Tube E, the range was 4.3 to 5.5; and for Tube G, 4.0 to 4.8. The magnitude of the enhancement again varies with both the type of fluted tube and the heat flux.

While Fig. 6-1 (p. 42) is useful for describing heat transfer ranges of the experiments and for determining whether the observed enhancement was merely an area effect, another dimensional presentation may be more meaningful for particular design situations. In Fig. 6-5, the data have been

ORNL-DWG 77-15225

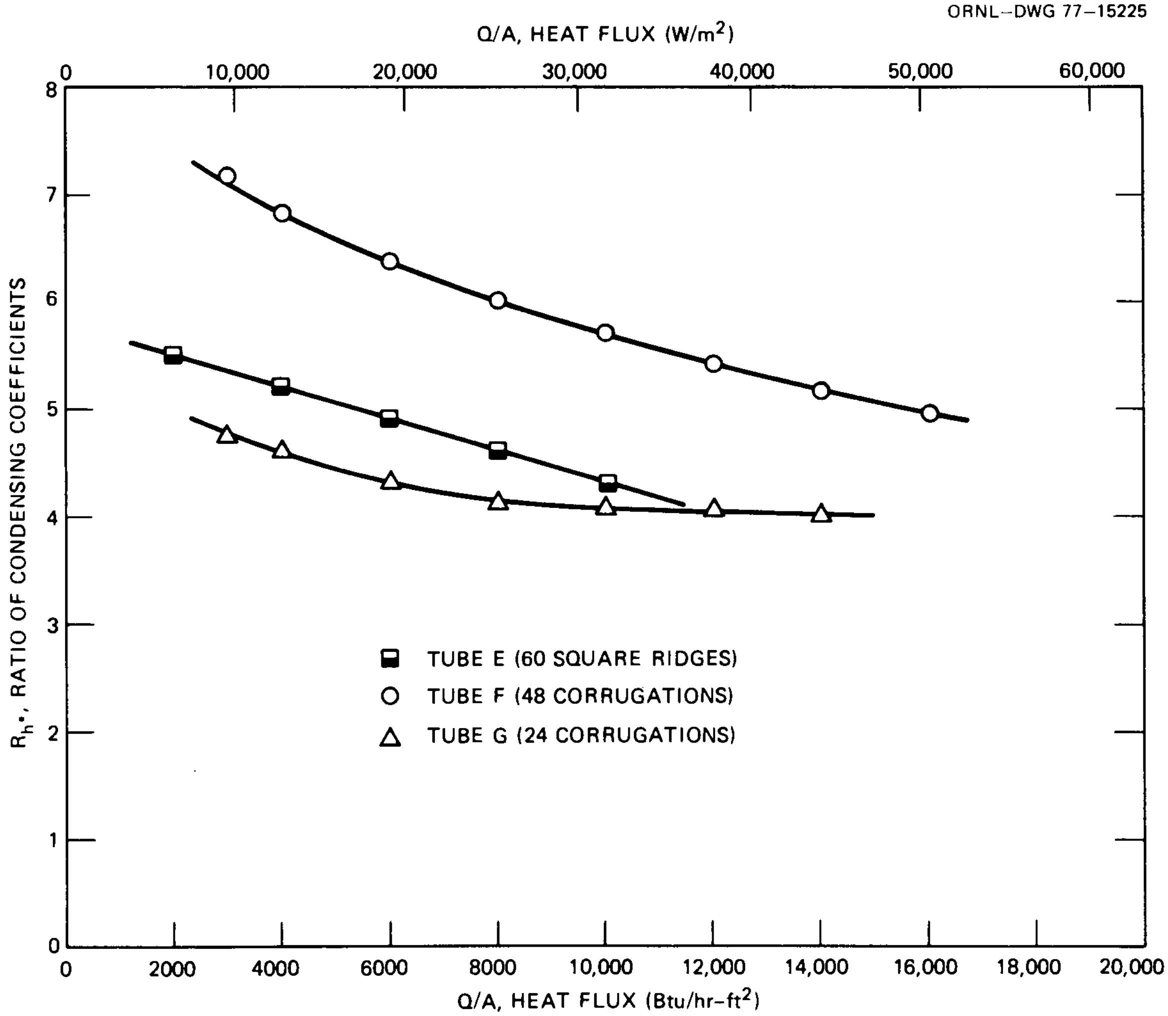

Fig. 6-4. Fluted-tube heat transfer enhancement plot for ammonia — ratio of condensing coefficients [R_{h*} = h* (fluted tube)/h* (smooth tube)] vs heat flux.

replotted as heat load versus condensing temperature difference. In this form (alternate to the previous total area basis), the designer can take "credit" for the increased area of the fluted tube. Thus, for fixed heat load or condensing temperature difference, enhancement factors can be evaluated. In Fig. 6-5, it can be seen that the performance rank order of test tubes is switched from the order in Fig. 6-1; that is, Tube A is

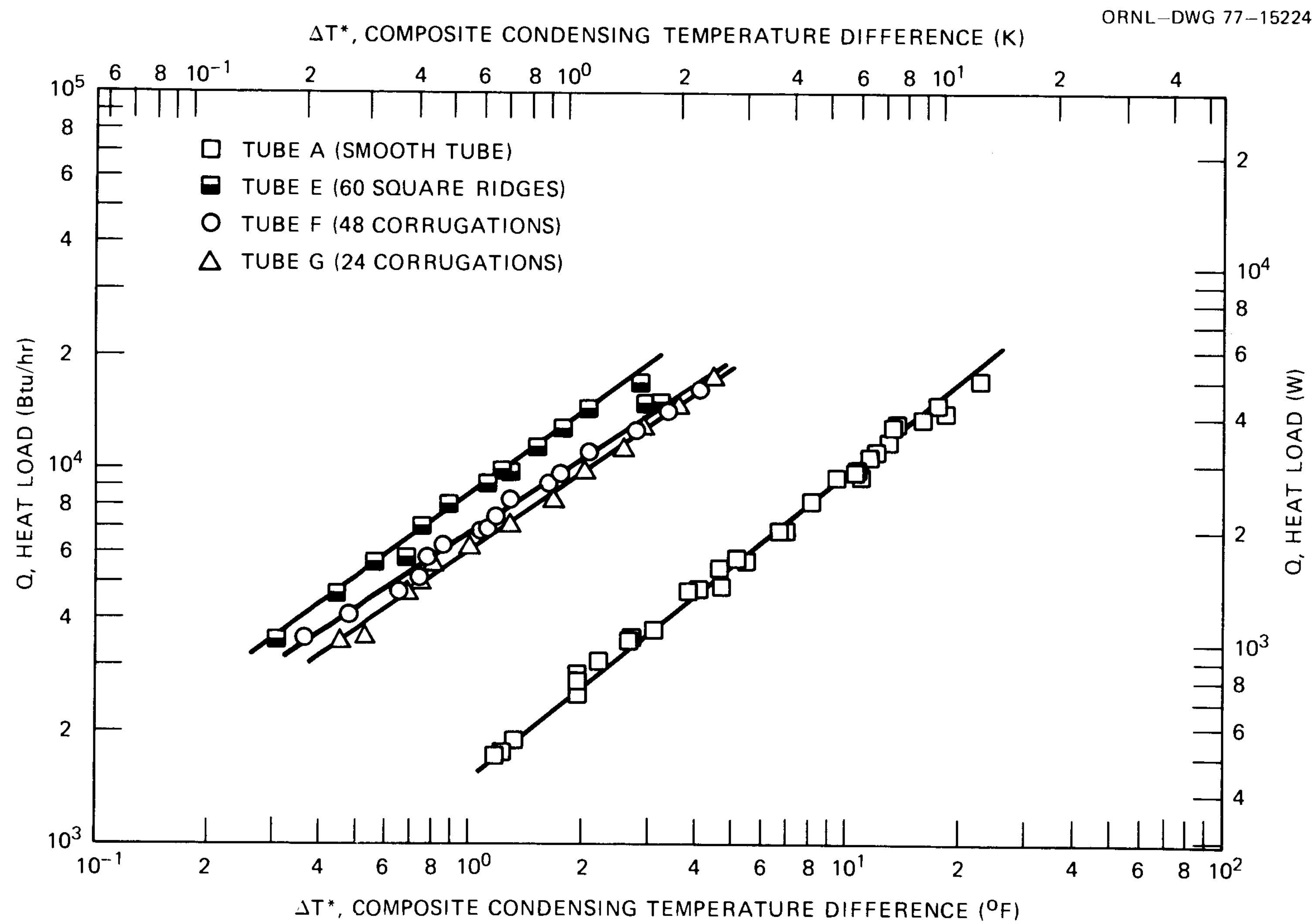

Fig. 6-5. Heat load vs composite condensing temperature difference for ammonia.

still the worst, but Tube E is now the best with Tube F second and Tube G third. It is clear that the relative positions of Tubes E and G improve when compared on the heat load-condensing temperature difference basis, because their total surface areas are greater than those of Tubes A and F (see Table 3-1, p. 20).

Figure 6-6 is an enhancement plot for the fluted tubes where the ratio of condensing temperature differences [$R_{\Delta T*}$ = $\Delta T*$ (smooth tube)/$\Delta T*$ (fluted tube)] is plotted as a function of heat load. The maximum condensing temperature difference ratio was 9.7 at the lowest heat load for Tube E; the minimum ratio was 4.8 at the highest heat load for Tube G.

In a similar manner, the ratio of heat loads [R_Q = Q (fluted tube)/ Q (smooth tube)] can be evaluated at a constant condensing temperature difference. The heat load ratio can be estimated from the curves sketched through the data in Fig. 6-5. The maximum heat load ratio achieved in these tests was 5.4 occurring with Tube E at a condensing temperature difference of 1.2°F (lowest value reported for Tube A). This indicates that Tube A could accommodate only a heat load of 1800 Btu/hr; whereas, Tube E could handle 9700 Btu/hr at a composite condensing temperature difference of 1.2°F. The minimum heat load ratio was 3.5 occurring at the highest condensing temperature difference (4.4°F) with Tube G.

Wilson-plot results for the fluted tubes with smooth inside surfaces (Tubes E and F) are compared in Appendix C (Tables C-2 and C-3) with the results obtained using water-side correlations [Eq. (5.20)]. The smooth-tube correlations for water-side coefficients were not applicable for Tube G, since it contained irregularities on the inside surface. The composite condensing coefficients from Eq. (5.20) were in fair agreement

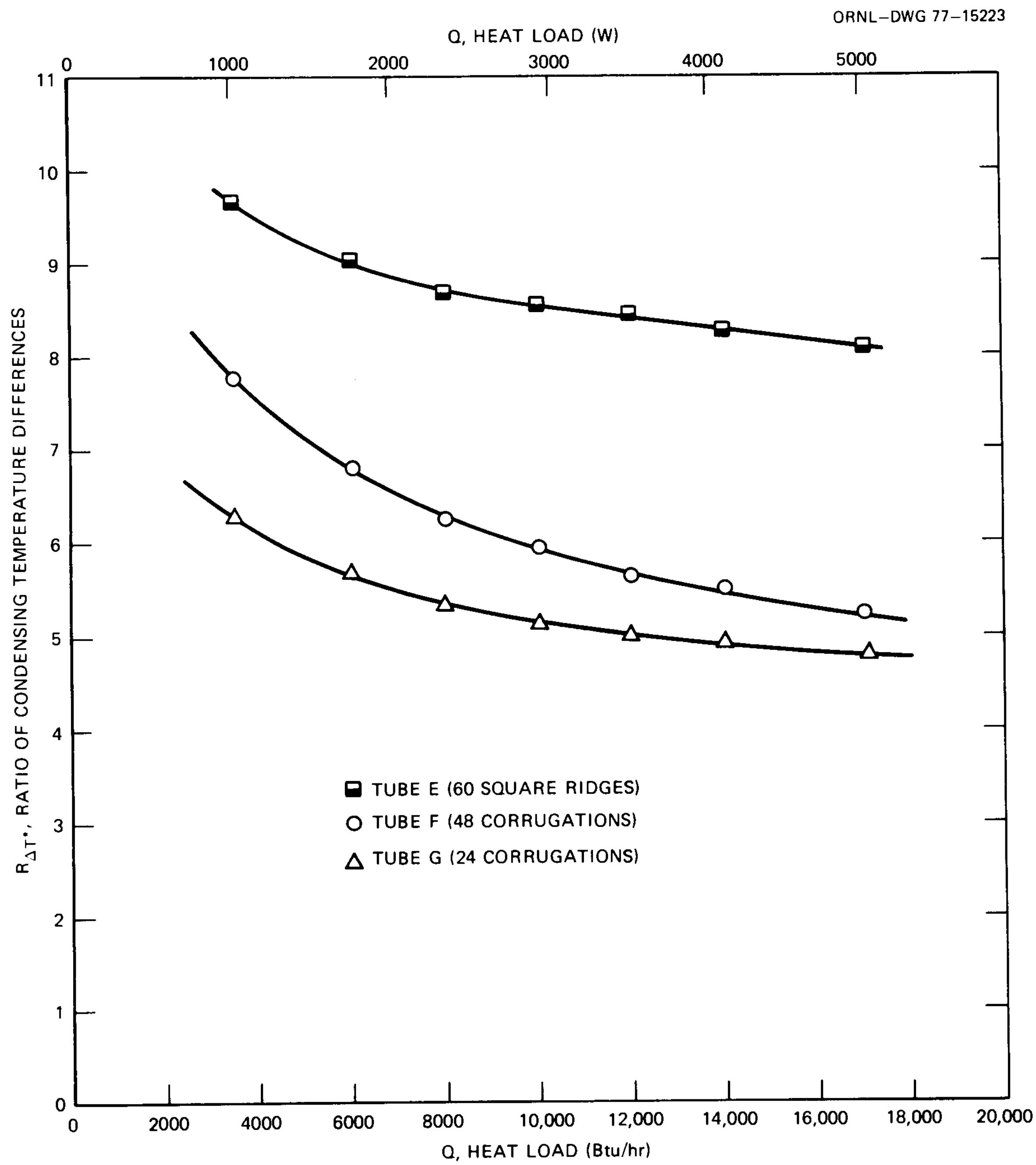

Fig. 6-6. Fluted-tube heat transfer enhancement plot for ammonia – ratio of condensing temperature differences [$R_{\Delta T*} = \Delta T*$ (smooth tube)/$\Delta T*$ (fluted tube)] vs heat load.

(−38 to +11.6%) with the corresponding Wilson-plot coefficients for the fluted tubes; the Colburn correlation gave the best agreement for both Tube E (−17 to +9.7%) and Tube F (−3.1 to +11.6%). In general, the coefficients for Tube F were in better agreement than those for Tube E. While agreement is not within ±12% as with the smooth-tube coefficients, it is fairly good considering the rough nature of the predicted water-side coefficients and the sensitivity of the Wilson-plot results to temperature measurement accuracy.

Tube Length Effects

Figures 6-7 and 6-8 show a comparison between the heat transfer data for Tube F (4 ft long) and Tube F-1 ("effectively" 2 ft long). As indicated in the two figures (6-7 and 6-8), the effect of tube length on performance is not detectable. The data for Tube F-1 fall within the normal scatter of the data for Tube F. Recent work at Oak Ridge National Laboratory with fluorocarbons has indicated significant effects of tube length on heat transfer performance with shorter condensing lengths improving the heat transfer performance. The decrease in heat transfer performance for longer condensing lengths is attributed to liquid flooding of the drainage channels or troughs. However, the large latent heat of vaporization for ammonia (see Table 6-2, p. 47) results in less condensate and thinner films on the tubes at the same heat flux and could explain why no length effects were observed for tubes of the lengths used in ammonia experiments.

ORNL DWG 77-15221

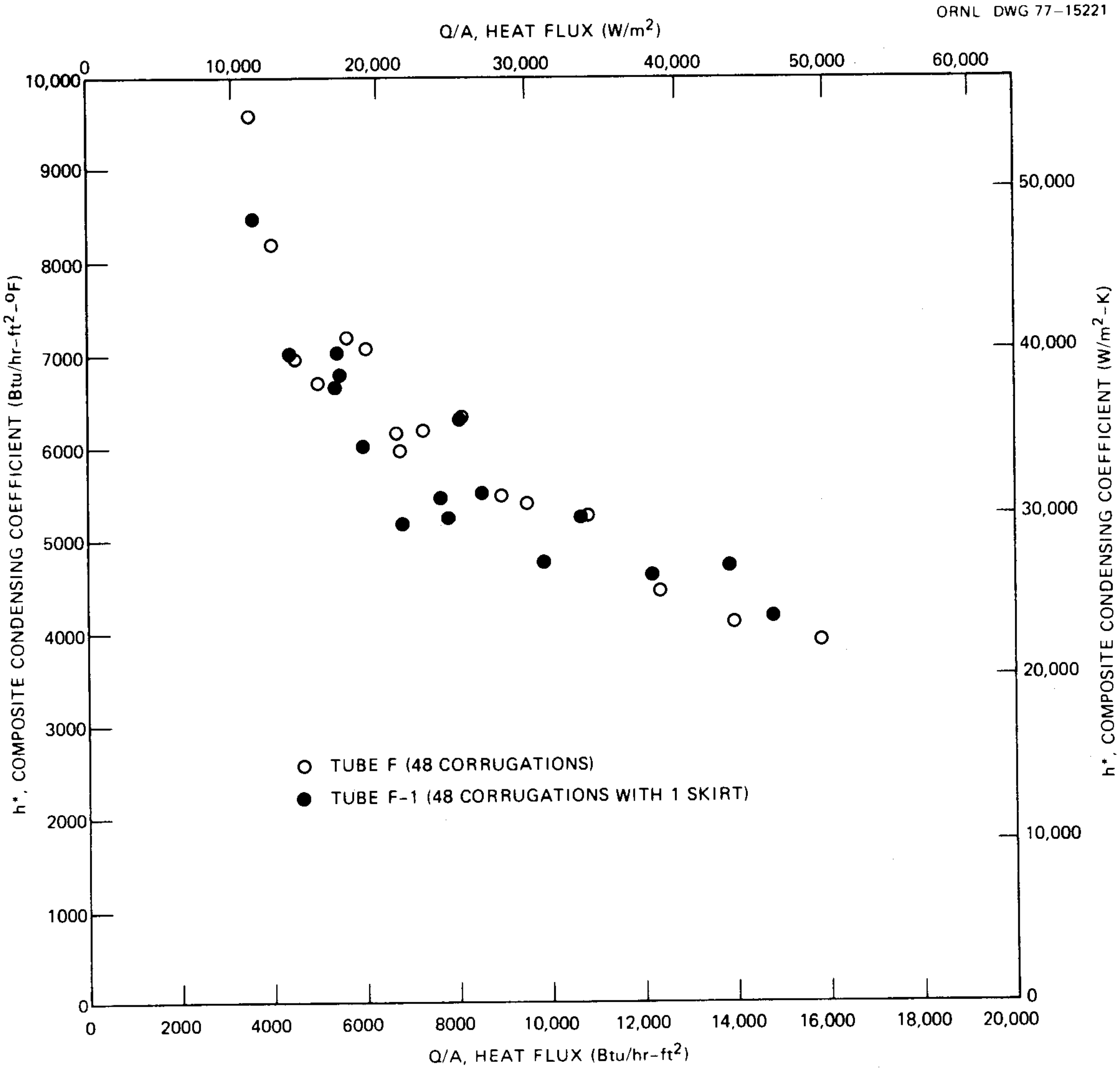

Fig. 6-7. Comparison of heat transfer performance between Tube F (48 corrugations) and a duplicate tube (F-1) containing a skirt at midpoint of the condensing length — h* vs Q/A.

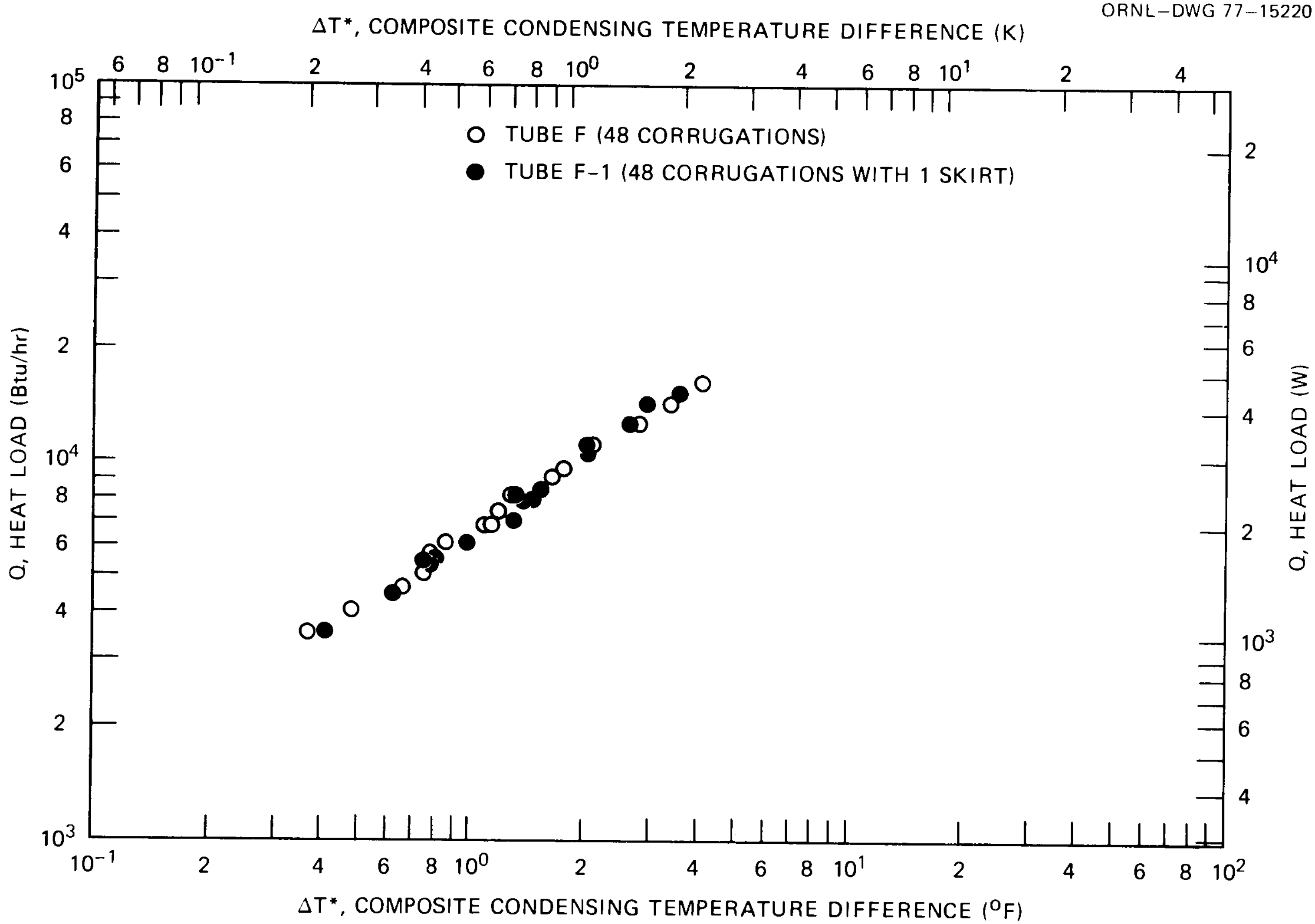

Fig. 6-8. Comparison of heat transfer performance between Tube F (48 corrugations) and a duplicate tube (F-1) containing a skirt at midpoint of the condensing length — Q vs ΔT*.

CHAPTER VII

CONCLUSIONS AND RECOMMENDATIONS

The following main conclusions were drawn from the experimental study for ammonia condensing on vertical tubes:

1. Heat transfer coefficients for ammonia condensing on the fluted outside surfaces of tubes are up to 7.2 times smooth tube values at a given heat flux; this augmentation cannot be accounted for by the greater surface area of the fluted tubes. These results confirm that fluted tubes, previously shown to enhance steam and fluorocarbon condensing coefficients significantly, are also effective with ammonia vapors.

2. The magnitude of the heat transfer enhancement varies with both the number of flutes on a tube of given diameter and the heat flux. Rounded flutes (corrugations) appear to be more effective than square flutes (square ridges) for enhancing heat transfer, indicating that the shape of the flute is also a key variable.

3. For a given heat load, a smooth tube can require condensing temperature differences up to 9.7 times the fluted tube values; conversely, fluted tubes can increase heat load capability up to 5.4 times smooth tube values for a given condensing temperature difference.

4. No appreciable effect on the heat transfer performance of a fluted tube condensing ammonia was detectable in going from an "effective" condensing length of 4 ft to 2 ft. In this respect the ammonia performance differed substantially from that of the fluorocarbons (for example, R-113), where heat transfer coefficients increased by up to 60% as the tube length was halved.

The ultimate goal of studies on fluted-tube condensation is to develop procedures for designing the optimum condensing surface for any particular fluid under any particular set of conditions. Thus, the data obtained in this study contribute with similar data (see Refs. 14 and 15) previously acquired with other fluids to the analytical modeling of the condensation process on fluted tubes. However, fluted-tube condensation is a very complicated process and complete models are not available at this time. To utilize the ammonia data in developing such models, the heat transfer coefficients should be in dimensionless form. This can be done only if the wall resistance can be substracted from the composite resistance. Describing the wall resistance is not an easy problem, since the heat flow paths are not simple as with smooth tubes and further vary with both gross and local tube geometry differences. Significant future effort is needed in this area.

The experimental equipment used in this investigation limited the heat flux to 16,000 Btu/hr$\cdot$ft^2. Experiments should be run at higher heat fluxes to provide more insight into the flooding mechanism for ammonia condensing on fluted tubes. This factor may well account for the lack of any observed effect of tube length on ammonia condensing coefficients in the present study.

In an ocean thermal plant, the condenser will operate at a temperature of around 50°F; this is a cooler condensing temperature than was obtained in any of the experiments in this investigation (range of 69 to 109°F). Although no significant effects on the heat transfer results are expected at lower temperatures, tests duplicating the actual planned operating conditions would provide additional confidence in heat exchanger design.

Fluted-tube coefficients are dependent on the surface tension of the fluid and the geometry of the flutes (size, number, shape, spacing, ratio of crest to trough area, etc.), in addition to the parameters in common with smooth-tube coefficients. Thus, experimental data are needed over a broader range of conditions, including various combinations of tube geometries and fluids, to aid in the development of models and correlations for condensation on fluted tubes. The experimental apparatus and techniques developed for this study should be useful for such an extended effort.

REFERENCES

1. L. G. Alexander and H. W. Hoffman, Improved Heat-Transfer Systems for Evaporators — Performance Characteristics of Advanced Evaporator Tubes for Long-Tube Vertical Evaporators, ORNL/TM-2951 (January 1971).

2. Lockheed Missiles & Space Company, Inc., Ocean Thermal Energy Conversion (OTEC) Power Plant Technical and Economic Feasibility, Report NSF/RANN/SE/GI-C937/FR/75/1, April 12, 1975.

3. TRW Systems Group, Ocean Thermal Energy Conversion Research on an Engineering Evaluation and Test Program, Vol. 3, Report for Contract No. NSF-C958, June 1975.

4. K. J. Bell, "Heat Exchangers for the Ocean Thermal Energy Power Plant," p. 701 in Future Energy Production Systems Heat and Mass Transfer Processes, Vol. 2, Academic Press, New York, 1976.

5. W. Nusselt, "Die Oberflächenkondensation des Wasserdampfes," *Z. Ver. Deutsch. Ing.*, 60, 541, 569 (1916).

6. W. H. McAdams, Heat Transmission, 3d ed., McGraw-Hill, New York, 1954.

7. S. S. Kutateladze, Fundamentals of Heat Transfer, p. 307, Academic Press, New York, 1963.

8. C. G. Kirkbride, "Heat Transfer by Condensing Vapors on Vertical Tubes," *Trans. Am. Inst. Chem. Engrs.*, 30, 170 (1933).

9. R. Gregorig, "Film Condensation on Finely Waved Surfaces with Consideration of Surface Tension," *Zeit. fur ang. Math. u. Physik*, 5, 36 (1954).

10. L. D. Landau and E. M. Lifshitz, Fluid Mechanics, p. 230, Pergman Press, New York, 1959.

11. T. C. Carnavos, "Thin Film Distillation," pp. 205–218 in Proceedings of First International Symposium on Water Desalination, Washington, D. C., October 3–9, 1965, Vol. 2, 1967.

12. D. G. Thomas, "Enhancement of Film Condensation Heat Transfer Rates on Vertical Tubes by Vertical Wires," *Ind. Eng. Chem. Fundamentals*, 6, 97 (1967).

13. D. G. Thomas, "Enhancement of Film Condensation Rate on Vertical Tubes by Longitudinal Fins," *Am. Inst. Chem. Eng. J.*, 14, 644 (1968).

14. Energy Division Annual Progr. Rep. Dec. 31, 1975, ORNL-5124, pp. 194–197.

15. Energy Division Annual Progr. Rept. Sept. 30, 1976, ORNL-5250, pp. 208–213.

16. A. P. Kratz, H. J. Macintire, and R. E. Gould, *University of Illinois, Engineering Experimental Station, Bull.* 171 (1927), 196 (1928), 209 (1930).

17. E. E. Wilson, "Basis for Rational Design of Heat Transfer Apparatus," *Trans. Am. Soc. Mech. Engrs.*, 37, 47 (1915).

18. D. Q. Kern, Process Heat Transfer, p. 281, McGraw-Hill, New York, 1950.

19. "Properties of Refrigerants," Chap. 14, ASHRAE Handbook of Fundamentals, p. 268, ASHRAE, New York, 1972.

20. Thermophysical Properties of Refrigerants, pp. 145–150, ASHRAE, New York, 1973.

21. Thermodynamic Properties of Refrigerants, pp. 131–150, ASHRAE, New York, 1969.

22. K. O. Beatty, Jr., and D. L. Katz, "Condensation of Vapors on Outside of Finned Tubes," *Chem. Eng. Progr.*, 44(1), 55 (1948).

23. W. M. Rohsenow and H. Y. Choi, Heat, Mass, and Momentum Transfer, Chap. 10, pp. 237–253, Prentice-Hall, New Jersey, 1961.

24. A. P. Colburn, "A Method of Correlating Forced Convection Heat Transfer Data and a Comparison with Fluid Friction," *Trans. Am. Inst. Chem. Engrs.*, 29, 174 (1933).

25. E. N. Sieder and C. E. Tate, "Heat Transfer and Pressure Drop of Liquids in Tubes," *Ind. Eng. Chem.*, 28, 1429 (1936).

APPENDIXES

APPENDIX A

SAMPLES OF DATA REDUCTION

Physical Properties for Ammonia

All property data for ammonia used in data reduction were taken from ASHRAE handbooks[19-21] where ammonia is designated as R-717. The accuracy of thermophysical properties is discussed in Ref. 20.

Fluted Tube

A sample of the experimental data required for computing the heat transfer rates and coefficients in the condenser is listed in Table A-1. The data are for ammonia condensing on Tube E (60 square ridges). Experimental Run 717-051E is used to demonstrate the procedure followed in reducing the data for an individual run, and the series of Runs 717-051E through 717-056E are used to demonstrate the Wilson plot.

For saturated vapor, the experimental pressure (P) of the vapor should agree with the saturation pressure (P_{sat}) of ammonia at the experimental vapor temperature (T_v). The saturation pressure in ASHRAE for a temperature of 77.2°F is 146 psia which agrees within the experimental accuracy of the instruments to the measured pressure (P) of 147 psia for Run 717-051E. This agreement also indicates that noncondensables were not present in the condenser in appreciable amounts during operation.

The heat transfer rate in the condenser can be computed both from condensate flow rate (F_c) and from the flow rate (F_w) and the temperature rise (ΔT_w) of the cooling water. To calculate the heat transfer from the condensate flow rate requires the latent heat (h_{fg}) of ammonia at the vapor

Table A-1. Sample of experimental data — ammonia condensing on Tube E

Run No.	Vapor feed to test section: Temperature T_v, °F	Vapor feed to test section: Pressure P, psia	Condensate: Flow rate F_c, gpm	Condensate: Temperature T_c, °F	Primary cooling water through test section: Flow rate F_w, gpm	Primary cooling water through test section: Inlet temp. $T_{w,in}$, °F	Primary cooling water through test section: Outlet temp. $T_{w,out}$, °F	Primary cooling water through test section: Temp. dif.[a] ΔT_w, °F
717-051E	77.16	147.2	0.03114	77.16	33.4	75.27	75.62	0.284
717-052E	78.39	150.2	0.03119	78.14	17.7	75.64	76.22	0.570
716-053E	78.96	151.7	0.03096	78.68	9.55	74.77	75.78	1.01
717-054E	79.84	154.2	0.03105	79.40	7.70	74.92	76.16	1.23
717-055E	82.02	159.7	0.03082	81.22	5.10	75.30	77.13	1.83
717-056E	82.69	161.7	0.03119	81.82	4.65	75.38	77.40	2.02

[a] Corrected for temperature offset of instruments and pressure drop effects.

temperature (T_v) and the density of liquid ammonia (ρ_c) at the temperature of the condensate (T_c) at the measuring station.

For

$$T_c = 77.2°F \qquad \rho_c = 37.6 \ lb_m/ft^3$$

$$T_v = 77.2°F \qquad h_{fg} = 502 \ Btu/lb_m$$

The heat transfer rate can be calculated from Eq. (5-2) with the condensate mass flow rate given by:

$$\dot{m}_c = F_c \rho_c , \tag{A-1}$$

so that

$$Q_c = F_c \rho_c h_{fg} \tag{A-2}$$

$$= (0.03114 \ gpm)(37.6 \ lb_m/ft^3)(502 \ Btu/lb_m)(1 \ ft^3/7.481 \ gal)(60 \ min/hr)$$

$$= 4710 \ Btu/hr .$$

The heat transfer rate also can be computed from the primary cooling water and is given by Eq. (5-3) where

$$\dot{m}_w = F_w \rho_w ; \tag{A-3}$$

and therefore,

$$Q_w = F_w \rho_w c_{pw} \Delta T_w , \tag{A-4}$$

where c_{pw} and ρ_w are the heat capacity and density of the primary cooling water, respectively. These values are calculated at the average temperature of the primary cooling water. In this particular example, the change in temperature is so small that the variation in properties is insignificant. The properties for water in this range (~75°F) is a density (ρ_w) of 62.2 lb_m/ft^3 and a heat capacity (c_{pw}) of 1.0 $Btu/lb_m \cdot °F$. With the information for Run 717-051E,

$$Q_w = (33.4 \ gpm)(62.2 \ lb_m/ft^3)(1.0 \ Btu/lb_m \cdot °F)(0.284°F)(1 \ ft^3/7.481 \ gal)$$
$$(60 \ min/hr) = 4730 \ Btu/hr .$$

The percent difference between the two heat loads is given by:

$$(\Delta Q/Q) \times 100 = (Q_w - Q_c)/Q_c \times 100 \qquad \text{(A-5)}$$

$$= (4730 - 4710)/4710 \times 100$$

$$= 0.4 \ .$$

The heat balance obtained by the two different methods thus agreed within acceptable limits.

The overall condensing coefficient can be computed from Eq. (5-5) with either Q_c or Q_w. However, since the heat rate from the condensate flow (Q_c) is considered the more accurate of the two, it is used in the calculation. The mean temperature difference ($\overline{\Delta T}$) is given by Eq. (5-4):

$$\overline{\Delta T} = T_v - (T_{w,in} + T_{w,out})/2 \ , \qquad \text{(5-4)}$$

and for Run 717-051E,

$$\overline{\Delta T} = 77.16 - (75.27 + 75.62)/2 = 1.71°F \ .$$

The outside surface area (A_o) of Tube E is listed in Table 3-1 (p. 20). Applying Eq. (5-5) and using the data for Run 717-051E,

$$U_o = \frac{Q}{A_o \ \overline{\Delta T}} = \frac{4710 \text{ Btu/hr}}{(1.60 \text{ ft}^2)(1.71°F)} = 1720 \text{ Btu/hr}\cdot\text{ft}^2\cdot°F \ . \qquad \text{(5-5)}$$

The same calculations illustrated for Run 717-051E can be carried out for the other five runs in Table A-1. The results of the calculations for all six runs are shown in Table A-2. The six heat rates can be averaged to obtain a mean heat load for the series of runs, so that

$$Q_{c,avg} = 4700 \text{ Btu/hr} \ ,$$

$$Q_{w,avg} = 4800 \text{ Btu/hr} \ .$$

Water velocities (v) are calculated from the volume flows of water (F_w) and the cross-sectional area of the annulus (A_c):

Table A-2. Sample information for the Wilson plot — ammonia condensing on Tube E

Run No.	Condenser heat load: Q_c,[a] Btu/hr	Condenser heat load: Q_w,[b] Btu/hr	Condenser heat load: $(\Delta Q/Q) \times 100$	Condenser mean temp. diff., $\overline{\Delta T}$, °F	Primary cooling water velocity, v, ft/sec	$(1/v)^{0.8}$	Overall coefficient, U_o, Btu/hr·ft^2·°F	$1/U_o$
717-051E	4710	4730	0.4	1.71	26.9	7.18×10^{-2}	1720	5.81×10^{-4}
717-052E	4700	5030	7.0	2.47	14.3	1.19×10^{-1}	1190	8.40×10^{-4}
717-053E	4660	4810	3.3	3.69	7.70	1.95×10^{-1}	790	1.27×10^{-3}
717-054E	4660	4740	1.7	4.30	6.20	2.32×10^{-1}	670	1.49×10^{-3}
717-055E	4590	4650	1.3	5.80	4.11	3.23×10^{-1}	490	2.04×10^{-3}
717-056E	4640	4690	1.1	6.30	3.75	3.47×10^{-1}	460	2.17×10^{-3}

[a]Calculated from condensate flow of ammonia.

[b]Calculated from temperature rise and flow of the primary cooling water.

$$v = F_w/A_c \ , \qquad \text{(A-6)}$$

and A_c is given by:

$$A_c = \pi D_i^2/4 - \pi D_r^2/4 \ , \qquad \text{(A-7)}$$

where D_i is the inside diameter of the test tube and D_r is the outside diameter of the solid rod inserted through the test tube (D_r = 0.5 in.). From Table 3-1 (p.20) for Tube E, D_i = 0.87 in. so that

$$A_c = \pi(0.87/12 \text{ ft})^2/4 - \pi(0.50/12 \text{ ft})^2/4 = 0.00276 \text{ ft}^2$$

and from Run 717-051E,

$$v = (33.4 \text{ gpm})\left(\frac{1 \text{ ft}^3}{7.481 \text{ gal}}\right)\left(\frac{1 \text{ min}}{60 \text{ sec}}\right)\Big/ 0.00276 \text{ ft}^2 = 26.9 \text{ ft/sec} \ .$$

To generate the Wilson plot, it is necessary to take the reciprocal of the overall coefficient and to raise the water velocity to the negative 0.8 power. These values are shown in Table A-2 and were used to construct the Wilson plot shown in Fig. A-1. The data points shown in Fig. A-1 were fitted by a least-squares method of the first order to determine the best linear fit to satisfy the following relationship:

$$1/U_o = a_o + a_1 \ v^{-0.8} \ , \qquad \text{(5-9)}$$

where a_1 is the slope of the straight line and a_o is the y-intercept. For this particular run series,

$$a_o = 1.51 \times 10^{-4} \ ,$$

$$a_1 = 5.81 \times 10^{-3} \ .$$

As indicated in Fig. A-1, the data show good linearity and allow extrapolation to infinite water velocity (zero water-side resistance)with some confidence. The reciprocal ($1/a_o$ or h*) gives the composite heat transfer coefficient of the condensing film and wall. For the series of Runs

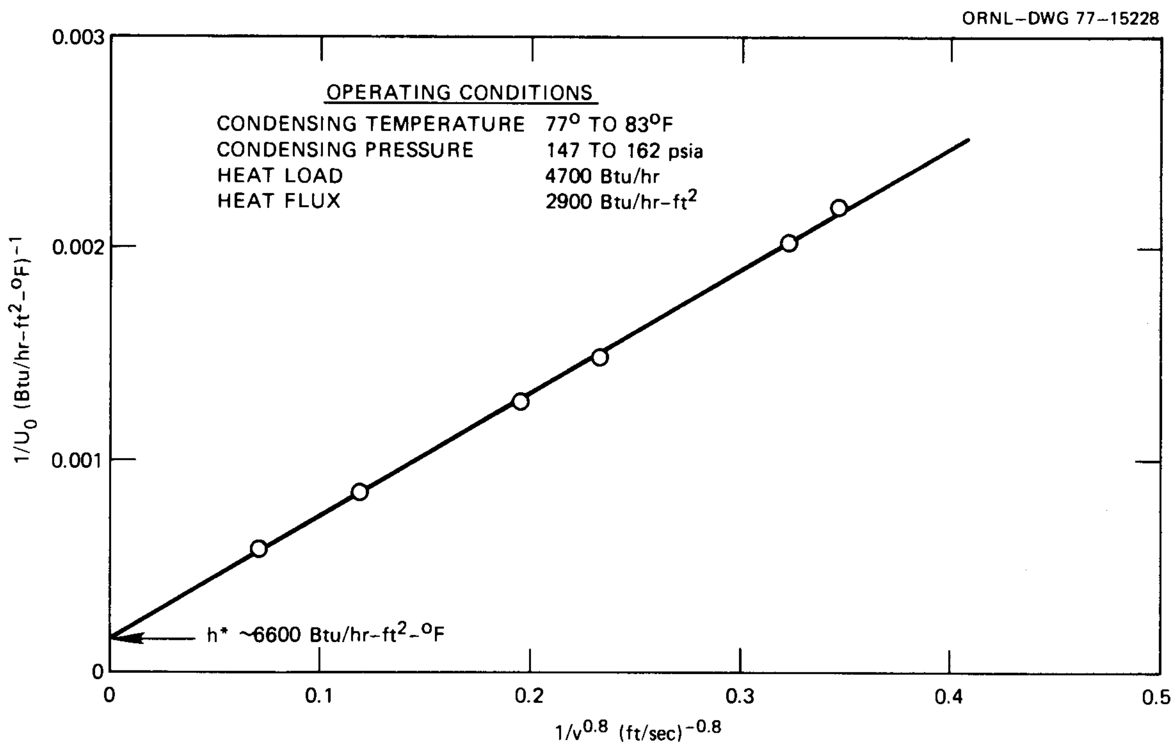

Fig. A-1. Wilson plot for ammonia condensing on Tube E (60 square ridges) — Runs 717-051E to 717-056E.

717-051E through 717-056E, the composite coefficient is 6600 Btu/hr·ft^2·°F as shown in Fig. A-1. The corresponding composite temperature difference is given by Eq. (5-14):

$$\Delta T^* = \frac{Q}{h^* A_o} = \frac{4700 \text{ Btu/hr}}{(6600 \text{ Btu/hr}\cdot\text{ft}^2\cdot°\text{F})(1.60 \text{ ft}^2)} = 0.4°\text{F} \ . \qquad (5.14)$$

Smooth Tube

A Wilson plot for the series of Runs 717-074A through 717-084A is shown in Fig. A-2. The data are for ammonia condensing on Tube A (smooth tube). The composite condensing heat transfer coefficient (h*) is 1300 Btu/hr·ft^2·°F, and the corresponding composite temperature difference

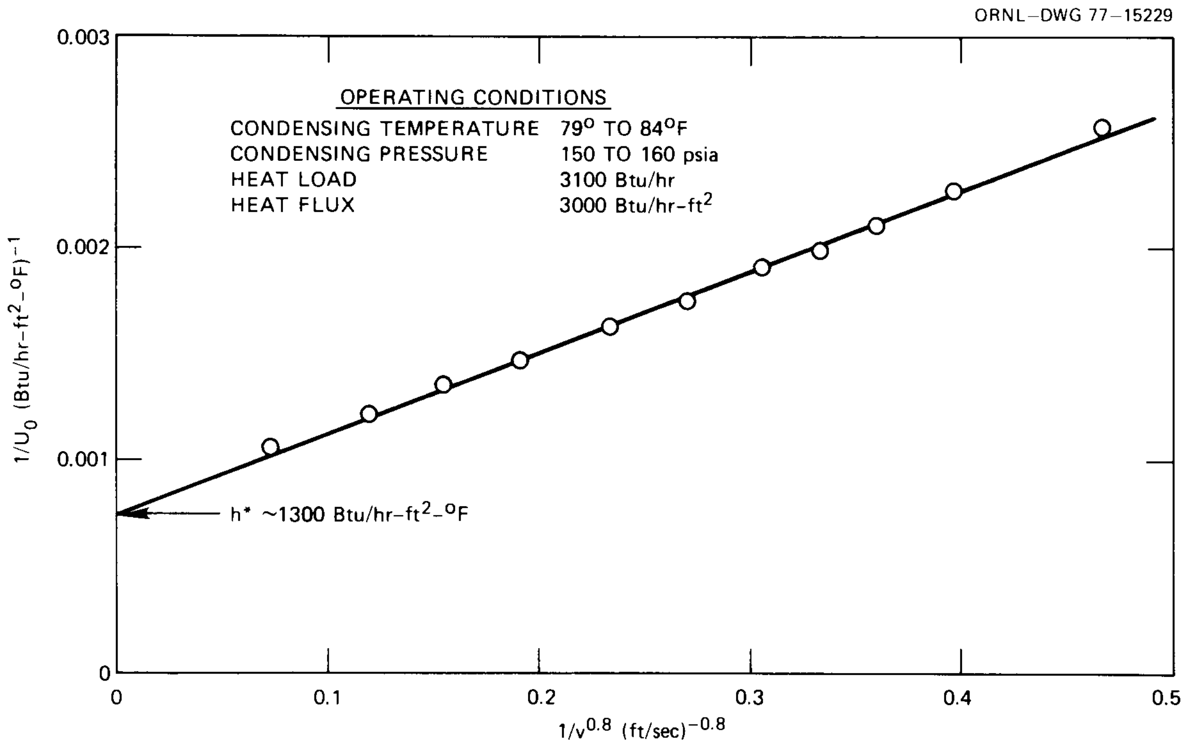

Fig. A-2. Wilson plot for ammonia condensing on Tube A (smooth tube) — Runs 717-074A to 717-084A.

($\Delta T^* = 2.2°F$) can be calculated from Eq. (5-14). The individual condensing-side coefficient can be computed by solving for h_v in Eq. (5-11):

$$h_v = \frac{1}{1/h^* - R_{wall}} , \tag{A-8}$$

where R_{wall} is given by Eq. (5-8) for Tube A:

$$R_{wall} = r_o \ln (r_o/r_i)/k . \tag{5-8}$$

The variables for Tube A are

$$r_o = 0.500 \text{ in.},$$

$$r_i = 0.435 \text{ in.},$$

$$k = 99 \text{ Btu/hr·ft·°F} ,$$

so that

$$R_w = [0.500 \text{ in. } (1 \text{ ft}/12 \text{ in.})] \ln(0.50/0.435)/(99 \text{ Btu/hr}\cdot\text{ft}\cdot{}^\circ\text{F})$$

$$= 5.9 \times 10^{-5} \ (\text{Btu/hr}\cdot\text{ft}^2\cdot{}^\circ\text{F})^{-1} \ .$$

From Fig. A-2, the y-intercept ($1/h^*$) is equal to 7.5×10^{-4}, and from Eq. (A-8):

$$h_v = \frac{1}{7.5 \times 10^{-4} - 5.9 \times 10^{-5}} = 1400 \text{ Btu/hr}\cdot\text{ft}^2\cdot{}^\circ\text{F} \ .$$

Nondimensional Quantities

The vapor-side heat transfer coefficient (h_v) is usually considered equal to the condensing film coefficient since the dominant resistance lies in the condensate film. Therefore, the condensing film heat transfer coefficient can be put into the standard nondimensional form given by Eq. (6-1):

$$H = h_v/(k^3\rho^2 g/\mu^2)^{1/3} \ , \qquad (6\text{-}1)$$

where all fluid properties are evaluated at the equivalent film temperature (T_f) as pointed out by McAdams[6] where

$$T_f = T_v - \frac{3}{4}(T_v - T_{wall}) \ , \qquad (A\text{-}9)$$

and T_{wall} is the outside wall temperature. The temperature of the vapor for the purpose of evaluating film temperatures was chosen as the lowest vapor temperature for the series of runs for a given Wilson plot. For Runs 717-074A through 717-084A, the vapor temperature was taken as 79°F (see Appendix B, Table B-1) for evaluation of the nondimensional coefficient. The temperature difference across the condensing film (ΔT_f) is given by:

$$\Delta T_f = T_v - T_{wall} = \frac{Q}{h_v\ A_o} . \tag{A-10}$$

For Runs 717-074A through 717-084A,

$$\Delta T_f = (T_v - T_{wall}) = \frac{(3100\ \text{Btu/hr})}{(1400\ \text{Btu/hr}\cdot\text{ft}^2\cdot{}^\circ\text{F})(1.05\ \text{ft}^2)} = 2.0^\circ\text{F} ,$$

so that

$$T_f = 79^\circ\text{F} - \frac{3}{4}(2.0^\circ\text{F}) = 77^\circ\text{F} .$$

Evaluating the fluid properties at the film temperature of 77°F,

$$k = 0.279\ \text{Btu/hr}\cdot\text{ft}\cdot{}^\circ\text{F} ,$$

$$\rho = 37.7\ \text{Btu/lb}_m ,$$

$$\mu = 0.350\ \text{lb}_m\text{/hr}\cdot\text{ft} ,$$

and

$$g = 4.17 \times 10^8\ \text{ft/hr}^2 ,$$

so that for $h_v = 1400$ Btu/hr·ft²·°F,

$$H = 1400/[(0.279)^3(37.7)^2(4.17 \times 10^8)/(0.350)^2]^{1/3} = 0.30 .$$

The liquid film Reynolds number is given by Eq. (6.2):

$$Re = 4(\Gamma/\mu) , \tag{6.2}$$

where Γ is the mass flow of condensate per unit length of perimeter on the tube. The mass flow per unit of perimeter can be computed from the heat load, latent heat of ammonia, and the perimeter of the tube:

$$\Gamma = \frac{Q}{h_{fg}\ P_t} , \tag{A-11}$$

where P_t is the outside perimeter of the tube (see Table 3-1, p. 20). The latent heat of ammonia is evaluated at the same vapor temperature as discussed for Eq. (A-9). For the series of Runs 717-074A through 717-084A,

$$\Gamma = \frac{(3100 \text{ Btu/hr})}{(500 \text{ Btu/lb}_m)(3.14 \text{ in.})(1 \text{ ft/12 in.})} = 23.7 \text{ lb}_m\text{/hr}\cdot\text{ft} ,$$

so that

$$\text{Re} = \frac{4\Gamma}{\mu} = \frac{4(23.7 \text{ lb}_m\text{/hr}\cdot\text{ft})}{(0.350 \text{ lb}_m\text{/hr}\cdot\text{ft})} = 270 .$$

The nondimensional heat transfer coefficients and liquid film Reynolds numbers were used to construct Figs. 6-2 (p. 44) and 6-3 (p. 46).

The nondimensional quantities (H and Re) were not found to be very sensitive to the temperature at which the properties were evaluated; therefore, the variation in vapor temperatures during a series of runs should not have affected the heat transfer results significantly. For Tube A, the vapor temperature variation ranged from 2 to 17°F for a given series of runs (a set heat load).

Water-Side Correlations

The water-side heat transfer coefficient can be estimated from Eqs. (5.17), (5.18), and (5.19). For example, Eq. (5.17) can be put in the following form:

$$h = 0.023 \, (k_b/D)(GD/\mu_b)^{0.8} \, (\mu c_p/k)_b^{0.4} , \qquad \text{(A-12)}$$

where D is taken as the hydraulic diameter (D_H) of the annulus given by:

$$D_H = D_i - D_r , \qquad \text{(A-13)}$$

so that for Tube E

$$D_H = 0.87 \text{ in.} - 0.50 \text{ in.} = 0.37 \text{ in.}$$

G is the mass flow rate per unit area of water given by:

$$G = \rho_w V \quad , \tag{A-14}$$

and for Run 717-051E at a bulk temperature of ~75°F,

$$G = (62.2\ lb_m/ft^3)(26.9\ ft/sec)(3600\ sec/hr)$$
$$= 6.02 \times 10^6\ lb_m/hr \cdot ft \ .$$

Evaluating the properties of water at 75°F,

$$k_b = 0.354\ Btu/hr \cdot ft \cdot {}^\circ F \ ,$$

$$\mu_b = 2.22\ lb_m/hr \cdot ft \ ,$$

$$c_p = 1.00\ Btu/lb_m \cdot {}^\circ F \ ,$$

so that

$$h = 0.023 \left(\frac{0.354}{0.37/12} \right) \left[\frac{(6.02 \times 10^6)(0.37/12)}{2.22} \right]^{0.8} \left[\frac{(2.22)(1.00)}{(0.354)} \right]^{0.4}$$

(McAdams) $h = 4800\ Btu/hr \cdot ft^2 \cdot {}^\circ F$.

Similar calculations with Eqs. (5-16) and (5-17) yield

(Colburn) $h = 4200\ Btu/hr \cdot ft^2 \cdot {}^\circ F$,

and

(Sieder and Tate) $h = 5000\ Btu/hr \cdot ft^2 \cdot {}^\circ F$.

Equation (5.20) can be used to calculate the composite condensing coefficient:

$$h^* = \frac{1}{(1/U_o) - (A_o/h_w A_i)} \ . \tag{5-20}$$

For Tube E, the ratio A_o/A_i can be calculated from Table 3-1 and is found to be 1.84. For Run 717-051E,

(McAdams) $h^* = \dfrac{1}{(1/1720) - 1.84/(4800)} = 5000\ Btu/hr \cdot ft^2 \cdot {}^\circ F$.

This compares with 6600 Btu/hr·ft^2·°F from the Wilson plot for the series of Runs 717-051E through 056E. Similar calculations can be done using results from Eqs. (5.18) and (5.19). The results from Eq. (5.20) are compared with the Wilson-plot results in Appendix C.

APPENDIX B

WILSON-PLOT RESULTS

Tables B-1 through B-5 summarize the experimental conditions for all series of runs used to construct Wilson plots. The results from the Wilson plots are also listed. The condenser heat load was taken as the average heat load based on the condensate flow ($Q_{c,avg}$) for a series of runs (see Appendix A for an example). Individual runs are documented in detail in Appendix D.

Table B-1. Summary of experimental conditions and results from Wilson plots for ammonia condensing on Tube A (smooth tube)

Series of runs	Condenser heat load		Condensing temperature range		Condensing heat transfer coefficient, h^*		Condensing temperature difference, ΔT^*	
	W	(Btu/hr)	K	(°F)	$W/m^2 \cdot K$	$(Btu/hr \cdot ft^2 \cdot °F)$	K	(°F)
717-001A to 004A	3800	(13100)	302–309	(84–96)	5200	(920)	7.5	(13.5)
717-005A to 007A	2400	(8200)	296–301	(74-82)	5500	(970)	4.5	(8.1)
717-009A to 011A	2800	(9600)	299–303	(78–86)	4800	(850)	6.0	(10.9)
717-013A to 015A	3200	(10800)	300–306	(80–90)	5200	(910)	6.3	(11.4)
717-017A to 019A	3800	(12900)	302–309	(83–97)	5200	(920)	7.5	(13.5)
717-021A to 023A	2900	(9800)	299–303	(78-87)	5100	(890)	5.9	(10.6)
717-025A to 029A	2800	(9500)	299–306	(78-90)	5500	(960)	5.2	(9.4)
717-030A to 033A	3500	(11900)	300–309	(81–96)	5000	(880)	7.2	(13.0)
717-034A to 037A	1600	(5400)	296–300	(72–80)	6300	(1100)	2.6	(4.6)
717-038A to 041A	1050	(3600)	296–299	(74–78)	6800	(1200)	1.6	(2.8)
717-042A to 045A	1000	(3500)	296–299	(74–78)	6800	(1200)	1.6	(2.8)
717-046A to 050A	800	(2800)	294–296	(70–74)	7700	(1350)	1.1	(2.0)
717-051A to 055A	800	(2800)	293–296	(69–72)	7900	(1400)	1.1	(2.0)
717-056A to 059A	1700	(5700)	295–300	(72–80)	6300	(1100)	2.8	(5.1)
717-060A to 063A	1400	(4700)	295–299	(71–78)	6800	(1200)	2.1	(3.8)
717-064A to 073A	1400	(4800)	295–298	(71–77)	6300	(1100)	2.3	(4.1)
717-074A to 084A	900	(3100)	299–302	(79–84)	7400	(1300)	1.2	(2.2)
717-085A to 088A	560	(1900)	298–299	(77–79)	7900	(1400)	0.7	(1.3)

Table B-1 (Continued)

Series of runs	Condenser heat load		Condensing temperature range		Condensing heat transfer coefficient, h*		Condensing temperature difference, ΔT*	
	W	(Btu/hr)	K	(°F)	$W/m^2 \cdot K$	$(Btu/hr \cdot ft^2 \cdot °F)$	K	(°F)
717-089A to 092A	500	(1700)	298–299	(76–78)	7900	(1400)	0.7	(1.2)
717-098A to 102A	500	(1700)	298–300	(77–80)	7700	(1350)	0.7	(1.2)
717-103A to 106A	3950	(13500)	300–310	(81–99)	4600	(800)	8.9	(16.0)
717-107A to 110A	5000	(17100)	305–313	(89–104)	4100	(720)	12.6	(22.7)
717-111A to 114A	4200	(14200)	306–313	(91–103)	4200	(740)	10.2	(18.3)
717-119A to 122A	3300	(11100)	300–308	(81–95)	5100	(890)	6.6	(12.0)
717-123A to 126A	2000	(6800)	301–306	(83–90)	5400	(940)	3.8	(6.9)
717-127A to 130A	2900	(9900)	300–308	(80–94)	5050	(890)	5.9	(10.6)
717-131A to 134A	2000	(6900)	299–304	(78–87)	5700	(1000)	3.6	(6.6)
717-135A to 138A	4300	(14800)	305–316	(89–109)	4600	(810)	9.7	(17.4)
717-139A to 142A	760	(2600)	302–304	(83–88)	7100	(1250)	1.1	(2.0)
717-143A to 145A	1400	(4800)	304–306	(87–91)	5600	(990)	2.6	(4.7)
717-146A to 149A	1100	(3700)	302–305	(84–89)	6300	(1100)	1.8	(3.2)
717-150A to 153A	1700	(5700)	304–309	(88–96)	5700	(1000)	3.0	(5.4)

Table B-2. Summary of experimental conditions and results from Wilson plots for ammonia condensing on Tube E (60 square ridges)

Series of runs	Condenser heat load		Condensing temperature range		Condensing heat transfer coefficient, h^*		Condensing temperature difference, ΔT^*	
	W	(Btu/hr)	K	(°F)	$W/m^2 \cdot K$	$(Btu/hr \cdot ft^2 \cdot °F)$	K	(°F)
717-009E to 016E	3300	(11300)	297–306	(76–92)	27,000	(4700)	0.8	(1.5)
717-017E to 024E	5000	(16900)	300–313	(81–104)	21,000	(3700)	1.6	(2.8)
717-025E to 031E	4200	(14400)	298–310	(77–98)	24,000	(4300)	1.1	(2.1)
717-032E to 038E	2400	(8100)	296–302	(73–84)	32,000	(5700)	0.5	(0.9)
717-039E to 045E	2050	(7000)	296–302	(73–84)	34,000	(5900)	0.4	(0.7)
717-046E to 050E	1700	(5800)	296–301	(73–82)	30,000	(5300)	0.4	(0.7)
717-051E to 056E	1400	(4700)	298–301	(77–83)	37,000	(6600)	0.2	(0.4)
717-057E to 062E	1000	(3500)	298–301	(76–82)	41,000	(7200)	0.2	(0.3)
717-063E to 068E	1700	(5700)	298–302	(77–84)	36,000	(6300)	0.3	(0.6)
717-069E to 074E	2900	(9900)	299-307	(78–92)	27,000	(4800)	0.7	(1.3)
717-075E to 081E	3800	(12800)	301–310	(82–99)	26,000	(4600)	1.0	(1.8)
717-082E to 086E	2900	(9900)	299–307	(79–92)	29,000	(5100)	0.7	(1.2)
717-087E to 093E	4300	(14600)	302–313	(83–104)	18,000	(3100)	1.6	(2.9)
717-094E to 099E	2700	(9200)	300–307	(80–93)	29,000	(5100)	0.6	(1.1)
717-100E to 106E	4400	(15100)	303–314	(85–105)	17,000	(3000)	1.8	(3.2)

Table B-3. Summary of experimental conditions and results from Wilson plots for ammonia condensing on Tube F (48 corrugations)

Series of runs	Condenser heat load		Condensing temperature range		Condensing heat transfer coefficient, h*		Condensing temperature difference, ΔT*	
	W	(Btu/hr)	K	(°F)	$W/m^2 \cdot K$	$(Btu/hr \cdot ft^2 \cdot °F)$	K	(°F)
717-001F to 006F	2400	(8300)	300–307	(80–92)	36,000	(6300)	0.7	(1.3)
717-007F to 011F	1000	(3500)	298–302	(77–83)	55,000	(9600)	0.2	(0.4)
717-012F to 018F	4800	(14400)	303–315	(85–107)	22,000	(3900)	2.3	(4.0)
717-024F to 029F	1700	(5800)	299–304	(79–87)	41,000	(7200)	0.4	(0.8)
717-030F to 035F	3300	(11200)	301–309	(82–97)	30,000	(5300)	1.1	(2.0)
717-042F to 047F	1400	(4700)	304–308	(88–95)	39,000	(6900)	0.4	(0.7)
717-048F to 053F	2000	(6900)	304–309	(87–97)	34,000	(6000)	0.6	(1.1)
717-054F to 059F	2900	(9800)	304–312	(87–101)	31,000	(5400)	1.0	(1.7)
716-060F to 065F	3700	(12700)	303–313	(86–104)	25,000	(4400)	1.5	(2.8)
717-066F to 071F	1800	(6200)	303–307	(85–93)	40,000	(7100)	0.5	(0.8)
717-072F to 078F	4200	(14400)	304–315	(88–107)	23,000	(4100)	1.9	(3.4)
717-079F to 084F	1200	(4100)	303–306	(86–91)	47,000	(8200)	0.3	(0.5)
717-085F to 090F	2200	(7500)	304–309	(87–97)	35,000	(6200)	0.7	(1.2)
717-091F to 096F	2700	(9200)	304–311	(87–100)	31,000	(5500)	0.9	(1.6)
717-097F to 102F	1500	(5100)	302–307	(84–92)	38,000	(6700)	0.4	(0.7)
717-103F to 108F	2000	(6900)	304–309	(88–97)	35,000	(6100)	0.6	(1.1)

Table B-4. Summary of experimental conditions and results from Wilson plots for ammonia condensing on Tube F-1 (48 corrugations with 1 skirt)

Series of runs	Condenser heat load		Condensing temperature range		Condensing heat transfer coefficient, h*		Condensing temperature difference, ΔT*	
	W	(Btu/hr)	K	(°F)	$W/m^2 \cdot K$	$(Btu/hr \cdot ft^2 \cdot °F)$	K	(°F)
717-019F1 to 024F1	1600	(5600)	301–306	(83–91)	39,000	(6800)	0.4	(0.8)
717-025F1 to 030F1	2400	(8300)	303–309	(85–97)	36,000	(6300)	0.7	(1.3)
717-031F1 to 036F1	3200	(11000)	304–313	(87–103)	30,000	(5300)	1.1	(2.0)
717-037F1 to 042F1	1050	(3600)	301–304	(82–87)	48,000	(8500)	0.2	(0.4)
717-043F1 to 048F1	4200	(14300)	304–315	(88–108)	27,000	(4700)	1.6	(2.9)
717-049F1 to 054F1	1300	(4500)	304–308	(87–94)	40,000	(7000)	0.3	(0.6)
717-055F1 to 059F1	4500	(15300)	306–315	(91–108)	24,000	(4200)	1.9	(3.5)
717-060F1 to 063F1	2050	(7000)	303–306	(85–91)	30,000	(5200)	0.7	(1.3)
717-064F1 to 069F1	2300	(8000)	302–309	(84–96)	30,000	(5200)	0.8	(1.5)
717-070F1 to 075F1	2300	(7900)	303–309	(86–97)	31,000	(5500)	0.8	(1.4)
717-076F1 to 081F1	1600	(5500)	306–310	(91–98)	37,000	(6600)	0.4	(0.8)
717-082F1 to 087F1	3700	(12500)	305–315	(90–107)	26,000	(4600)	1.4	(2.6)
717-088F1 to 093F1	1600	(5600)	302–307	(84–93)	40,000	(7000)	0.4	(0.8)
717-094F1 to 098F1	3000	(10100)	304–309	(87–97)	27,000	(4800)	1.2	(2.1)
717-105F1 to 110F1	2600	(8800)	305–313	(90–103)	31,000	(5500)	0.8	(1.5)
717-111F1 to 116F1	1800	(6100)	304–308	(87–95)	34,000	(6000)	0.6	(1.0)

Table B-5. Summary of experimental conditions and results from Wilson plots for ammonia condensing on Tube G (24 corrugations)

Series of runs	Condenser heat load		Condensing temperature range		Condensing heat transfer coefficient, h*		Condensing temperature difference, ΔT*	
	W	(Btu/hr)	K	(°F)	$W/m^2 \cdot K$	$(Btu/hr \cdot ft^2 \cdot °F)$	K	(°F)
717-001G to 006G	2400	(8200)	304–310	(87–99)	23,000	(4000)	0.9	(1.7)
717-007G to 010G	1600	(5500)	303–308	(85–94)	32,000	(5600)	0.4	(0.8)
717-011G to 016G	1050	(3600)	303–307	(85–92)	31,000	(5400)	0.3	(0.5)
717-017G to 022G	3300	(11200)	306–315	(91–108)	20,000	(3600)	1.4	(2.5)
717-023G to 028G	4200	(14500)	303–316	(86–109)	19,000	(3300)	2.0	(3.6)
717-029G to 034G	1400	(4700)	302–306	(83–91)	32,000	(5600)	0.4	(0.7)
717-035G to 040G	2100	(7100)	303–310	(86–98)	26,000	(4600)	0.7	(1.3)
717-041G to 046G	1500	(5000)	307–310	(92–99)	31,000	(5500)	0.4	(0.7)
717-047G to 051G	5100	(17400)	302–316	(84–109)	18,000	(3200)	2.5	(4.4)
717-052G to 057G	1800	(6100)	305–310	(89–98)	28,000	(5000)	0.6	(1.0)
717-058G to 063G	2900	(9800)	304–312	(87–102)	23,000	(4000)	1.1	(2.0)
717-064G to 069G	1000	(3500)	303–307	(86–92)	36,000	(6300)	0.3	(0.5)
717-070G to 075G	3700	(12800)	304–314	(87–106)	20,000	(3600)	1.6	(2.9)

APPENDIX C

COMPARISON OF RESULTS FROM WATER-SIDE CORRELATIONS AND WILSON PLOTS

The results from the water-side correlations are compared with the Wilson-plot coefficients in Tables C-1 through C-3 for the test tubes with smooth inside surfaces (Tubes A, E, and F). The correlations of McAdams, Colburn, and Sieder and Tate were used to generate the water-side coefficients. Then, the composite condensing coefficients were estimated from Eq. (5.20) as outlined in Appendix A. The runs listed in Tables C-1 through C-3 represent the highest water velocity for a given series of runs. The highest water velocity was chosen since the sensitivity of Eq. (5.20) is much lower to the predicted coefficients at high water velocities (higher water-side coefficients).

Table C-1. Comparison of condensing coefficients from water-side correlations and the Wilson plot — ammonia condensing on Tube A (smooth tube)

Run No.	Estimated composite condensing coefficient, Btu/hr•ft^2•°F			Composite condensing coefficient from Wilson plot, Btu/hr•ft^2•°F	Percent difference based on the Wilson-plot coefficient		
	McAdams	Colburn	Sieder & Tate		McAdams	Colburn	Sieder & Tate
717-001A	920	960	920	920	0	4.4	0
717-005A	970	1000	960	970	0	3.1	−1.0
717-009A	850	880	850	850	0	3.5	0
717-013A	900	930	900	910	−1.1	2.2	−1.1
717-017A	900	930	890	920	−2.2	1.1	−3.3
717-021A	890	920	890	890	0	3.4	0
717-025A	930	960	920	960	−3.1	0	−4.2
717-030A	860	880	850	880	−2.3	0	−3.4
717-034A	1070	1120	1070	1100	−2.7	1.8	−2.7
717-038A	1180	1230	1160	1200	−1.7	2.5	−3.3
717-042A	1140	1190	1130	1200	−5.0	−0.8	−5.8
717-046A	1300	1370	1290	1350	−3.7	1.5	−4.4
717-051A	1310	1380	1300	1400	−6.4	−1.4	−7.1
717-056A	1020	1060	1020	1100	−7.3	−3.6	−7.3
717-060A	1120	1170	1110	1200	−6.7	−2.5	−7.5
717-064A	1060	1110	1050	1100	−3.6	0.9	−4.6
717-074A	1220	1270	1210	1300	−6.2	−2.3	−6.9
717-085A	1260	1310	1240	1400	−10.0	−6.4	−11.4

Table C-1 (Continued)

Run No.	Estimated composite condensing coefficient, Btu/hr·ft^2·°F			Composite condensing coefficient from Wilson plot, Btu/hr·ft^2·°F	Percent difference based on the Wilson-plot coefficient		
	McAdams	Colburn	Sieder & Tate		McAdams	Colburn	Sieder & Tate
717-089A	1270	1320	1250	1400	–9.3	–5.7	–10.7
717-100A	1240	1300	1230	1350	–8.2	–3.9	–8.9
717-103A	780	810	780	800	–2.5	1.3	–2.5
717-108A	750	770	740	720	4.2	6.9	2.8
717-111A	740	760	740	740	0	2.7	0
717-119A	860	890	860	890	–3.4	0	–3.4
717-123A	900	930	900	940	–4.3	–1.1	–4.3
717-127A	860	890	850	890	–3.4	0	–4.5
717-131A	940	970	930	1000	–6.0	–3.0	–7.0
717-135A	790	810	790	810	–2.5	0	–2.5
717-139A	1180	1220	1160	1250	–5.6	–2.4	–7.2
717-143A	970	1000	960	990	–2.0	1.0	–3.0
717-146A	1060	1100	1050	1100	–3.6	0	–4.6
716-150A	980	1010	970	1000	–2.0	1.0	–3.0

Table C-2. Comparison of condensing coefficients from water-side correlations and the Wilson plot — ammonia condensing on Tube E (60 square ridges)

Run No.	Estimated composite condensing coefficient, Btu/hr·ft²·°F			Composite condensing coefficient from Wilson plot, Btu/hr·ft²·°F	Percent difference based on the Wilson-plot coefficient		
	McAdams	Colburn	Sieder & Tate		McAdams	Colburn	Sieder & Tate
717-009E	3400	4100	3300	4700	–27.7	–12.8	–29.8
717-017E	3200	3800	3100	3700	–13.5	2.7	–16.2
717-025E	3500	4300	3300	4300	–18.6	0	–23.3
717-032E	4100	5200	3900	5700	–28.1	–8.8	–31.6
717-039E	3900	4900	3700	5900	–33.9	–17.0	–37.3
717-046E	3900	5000	3700	5300	–26.4	–6.0	–30.2
717-051E	5000	6800	4700	6600	–24.2	3.0	–28.8
717-057E	4800	6400	4500	7200	–33.3	–11.1	–37.5
717-063E	4400	5700	4200	6300	–30.2	–10.5	–33.3
717-069E	3500	4300	3400	4800	–27.1	–11.6	–29.2
717-075E	3500	4200	3300	4600	–23.9	–8.7	–28.3
717-082E	4100	5100	3800	5100	–19.6	0	–25.5
717-087E	2900	3400	2800	3100	– 6.5	9.7	– 9.7
717-094E	4100	5100	3800	5100	–19.6	0	–25.5
717-100E	2600	3000	2500	3000	–13.3	0	–16.7

Table C-3. Comparison of condensing coefficients from water-side correlations and the Wilson plot — ammonia condensing on Tube F (48 corrugations)

Run No.	Estimated composite condensing coefficient, Btu/hr•ft^2•°F			Composite condensing coefficient from Wilson plot, Btu/hr•ft^2•°F	Percent difference based on the Wilson-plot coefficient		
	McAdams	Colburn	Sieder & Tate		McAdams	Colburn	Sieder & Tate
717-001F	5400	6700	5200	6300	−14.3	6.4	−17.5
717-007F	7100	9300	6600	9600	−26.0	−3.1	−31.3
717-012F	3600	4100	3400	3900	− 7.7	5.1	−12.8
717-024F	6300	8000	6000	7200	−12.5	11.1	−16.7
717-030F	4600	5400	4400	5300	−13.2	1.9	−20.8
717-042F	6300	7700	5900	6900	− 8.7	11.6	−14.5
717-048F	5200	6200	4900	6000	−13.3	3.3	−18.3
717-054F	4900	5800	4600	5400	− 9.3	7.4	−14.8
717-060F	4000	4600	3900	4400	−10.0	4.6	−11.4
717-066F	6000	7300	5600	7100	−15.5	2.8	−21.1
717-072F	3800	4300	3700	4100	− 7.3	4.9	− 9.8
717-079F	6900	8600	6400	8200	−15.9	4.9	−22.0
717-085F	5500	6500	5200	6200	−11.3	4.8	−16.1
717-091F	5000	5900	4800	5500	− 9.1	7.3	−12.7
717-097F	5900	7200	5500	6700	−11.9	6.9	−17.9
717-103F	5500	6600	5200	6100	− 9.8	8.2	−14.8

APPENDIX D

EXPERIMENTAL DATA

Tables D-1 through D-5 document 501 runs which yielded 92 data points or Wilson plots. The tables summarize the experimental data used in data reduction. In addition, the tables list saturation pressures and heat balance checks. Velocities are presented along with Reynolds number for the water flows. Also, overall heat transfer coefficients are tabulated. The information was generated by a computer code used for data reduction, and the runs are grouped in series corresponding to Wilson plots. Several series of runs were discarded because of problems with operation and/or instrumentation.

Table D-1. Experimental data for ammonia condensing on Tube A (smooth tube)

Run No.	T_v, °F	P, psia	P_{sat}, psia	F_c, gpm	T_c, °F	$\dot{m}_c$, lb_m/hr	F_w, gpm	v, ft/sec	Re	$T_{w,in}$, °F	$T_{w,out}$, °F	ΔT_w, °F	$\overline{\Delta T}$, °F	Q_c, Btu/hr	Q_w, Btu/hr	$\frac{\Delta Q}{Q}$ X 100	U_o, $\frac{Btu}{hr \cdot ft^2 \cdot °F}$
R-717-001A	84.42	165.7	164.8	0.0896	79.38	26.97	32.6	26.3	73894.	66.94	67.81	0.78	17.05	13323.	12739.	-4.4	746.
R-717-002A	91.89	186.7	186.3	0.0892	84.04	26.65	7.4	6.0	17056.	66.92	70.26	3.34	23.30	12962.	12335.	-4.8	531.
R-717-003A	95.87	197.7	198.5	0.0893	86.77	26.60	5.1	4.1	11901.	66.70	71.43	4.72	26.81	12824.	12088.	-5.7	457.
R-717-004A	89.10	178.7	178.0	0.0898	82.69	26.90	11.8	9.5	27139.	67.30	69.57	2.25	20.67	13162.	13254.	0.7	608.
R-717-005A	73.72	138.7	137.4	0.0540	72.76	16.41	32.6	26.3	69924.	63.13	63.73	0.51	10.23	8281.	8356.	0.9	769.
R-717-006A	78.73	150.7	149.8	0.0535	76.39	16.18	7.5	6.0	16343.	63.46	65.63	2.16	14.19	8085.	8102.	0.2	544.
R-717-007A	81.81	159.2	157.8	0.0540	78.51	16.26	5.2	4.2	11421.	63.56	66.65	3.09	16.71	8079.	8026.	-0.7	462.
R-717-009A	78.24	147.2	148.5	0.0653	76.17	19.74	32.6	26.3	71213.	64.38	65.06	0.60	13.52	9876.	9708.	-1.7	698.
R-717-010A	82.81	161.7	160.4	0.0644	80.09	19.38	7.4	6.0	16355.	64.04	66.67	2.62	17.45	9605.	9710.	1.1	526.
R-717-011A	85.75	169.2	168.5	0.0635	82.42	19.03	5.2	4.2	11525.	63.93	67.59	3.65	19.99	9375.	9484.	1.2	448.
R-717-013A	79.71	152.7	152.3	0.0729	78.05	21.98	32.6	26.3	71837.	64.96	65.72	0.68	14.37	10967.	11093.	1.1	729.
R-717-014A	85.65	169.2	168.2	0.0728	82.70	21.80	7.9	6.4	17680.	64.79	67.57	2.77	19.47	10744.	10992.	2.3	527.
R-717-015A	90.28	182.7	181.5	0.0742	86.95	22.09	5.2	4.2	11733.	64.98	69.11	4.13	23.24	10780.	10728.	-0.5	443.
R-717-017A	83.23	163.2	161.6	0.0881	81.04	26.44	32.6	26.3	72503.	65.54	66.46	0.83	17.23	13094.	13487.	3.0	726.
R-717-018A	87.79	175.2	174.2	0.0879	84.63	26.26	12.0	9.7	27077.	65.93	68.15	2.20	20.75	12881.	13221.	2.6	593.
R-717-019A	91.51	186.2	185.1	0.0882	87.70	26.24	7.9	6.4	18208.	66.50	69.76	3.26	23.38	12774.	12942.	1.3	522.
R-717-021A	77.92	147.7	147.7	0.0663	76.31	20.03	32.6	26.3	71146.	64.30	65.01	0.63	13.27	10027.	10181.	1.5	722.
R-717-022A	82.77	161.7	160.3	0.0653	79.96	19.62	7.7	6.2	16964.	64.04	66.61	2.56	17.44	9728.	9834.	1.1	533.
R-717-023A	86.53	172.2	170.7	0.0656	83.00	19.64	5.1	4.1	11394.	64.04	67.78	3.73	20.63	9663.	9569.	-1.0	447.
R-717-025A	78.02	148.7	148.0	0.0638	76.15	19.29	32.6	26.3	72141.	65.30	65.99	0.61	12.39	9658.	9920.	2.7	745.
R-717-026A	80.41	154.7	154.1	0.0636	78.17	19.17	13.8	11.1	30656.	65.18	66.65	1.45	14.50	9551.	10033.	5.0	629.
R-717-027A	83.29	162.7	161.7	0.0636	80.40	19.11	8.0	6.4	17889.	65.17	67.61	2.44	16.90	9466.	9757.	3.1	535.
R-717-028A	88.00	175.7	174.8	0.0638	84.17	19.07	4.7	3.8	10599.	64.98	69.02	4.02	21.00	9350.	9448.	1.0	425.
R-717-029A	90.27	182.7	181.4	0.0644	86.27	19.20	4.0	3.2	9061.	64.96	69.69	4.73	22.94	9369.	9448.	0.8	390.
R-717-030A	80.75	154.2	155.0	0.0806	78.27	24.30	32.5	26.2	70458.	63.75	64.61	0.77	16.57	12096.	12569.	3.9	697.
R-717-031A	86.42	169.7	170.3	0.0816	83.27	24.41	9.8	7.9	21704.	64.08	66.59	2.49	21.08	12010.	12280.	2.2	544.
R-717-032A	91.28	184.2	184.4	0.0816	87.51	24.26	5.4	4.4	12034.	63.26	67.72	4.45	25.79	11814.	12113.	2.5	438.
R-717-033A	96.04	199.7	199.0	0.0825	91.60	24.39	3.9	3.2	8760.	63.16	69.16	5.99	29.88	11752.	11760.	0.1	376.
R-717-034A	72.25	135.2	134.0	0.0350	71.22	10.64	32.6	26.3	72622.	65.91	66.33	0.33	6.13	5386.	5424.	0.7	840.
R-717-035A	74.69	140.7	139.8	0.0355	72.85	10.78	9.8	7.9	22013.	65.78	66.92	1.13	8.34	5431.	5571.	2.6	622.
R-717-036A	77.23	146.2	146.0	0.0358	74.72	10.84	5.4	4.4	12214.	65.53	67.58	2.04	10.68	5436.	5550.	2.1	486.
R-717-037A	79.92	153.7	152.8	0.0365	76.90	11.01	3.9	3.2	8873.	65.70	68.48	2.78	12.83	5490.	5453.	-0.7	409.
R-717-038A	73.86	138.7	137.8	0.0236	70.68	7.19	32.6	26.3	76619.	69.88	70.18	0.21	3.83	3630.	3356.	-7.6	905.
R-717-039A	75.47	142.2	141.7	0.0234	72.12	7.11	9.8	7.9	23210.	69.84	70.60	0.76	5.25	3577.	3745.	4.7	650.
R-717-040A	77.00	146.2	145.4	0.0234	73.09	7.12	5.4	4.4	12845.	69.55	70.92	1.36	6.76	3569.	3714.	4.1	504.
R-717-041A	78.20	148.7	148.4	0.0237	74.12	7.19	3.9	3.2	9251.	69.23	71.06	1.82	8.05	3596.	3582.	-0.4	427.
R-717-042A	73.95	138.7	138.0	0.0231	70.11	7.03	32.6	26.3	76717.	69.97	70.28	0.23	3.82	3546.	3698.	4.3	886.
R-717-043A	75.53	142.2	141.8	0.0227	71.47	6.91	9.8	7.9	23215.	69.85	70.63	0.77	5.29	3478.	3809.	9.5	628.
R-717-044A	77.00	146.2	145.4	0.0228	72.24	6.94	5.4	4.4	12839.	69.53	70.89	1.36	6.79	3478.	3695.	6.2	489.
R-717-045A	78.31	149.2	148.7	0.0231	73.39	7.00	3.9	3.2	9256.	69.26	71.11	1.86	8.12	3503.	3647.	4.1	412.

Table D-1 (Continued)

Run No.	T_v, °F	P, psia	P_{sat}, psia	F_c, gpm	T_c, °F	$\dot{m}_c$, lb_m/hr	F_w, gpm	v, ft/sec	Re	$T_{w,in}$, °F	$T_{w,out}$, °F	ΔT_w, °F	$\overline{\Delta T}$, °F	Q_c, Btu/hr	Q_w, Btu/hr	$\frac{\Delta Q}{Q}$ X 100	U_o, $\frac{Btu}{hr \cdot ft^2 \cdot °F}$
R-717-046A	69.65	128.7	128.0	0.0176	67.64	5.38	32.6	26.3	73482.	66.84	67.03	0.17	2.68	2735.	2737.	0.1	974.
R-717-047A	70.31	130.2	129.5	0.0177	68.46	5.40	23.0	18.5	52142.	67.25	67.52	0.22	2.92	2744.	2551.	-7.0	897.
R-717-048A	71.29	132.2	131.7	0.0178	69.41	5.42	9.8	7.9	22368.	67.21	67.80	0.58	3.78	2751.	2850.	3.6	695.
R-717-049A	72.43	134.7	134.4	0.0179	69.88	5.45	5.4	4.4	12386.	67.07	68.06	0.98	4.87	2759.	2677.	-3.0	541.
R-717-050A	73.55	137.7	137.0	0.0179	70.75	5.47	3.9	3.2	8939.	66.93	68.31	1.37	5.93	2760.	2682.	-2.8	445.
R-717-051A	68.99	127.2	126.5	0.0183	67.86	5.60	32.6	26.3	72712.	66.08	66.34	0.17	2.78	2854.	2851.	-0.1	979.
R-717-052A	69.41	128.2	127.5	0.0183	68.43	5.60	23.0	18.5	51442.	66.26	66.55	0.24	3.00	2852.	2793.	-2.1	908.
R-717-053A	70.22	130.2	129.3	0.0184	68.84	5.63	9.8	7.9	22007.	66.04	66.62	0.56	3.89	2860.	2771.	-3.1	702.
R-717-054A	71.33	132.7	131.8	0.0183	69.46	5.59	5.4	4.4	12165.	65.74	66.78	1.03	5.07	2833.	2799.	-1.2	534.
R-717-055A	72.43	135.2	134.4	0.0182	69.93	5.54	3.9	3.2	8781.	65.63	67.04	1.40	6.10	2802.	2753.	-1.7	439.
R-717-056A	72.05	134.7	133.5	0.0378	71.68	11.49	32.6	26.3	71657.	64.94	65.38	0.35	6.89	5818.	5783.	-0.6	807.
R-717-057A	74.33	140.2	138.9	0.0377	73.41	11.45	9.8	7.9	21696.	64.70	65.92	1.21	9.02	5772.	5945.	3.0	611.
R-717-058A	77.03	146.7	145.5	0.0377	75.43	11.41	5.4	4.4	12070.	64.62	66.78	2.14	11.33	5723.	5838.	2.0	482.
R-717-059A	79.73	153.7	152.4	0.0377	77.53	11.39	3.8	3.1	8577.	64.64	67.61	2.96	13.61	5681.	5700.	0.3	399.
R-717-060A	71.07	131.7	131.2	0.0301	68.55	9.20	32.6	26.3	72439.	65.75	66.12	0.29	5.13	4666.	4659.	-0.2	869.
R-717-061A	73.48	137.2	136.9	0.0308	70.42	9.39	9.8	7.9	21802.	65.88	66.90	1.01	7.09	4742.	4935.	4.1	639.
R-717-062A	75.98	143.7	142.9	0.0310	72.67	9.41	5.4	4.3	12100.	65.91	67.70	1.78	9.19	4730.	4790.	1.3	492.
R-717-063A	77.79	147.7	147.4	0.0309	73.73	9.38	3.8	3.1	8664.	65.64	68.06	2.41	10.94	4699.	4636.	-1.3	410.
R-717-064A	70.94	132.2	130.9	0.0316	70.96	9.62	32.6	26.3	71823.	65.13	65.52	0.31	5.61	4884.	4984.	2.1	831.
R-717-065A	72.16	135.2	133.8	0.0315	72.26	9.58	12.6	10.2	27827.	65.10	65.90	0.79	6.66	4850.	4974.	2.6	695.
R-717-066A	72.86	136.7	135.4	0.0308	72.98	9.36	9.8	7.9	21757.	64.99	66.03	1.02	7.36	4731.	5035.	6.4	614.
R-717-067A	71.83	134.7	133.0	0.0302	71.92	9.18	17.7	14.3	39157.	65.31	65.93	0.58	6.21	4650.	5174.	11.3	715.
R-717-068A	73.59	138.7	137.1	0.0311	73.10	9.43	7.7	6.2	17023.	64.92	66.22	1.29	8.02	4762.	4971.	4.4	567.
R-717-069A	74.15	139.7	138.5	0.0313	73.66	9.50	6.4	5.2	14182.	64.75	66.28	1.53	8.63	4790.	4895.	2.2	530.
R-717-070A	74.81	141.2	140.1	0.0311	73.90	9.42	5.4	4.4	11931.	64.64	66.42	1.77	9.28	4744.	4781.	0.8	488.
R-717-071A	75.54	143.2	141.8	0.0313	74.48	9.48	4.8	3.9	10742.	64.70	66.71	2.00	9.84	4767.	4844.	1.6	463.
R-717-072A	75.95	144.2	142.8	0.0313	74.78	9.48	4.5	3.6	9969.	64.65	66.80	2.14	10.23	4763.	4814.	1.1	445.
R-717-073A	76.82	146.2	145.0	0.0309	75.10	9.36	3.9	3.2	8720.	64.61	67.05	2.43	10.99	4695.	4772.	1.6	408.
R-717-074A	78.57	150.2	149.4	0.0201	75.85	6.08	33.0	26.6	83221.	75.37	75.62	0.18	3.08	3041.	3013.	-0.9	943.
R-717-075A	79.34	152.2	151.3	0.0201	76.70	6.07	17.7	14.3	44816.	75.61	76.00	0.34	3.53	3032.	3046.	0.5	821.
R-717-076A	79.96	153.9	152.9	0.0204	78.08	6.15	12.6	10.2	31980.	75.73	76.26	0.52	3.97	3066.	3281.	7.0	739.
R-717-077A	80.34	154.7	153.9	0.0204	78.56	6.16	9.8	7.9	25015.	75.72	76.36	0.64	4.30	3069.	3135.	2.1	682.
R-717-078A	80.65	155.7	154.7	0.0207	78.28	6.23	7.6	6.1	19305.	75.42	76.28	0.85	4.80	3100.	3231.	4.2	617.
R-717-079A	81.06	156.2	155.8	0.0205	78.36	6.17	6.4	5.1	16148.	75.40	76.40	0.99	5.16	3072.	3156.	2.7	569.
R-717-080A	81.47	157.2	156.9	0.0205	78.57	6.17	5.4	4.4	13815.	75.31	76.48	1.16	5.59	3068.	3165.	3.1	526.
R-717-081A	81.72	157.7	157.5	0.0206	78.93	6.21	4.9	3.9	12414.	75.21	76.49	1.28	5.87	3085.	3119.	1.1	502.
R-717-082A	82.18	159.7	158.8	0.0207	79.26	6.22	4.4	3.6	11291.	75.26	76.68	1.42	6.22	3086.	3143.	1.8	474.
R-717-083A	82.68	161.2	160.1	0.0206	79.57	6.20	3.9	3.2	9976.	75.20	76.80	1.60	6.67	3074.	3137.	2.0	440.
R-717-084A	83.54	162.7	162.4	0.0206	80.05	6.20	3.2	2.6	8173.	75.03	76.97	1.93	7.54	3067.	3100.	1.1	389.
R-717-085A	76.78	146.2	144.9	0.0125	74.59	3.78	33.0	26.6	82580.	74.79	75.00	0.13	1.89	1899.	2190.	15.3	961.
R-717-086A	77.51	147.7	146.7	0.0127	75.29	3.85	9.8	7.9	24642.	74.67	75.08	0.41	2.63	1930.	2024.	4.9	701.
R-717-087A	78.28	149.7	148.6	0.0126	75.72	3.80	5.4	4.3	13396.	74.42	75.18	0.76	3.48	1900.	2043.	7.5	521.
R-717-088A	79.05	151.7	150.6	0.0125	76.25	3.77	3.9	3.2	9836.	74.40	75.42	1.01	4.14	1883.	1986.	5.5	434.
R-717-089A	76.21	144.7	143.5	0.0114	74.97	3.46	33.0	26.6	82150.	74.39	74.60	0.13	1.72	1738.	2140.	23.1	967.
R-717-090A	76.88	145.7	145.1	0.0113	75.35	3.43	9.8	7.9	24276.	74.32	74.70	0.38	2.37	1722.	1848.	7.4	693.
R-717-091A	77.48	147.2	146.6	0.0113	75.93	3.43	5.4	4.3	13366.	74.00	74.68	0.68	3.14	1718.	1822.	6.1	523.
R-717-092A	77.97	149.0	147.9	0.0112	76.35	3.40	3.9	3.1	9671.	73.74	74.66	0.92	3.77	1700.	1792.	5.4	431.

Table D-1 (Continued)

Run No.	T_v, °F	P, psia	P_{sat}, psia	F_c, gpm	T_c, °F	$\dot{m}_c$, lb_m/hr	F_w, gpm	v, ft/sec	Re	$T_{w,in}$, °F	$T_{w,out}$, °F	ΔT_w, °F	$\overline{\Delta T}$, °F	Q_c, Btu/hr	Q_w, Btu/hr	$\frac{\Delta Q}{Q}$ X 100	U_o, $\frac{Btu}{hr \cdot ft^2 \cdot °F}$
R-717-098A	77.79	148.7	147.4	0.0114	77.14	3.43	9.8	7.9	24675.	75.18	75.57	0.39	2.42	1717.	1882.	9.6	678.
R-717-099A	78.45	150.2	149.1	0.0114	77.40	3.46	5.3	4.2	13221.	74.88	75.60	0.72	3.21	1728.	1884.	9.0	513.
R-717-100A	77.20	147.4	145.9	0.0119	77.19	3.59	33.0	26.6	83119.	75.30	75.50	0.13	1.80	1799.	2074.	15.3	955.
R-717-101A	77.76	148.2	147.3	0.0117	77.19	3.54	18.0	14.5	45536.	75.61	75.86	0.23	2.02	1775.	2083.	17.4	840.
R-717-102A	79.60	153.2	152.0	0.0114	78.19	3.43	3.9	3.1	9871.	75.30	76.26	0.96	3.82	1712.	1860.	8.7	428.
R-717-103A	81.17	153.7	156.1	0.0911	79.18	27.43	32.6	26.3	67488.	60.48	61.44	0.89	20.21	13644.	14253.	4.5	645.
R-717-104A	87.16	170.4	172.4	0.0920	85.26	27.45	9.8	7.9	20726.	60.66	63.52	2.84	25.07	13485.	13973.	3.6	514.
R-717-105A	93.58	189.7	191.4	0.0938	91.01	27.76	5.4	4.4	11448.	60.05	65.16	5.10	30.97	13451.	13774.	2.4	415.
R-717-106A	98.84	206.7	208.1	0.0943	95.01	27.73	3.9	3.1	8342.	59.79	66.68	6.89	35.61	13281.	13415.	1.0	356.
R-717-107A	95.27	192.7	196.6	0.1191	91.98	35.21	9.8	7.9	21033.	61.32	64.91	3.59	32.16	16997.	17669.	4.0	505.
R-717-108A	88.60	171.7	176.6	0.1174	85.31	35.04	32.6	26.3	68752.	61.66	62.83	1.09	26.36	17164.	17739.	3.4	622.
R-717-109A	104.13	221.7	225.9	0.1232	100.34	35.96	5.4	4.4	11749.	61.22	67.65	6.42	39.70	17012.	17333.	1.9	409.
R-717-110A	94.44	184.7	194.0	0.1211	89.80	35.89	17.7	14.3	38106.	62.63	64.75	2.12	30.75	17359.	18599.	7.1	539.
R-717-111A	90.93	178.9	183.4	0.0987	87.84	29.36	32.6	26.3	75569.	68.49	69.53	0.94	21.92	14307.	15361.	7.4	623.
R-717-112A	94.30	189.2	193.6	0.0997	90.69	29.51	17.7	14.3	41623.	69.19	70.95	1.75	24.23	14275.	15459.	8.3	563.
R-717-113A	97.37	199.2	203.3	0.1004	93.74	29.60	9.8	7.9	22867.	68.29	71.46	3.17	27.50	14221.	15434.	8.5	494.
R-717-114A	103.36	218.7	223.2	0.1018	99.48	29.76	5.4	4.4	12901.	67.84	73.28	5.44	32.80	14108.	14817.	5.0	411.
R-717-119A	80.76	154.7	155.0	0.0754	79.74	22.68	32.6	26.3	71961.	65.06	65.87	0.72	15.29	11289.	11712.	3.7	705.
R-717-120A	85.51	168.2	167.8	0.0761	84.16	22.73	9.8	7.9	21981.	65.05	67.44	2.39	19.27	11207.	11709.	4.5	556.
R-717-121A	90.17	182.2	181.1	0.0763	88.32	22.68	5.4	4.4	12240.	64.58	68.83	4.24	23.47	11070.	11538.	4.2	451.
R-717-122A	95.05	197.2	195.9	0.0772	92.92	22.79	3.9	3.2	8925.	64.60	70.42	5.82	27.54	11008.	11421.	3.7	382.
R-717-123A	82.48	158.7	159.6	0.0468	80.57	14.07	32.6	26.3	80043.	73.19	73.69	0.43	9.04	6977.	7042.	0.9	737.
R-717-124A	84.58	166.7	165.2	0.0459	82.61	13.76	9.8	7.9	24377.	73.31	74.77	1.45	10.53	6794.	7135.	5.0	616.
R-717-125A	87.51	174.7	173.4	0.0458	84.98	13.67	5.4	4.4	13558.	73.16	75.72	2.55	13.07	6709.	6944.	3.5	490.
R-717-126A	90.40	183.2	181.8	0.0462	87.80	13.75	3.9	3.2	9879.	73.09	76.62	3.52	15.54	6706.	6932.	3.4	412.
R-717-127A	79.96	153.7	152.9	0.0665	79.15	20.01	33.3	26.8	74501.	66.08	66.70	0.62	13.53	9978.	10250.	2.7	704.
R-717-128A	85.66	168.7	168.2	0.0677	84.30	20.22	9.6	7.7	21723.	66.17	68.33	2.15	18.41	9964.	10337.	3.7	517.
R-717-129A	90.19	181.7	181.2	0.0678	88.24	20.16	5.4	4.4	12414.	65.88	69.59	3.70	22.46	9840.	10087.	2.5	419.
R-717-130A	94.17	193.7	193.2	0.0681	91.89	20.13	3.9	3.2	9026.	65.76	70.90	5.13	25.84	9740.	10080.	3.5	360.
R-717-131A	78.25	149.7	148.6	0.0468	77.36	14.11	33.4	26.9	77790.	69.10	69.62	0.42	8.83	7061.	7043.	-0.3	759.
R-717-132A	81.08	157.2	155.8	0.0464	79.67	13.96	9.8	7.9	23012.	68.88	70.29	1.41	11.49	6943.	6925.	-0.3	577.
R-717-133A	84.55	166.7	165.2	0.0461	82.78	13.80	5.4	4.4	12793.	68.66	71.21	2.54	14.61	6818.	6914.	1.4	446.
R-717-134A	87.08	173.7	172.2	0.0455	84.87	13.57	3.9	3.2	9269.	68.54	72.03	3.50	16.79	6670.	6873.	3.0	379.
R-717-135A	88.55	176.7	176.4	0.1025	86.31	30.54	33.4	26.9	75162.	66.35	67.35	0.91	21.70	14960.	15120.	1.1	658.
R-717-136A	95.37	197.7	196.9	0.1049	93.22	30.94	9.8	7.9	22447.	66.34	69.46	3.12	27.46	14935.	15320.	2.6	519.
R-717-137A	101.94	219.7	218.4	0.1055	99.34	30.84	5.4	4.4	12593.	66.04	71.51	5.46	33.17	14664.	14863.	1.4	422.
R-717-138A	108.53	242.2	241.6	0.1079	105.66	31.24	3.8	3.1	8926.	65.88	73.71	7.83	38.74	14625.	14906.	1.9	361.
R-717-139A	83.03	162.2	161.0	0.0175	80.40	5.26	34.0	27.4	91169.	80.22	80.47	0.18	2.69	2607.	3036.	16.5	926.
R-717-140A	85.10	168.2	166.7	0.0172	82.24	5.16	9.8	7.9	26445.	80.98	81.55	0.56	3.83	2546.	2719.	6.8	635.
R-717-141A	86.50	171.7	170.6	0.0174	83.34	5.19	5.4	4.4	14697.	81.05	82.05	1.00	4.95	2556.	2683.	5.0	493.
R-717-142A	87.78	175.7	174.2	0.0175	84.28	5.24	3.9	3.2	10746.	81.23	82.62	1.39	5.86	2569.	2727.	6.2	419.
R-717-143A	86.60	171.7	170.9	0.0337	84.92	10.07	34.0	27.4	91501.	80.45	80.82	0.31	5.97	4952.	5241.	5.8	793.
R-717-144A	88.63	177.7	176.6	0.0328	85.89	9.79	9.8	7.9	26649.	80.56	81.56	0.99	7.56	4797.	4884.	1.8	606.
R-717-145A	90.77	184.2	182.9	0.0326	87.39	9.69	5.5	4.4	14951.	80.59	82.31	1.71	9.32	4725.	4686.	-0.8	484.

Table D-1 (Continued)

Run No.	T_v, °F	P, psia	P_{sat}, psia	F_c, gpm	T_c, °F	$\dot{m}_c$, lb_m/hr	F_w, gpm	v, ft/sec	Re	$T_{w,in}$, °F	$T_{w,out}$, °F	ΔT_w, °F	$\overline{\Delta T}$, °F	Q_c, Btu/hr	Q_w, Btu/hr	$\frac{\Delta Q}{Q}$ X 100	U_o, $\frac{Btu}{hr \cdot ft^2 \cdot °F}$
R-717-146A	84.53	167.2	165.1	0.0257	82.72	7.71	34.0	27.4	91091.	80.12	80.43	0.24	4.26	3808.	4020.	5.6	854.
R-717-147A	86.18	170.7	169.7	0.0256	83.59	7.66	9.8	7.9	26427.	79.99	80.79	0.79	5.79	3771.	3867.	2.5	622.
R-717-148A	87.89	175.7	174.5	0.0253	84.39	7.55	5.4	4.4	14660.	79.89	81.30	1.40	7.23	3705.	3820.	3.1	485.
R-717-149A	89.25	179.7	178.4	0.0250	85.70	7.46	3.9	3.2	10609.	79.94	81.83	1.88	8.37	3648.	3688.	1.1	416.
R-717-150A	88.20	177.2	175.4	0.0396	85.97	11.82	34.0	27.4	92240.	81.07	81.50	0.35	6.91	5793.	5953.	2.8	801.
R-717-151A	90.98	184.7	183.5	0.0394	88.42	11.69	9.8	7.9	26876.	81.16	82.34	1.17	9.23	5698.	5749.	0.9	590.
R-717-152A	93.88	193.7	192.3	0.0399	90.92	11.80	5.4	4.4	15012.	81.50	83.54	2.04	11.35	5714.	5541.	-3.0	481.
R-717-153A	95.90	199.7	198.6	0.0399	92.42	11.77	3.9	3.2	10835.	81.15	84.05	2.90	13.30	5676.	5687.	0.2	408.

Table D-2. Experimental data for ammonia condensing on Tube E (60 square ridges)

Run No.	T_v, °F	P, psia	P_{sat}, psia	F_c, gpm	T_c, °F	$\dot{m}_c$, lb_m/hr	F_w, gpm	v, ft/sec	Re	$T_{w,in}$, °F	$T_{w,out}$, °F	ΔT_w, °F	$\overline{\Delta T}$, °F	Q_c, Btu/hr	Q_w, Btu/hr	$\frac{\Delta Q}{Q}$ X 100	U_o, Btu/hr·ft²·°F
R-717-009E	75.72	143.2	142.3	0.0746	75.58	22.57	33.4	26.9	79349.	70.44	71.22	0.69	4.88	11350.	11599.	2.2	1448.
R-717-010E	77.63	148.2	147.0	0.0754	77.38	22.76	18.5	14.9	44154.	70.54	71.82	1.24	6.45	11402.	11490.	0.8	1101.
R-717-011E	79.36	152.7	151.4	0.0755	79.04	22.72	12.6	10.2	30146.	70.44	72.29	1.84	8.00	11342.	11591.	2.2	884.
R-717-012E	80.87	156.7	155.3	0.0760	80.42	22.84	9.8	7.9	23610.	70.33	72.67	2.33	9.37	11368.	11492.	1.1	756.
R-717-013E	82.78	161.7	160.4	0.0762	82.22	22.84	7.7	6.2	18516.	70.25	73.23	2.98	11.04	11321.	11454.	1.2	639.
R-717-014E	86.50	171.7	170.6	0.0772	85.62	23.02	5.4	4.4	13185.	70.23	74.41	4.18	14.18	11326.	11362.	0.3	498.
R-717-015E	89.53	181.2	179.3	0.0772	88.32	22.93	4.4	3.6	10846.	70.31	75.45	5.14	16.65	11210.	11419.	1.9	419.
R-717-016E	91.51	186.7	185.1	0.0778	90.12	23.05	3.9	3.2	9611.	70.24	76.03	5.79	18.37	11218.	11355.	1.2	380.
R-717-017E	80.51	155.2	154.4	0.1137	79.55	34.22	33.4	26.9	81571.	72.47	73.59	1.03	7.49	17041.	17195.	0.9	1419.
R-717-018E	85.64	168.7	168.2	0.1171	84.48	34.98	17.7	14.3	44561.	74.35	76.39	2.00	10.29	17239.	17642.	2.3	1045.
R-717-019E	87.27	173.2	172.8	0.1181	86.02	35.20	12.6	10.2	31446.	73.26	76.12	2.85	12.59	17287.	17895.	3.5	856.
R-717-020E	89.28	178.2	178.5	0.1131	87.58	33.65	9.8	7.9	24561.	72.85	76.40	3.55	14.66	16454.	17429.	5.9	699.
R-717-021E	91.82	185.7	186.1	0.1182	89.96	35.02	7.8	6.3	19517.	72.67	77.11	4.43	16.93	17036.	17253.	1.3	627.
R-717-022E	96.92	201.7	201.9	0.1183	94.74	34.82	5.4	4.4	13759.	72.46	78.70	6.22	21.34	16746.	16925.	1.1	489.
R-717-023E	100.61	214.2	213.9	C.1201	98.17	35.16	4.6	3.7	11707.	72.46	79.95	7.49	24.41	16772.	17183.	2.5	428.
R-717-024E	103.58	224.7	224.0	0.1193	100.94	34.78	3.9	3.2	10067.	72.43	80.99	8.56	26.87	16477.	16789.	1.9	382.
R-717-025E	77.32	147.2	146.2	0.0935	76.73	28.24	33.4	26.9	79854.	70.85	71.77	0.83	6.01	14155.	13818.	-2.4	1466.
R-717-026E	81.30	157.2	156.4	0.0963	80.37	28.93	17.7	14.3	43134.	72.02	73.71	1.66	8.43	14384.	14658.	1.9	1063.
R-717-027E	83.02	161.7	161.0	0.0971	82.01	29.10	12.6	10.2	30616.	71.45	73.84	2.39	10.37	14421.	15004.	4.0	866.
R-717-028E	85.04	167.2	166.5	0.0986	83.90	29.48	9.8	7.9	24059.	71.55	74.53	2.97	12.00	14548.	14604.	0.4	755.
R-717-029E	87.44	174.2	173.2	0.0991	86.13	29.52	7.7	6.2	18897.	71.51	75.30	3.78	14.03	14495.	14520.	0.2	644.
R-717-030E	91.57	186.2	185.3	0.0996	89.88	29.54	5.4	4.4	13416.	70.99	76.28	5.28	17.94	14374.	14369.	-0.0	499.
R-717-031E	97.57	204.7	203.9	0.1008	95.25	29.63	3.9	3.2	9777.	70.80	78.09	7.30	23.12	14233.	14306.	0.5	384.
R-717-032E	73.41	137.7	136.7	0.0547	73.22	16.62	33.4	26.9	78511.	69.74	70.34	0.51	3.37	8393.	8528.	1.6	1553.
R-717-033E	75.00	141.7	140.5	0.0532	74.70	16.10	17.7	14.3	41849.	69.99	70.95	0.93	4.53	8109.	8225.	1.4	1116.
R-717-034E	76.24	144.7	143.5	0.0536	75.86	16.20	12.6	10.2	29842.	69.93	71.28	1.35	5.64	8137.	8474.	4.1	899.
R-717-035E	77.27	147.2	146.1	0.0534	76.79	16.12	9.8	7.9	23361.	69.88	71.53	1.65	6.57	8083.	8121.	0.5	767.
R-717-036E	81.05	156.7	155.8	0.0530	80.03	15.93	5.4	4.4	13018.	69.78	72.69	2.90	9.82	7924.	7897.	-0.3	503.
R-717-037E	83.07	162.2	161.1	0.0534	81.82	16.02	4.4	3.6	10646.	69.55	73.16	3.61	11.72	7936.	8027.	1.1	422.
R-717-038E	84.49	166.7	165.0	0.0535	83.22	16.01	3.9	3.2	9436.	69.60	73.65	4.04	12.87	7909.	7941.	0.4	383.
R-717-039E	73.42	138.2	136.7	0.0460	73.45	13.97	33.4	26.9	79050.	70.29	70.81	0.43	2.87	7056.	7176.	1.7	1533.
R-717-040E	74.61	141.2	139.6	0.0463	74.49	14.02	17.7	14.3	41988.	70.31	71.13	0.80	3.89	7065.	7049.	-0.2	1131.
R-717-041E	75.81	143.7	142.5	0.0463	75.55	14.00	12.6	10.2	29993.	70.41	71.55	1.14	4.83	7038.	7171.	1.9	908.
R-717-042E	76.75	146.2	144.8	0.0463	76.52	13.98	10.0	8.1	23860.	70.43	71.89	1.45	5.59	7015.	7230.	3.1	781.
R-717-043E	78.78	150.7	149.9	0.0461	78.37	13.89	6.5	5.2	15569.	70.26	72.40	2.13	7.45	6941.	6915.	-0.4	580.
R-717-044E	80.39	154.7	154.0	0.0465	79.80	13.98	5.4	4.4	13114.	70.51	73.07	2.56	8.60	6967.	6982.	0.2	505.
R-717-045E	83.80	164.2	163.1	0.0467	82.67	13.98	3.8	3.1	9183.	70.39	74.08	3.69	11.56	6917.	7001.	1.2	373.
R-717-046E	73.29	137.2	136.4	0.0377	73.34	11.45	33.4	26.9	79475.	70.73	71.17	0.36	2.34	5783.	5941.	2.7	1539.
R-717-047E	76.14	144.2	143.3	0.0382	76.00	11.56	9.8	7.9	23595.	70.86	72.04	1.16	4.69	5807.	5709.	-1.7	772.
R-717-048E	78.24	149.2	148.5	0.0383	78.04	11.55	6.5	5.2	15677.	71.05	72.88	1.83	6.27	5780.	5944.	2.8	574.
R-717-049E	81.74	158.7	157.6	0.0384	80.99	11.53	3.9	3.2	9527.	71.00	73.94	2.94	9.27	5731.	5762.	0.5	385.
R-717-050E	79.71	153.7	152.3	0.0386	79.61	11.63	5.3	4.3	12834.	71.29	73.49	2.20	7.32	5800.	5811.	0.2	494.
R-717-051E	77.16	147.2	145.8	0.0311	77.16	9.40	33.4	26.9	84175.	75.27	75.62	0.28	1.71	4713.	4732.	0.4	1716.
R-717-052E	78.39	150.2	148.9	0.0312	78.14	9.40	17.7	14.3	44885.	75.64	76.21	0.57	2.47	4703.	5033.	7.0	1188.
R-717-053E	78.96	151.7	150.4	0.0310	78.68	9.33	9.5	7.7	24015.	74.77	75.78	1.01	3.69	4659.	4812.	3.3	787.
R-717-054E	79.84	154.2	152.6	0.0310	79.40	9.34	7.7	6.2	19429.	74.92	76.16	1.23	4.30	4660.	4740.	1.7	674.
R-717-055E	82.02	159.7	158.3	0.0308	81.22	9.25	5.1	4.1	12981.	75.30	77.13	1.83	5.80	4593.	4653.	1.3	493.
R-717-056E	82.69	161.7	160.1	0.0312	81.81	9.35	4.6	3.7	11862.	75.38	77.40	2.02	6.30	4638.	4688.	1.1	458.

Table D-2 (Continued)

Run No.	T_v, °F	P, psia	P_{sat}, psia	F_c, gpm	T_c, °F	$\dot{m}_c$, lb_m/hr	F_w, gpm	v, ft/sec	Re	$T_{w,in}$, °F	$T_{w,out}$, °F	ΔT_w, °F	$\overline{\Delta T}$, °F	Q_c, Btu/hr	Q_w, Btu/hr	$\frac{\Delta Q}{Q}$ X 100	U_o, $\frac{Btu}{hr \cdot ft^2 \cdot °F}$
R-717-057E	76.37	144.7	143.9	0.0237	75.96	7.16	33.4	26.9	93732.	74.89	75.18	0.22	1.33	3596.	3716.	3.3	1684.
R-717-058E	76.82	145.7	145.0	0.0235	76.37	7.11	17.7	14.3	44303.	74.70	75.13	0.42	1.90	3569.	3709.	3.9	1169.
R-717-059E	78.22	149.2	148.5	0.0231	77.63	6.97	9.5	7.7	23937.	75.04	75.82	0.77	2.79	3490.	3644.	4.4	778.
R-717-060E	79.88	153.7	152.7	0.0231	78.94	6.95	5.4	4.4	13642.	74.95	76.31	1.35	4.25	3466.	3634.	4.9	508.
R-717-061E	80.85	156.2	155.2	0.0233	79.78	7.00	4.7	3.8	11863.	75.29	76.83	1.54	4.79	3482.	3578.	2.8	453.
R-717-062E	81.82	158.7	157.8	0.0232	80.60	6.97	3.9	3.2	10014.	75.39	77.21	1.82	5.52	3464.	3574.	3.2	391.
R-717-063E	77.47	147.7	146.6	0.0380	76.76	11.48	33.4	26.9	83999.	75.07	75.50	0.36	2.19	5751.	5998.	4.3	1636.
R-717-064E	79.87	153.7	152.7	0.0379	80.18	11.41	9.9	8.0	25080.	74.86	76.05	1.19	4.41	5689.	5917.	4.0	803.
R-717-065E	82.24	159.7	158.9	0.0379	81.01	11.38	6.6	5.3	16756.	75.49	77.25	1.75	5.87	5649.	5749.	1.8	599.
R-717-066E	83.26	162.7	161.7	0.0379	82.09	11.38	5.4	4.4	13923.	75.46	77.54	2.08	6.76	5634.	5661.	0.5	519.
R-717-067E	84.27	165.7	164.4	0.0380	82.97	11.39	4.6	3.7	11876.	75.24	77.72	2.47	7.78	5629.	5737.	1.9	451.
R-717-068E	85.64	169.2	168.2	0.0382	84.03	11.43	3.9	3.2	10079.	75.36	78.25	2.89	8.84	5632.	5664.	0.6	397.
R-717-069E	78.43	149.7	149.0	0.0670	77.91	20.20	33.4	26.9	82834.	73.85	74.56	0.64	4.22	10103.	10680.	5.7	1490.
R-717-070E	81.54	158.2	157.1	0.0667	80.70	20.03	12.6	10.2	31435.	73.83	75.50	1.66	6.88	9953.	10453.	5.0	901.
R-717-071E	83.75	163.7	163.0	0.0669	82.66	20.04	10.0	8.1	25361.	74.92	76.94	2.02	7.82	9914.	10077.	1.6	790.
R-717-072E	87.92	175.7	174.6	0.0670	86.36	19.96	5.4	4.4	13842.	74.24	77.85	3.61	11.87	9791.	9818.	0.3	514.
R-717-073E	90.15	182.2	181.1	0.0672	98.26	19.97	4.6	3.7	11895.	74.47	78.73	4.26	13.55	9750.	9887.	1.4	448.
R-717-074E	92.34	188.7	187.6	0.0677	90.22	20.05	3.9	3.2	10073.	74.26	79.25	4.99	15.59	9741.	9775.	0.4	389.
R-717-075E	82.29	159.7	159.1	0.0885	81.26	26.56	33.4	26.9	85674.	76.37	77.27	0.83	5.48	13179.	13896.	5.4	1500.
R-717-076E	86.40	170.7	170.3	0.0877	84.97	26.18	12.6	10.2	32562.	76.34	78.47	2.11	8.99	12880.	13294.	3.2	892.
R-717-077E	87.88	175.2	174.5	0.0879	86.24	26.20	10.0	8.1	25904.	76.29	78.89	2.60	10.29	12850.	12985.	1.1	778.
R-717-078E	91.77	186.7	185.9	0.0891	89.89	26.40	6.4	5.2	16668.	75.86	79.92	4.05	13.88	12845.	12967.	1.0	577.
R-717-079E	93.61	191.7	191.5	0.0894	91.56	26.45	5.4	4.4	14148.	75.37	80.15	4.78	15.85	12814.	12990.	1.4	504.
R-717-080E	95.85	198.7	198.4	0.0894	93.64	26.35	4.6	3.7	11985.	75.24	80.85	5.60	17.80	12705.	12860.	1.2	445.
R-717-081E	98.65	207.7	207.4	0.0897	96.10	26.36	3.9	3.1	10122.	75.05	81.65	6.60	20.29	12630.	12742.	0.9	388.
R-717-082E	78.81	150.2	150.0	0.0668	77.79	20.13	33.4	26.9	83517.	74.50	75.17	0.60	3.97	10062.	9964.	-1.0	1580.
R-717-083E	82.48	160.2	159.6	0.0672	81.34	20.17	12.6	10.2	31853.	74.86	76.51	1.65	6.80	10007.	10371.	3.6	917.
R-717-084E	83.84	163.7	163.2	0.0673	82.56	20.16	9.8	7.9	25027.	75.07	77.09	2.01	7.76	9975.	9896.	-0.8	801.
R-717-085E	88.40	176.7	176.0	0.0676	86.65	20.13	5.5	4.4	14147.	74.98	78.53	3.55	11.64	9863.	9765.	-1.0	528.
R-717-086E	92.09	187.2	186.9	0.0679	89.90	20.12	4.0	3.2	10299.	74.70	79.52	4.82	14.98	9778.	9622.	-1.6	407.
R-717-087E	83.38	161.2	162.0	0.1002	82.14	30.04	33.4	26.9	85465.	76.14	77.12	0.91	6.76	14872.	15162.	2.0	1371.
R-717-088E	88.38	175.2	175.9	0.1015	86.83	30.22	12.6	10.2	32594.	76.24	78.72	2.47	10.90	14806.	15557.	5.1	846.
R-717-089E	90.09	180.2	180.9	0.1015	88.47	30.14	10.0	8.1	25972.	76.29	79.31	3.02	12.29	14717.	15076.	2.4	746.
R-717-090E	94.94	195.2	195.6	0.1023	93.10	30.19	6.5	5.2	17127.	76.64	81.24	4.59	16.00	14586.	14887.	2.1	568.
R-717-091E	97.70	203.7	204.3	0.1032	95.80	30.32	5.4	4.4	14338.	76.82	82.29	5.47	18.15	14559.	14730.	1.2	500.
R-717-092E	100.10	213.2	212.2	0.1036	98.05	30.35	4.7	3.8	12632.	77.07	83.30	6.22	19.92	14495.	14653.	1.1	453.
R-717-093E	103.49	223.7	223.7	0.1043	101.25	30.40	3.9	3.2	10606.	77.17	84.56	7.39	22.63	14406.	14490.	0.6	397.
R-717-094E	79.61	152.7	152.0	0.0624	79.79	18.76	33.4	26.9	84706.	75.60	76.26	0.58	3.67	9362.	9747.	4.1	1587.
R-717-095E	82.86	161.2	160.6	0.0623	82.70	18.67	12.6	10.2	32253.	75.91	77.40	1.49	6.20	9257.	9340.	0.9	930.
R-717-096E	84.38	165.7	164.7	0.0623	84.15	18.64	9.8	7.9	25399.	76.29	78.18	1.89	7.15	9209.	9272.	0.7	803.
R-717-097E	88.69	178.2	176.8	0.0626	88.09	18.60	5.4	4.4	14037.	76.18	79.55	3.36	10.82	9108.	9054.	-0.6	524.
R-717-098E	90.79	184.2	183.0	0.0626	89.98	18.55	4.7	3.8	12221.	76.63	80.50	3.87	12.22	9042.	8997.	-0.5	461.
R-717-099E	92.91	190.7	189.3	0.0626	91.84	18.50	3.9	3.2	10375.	76.82	81.37	4.55	13.81	8976.	8922.	-0.6	405.

Table D-2 (Continued)

Run No.	T_v, °F	P, psia	P_{sat}, psia	F_c, gpm	T_c, °F	$\dot{m}_c$, lb_m/hr	F_w, gpm	v, ft/sec	Re	$T_{w,in}$, °F	$T_{w,out}$, °F	ΔT_w, °F	$\overline{\Delta T}$, °F	Q_c, Btu/hr	Q_w, Btu/hr	$\frac{\Delta Q}{Q}$ X 100	U_o, $\frac{Btu}{hr \cdot ft^2 \cdot °F}$
R-717-100E	84.94	164.7	166.2	0.1037	83.87	31.01	33.4	26.9	86634.	77.19	73.20	0.94	7.25	15304.	15646.	2.2	1316.
R-717-101E	89.82	179.2	180.1	0.1044	88.56	31.00	12.6	10.2	33003.	77.19	79.75	2.55	11.35	15143.	16028.	5.8	831.
R-717-102E	91.79	185.2	186.0	0.1054	90.44	31.23	10.0	8.1	26347.	77.37	80.50	3.13	12.85	15191.	15634.	2.9	736.
R-717-103E	93.84	191.7	192.2	0.1060	92.51	31.30	7.7	6.2	20308.	76.70	80.71	4.00	15.14	15156.	15440.	1.9	624.
R-717-104E	98.40	207.2	206.6	0.1063	96.85	31.20	5.4	4.4	14445.	76.58	82.23	5.65	18.99	14957.	15350.	2.6	491.
R-717-105E	100.69	214.2	214.2	0.1067	99.05	31.20	4.6	3.7	12389.	76.57	83.08	6.50	20.87	14880.	15085.	1.4	444.
R-717-106E	104.69	227.2	227.8	0.1089	102.87	31.67	3.9	3.2	10598.	76.91	84.68	7.77	23.89	14965.	15243.	1.9	390.

Table D-3. Experimental data for ammonia condensing on Tube F (48 corrugations)

Run No.	T_v, °F	P, psia	P_{sat}, psia	F_c, gpm	T_c, °F	$\dot{m}_c$, lb_m/hr	F_w, gpm	v, ft/sec	Re	$T_{w,in}$, °F	$T_{w,out}$, °F	ΔT_w, °F	$\overline{\Delta T}$, °F	Q_c, Btu/hr	Q_w, Btu/hr	$\frac{\Delta Q}{Q}$ X 100	U_o, $\frac{Btu}{hr \cdot ft^2 \cdot °F}$
R-717-001F	79.94	154.2	152.9	0.0565	79.64	16.99	34.0	24.8	84808.	76.03	76.62	0.51	3.62	8469.	8684.	2.5	2255.
R-717-002F	82.14	159.7	158.6	0.0562	81.51	16.86	17.7	12.9	44655.	76.70	77.73	1.03	4.92	8371.	9059.	8.2	1640.
R-717-003F	84.17	165.2	164.1	0.0569	83.34	17.02	9.8	7.2	24836.	76.27	78.07	1.79	7.00	8415.	8806.	4.6	1158.
R-717-004F	88.21	176.7	175.4	0.0565	86.84	16.83	5.3	3.9	13453.	76.08	79.31	3.23	10.52	8250.	8532.	3.4	756.
R-717-005F	90.25	182.2	181.4	0.0570	88.70	16.93	4.6	3.4	11786.	76.57	80.30	3.73	11.81	8263.	8550.	3.5	674.
R-717-006F	91.79	187.2	186.0	0.0564	89.88	16.73	3.9	2.9	10085.	76.41	80.71	4.29	13.23	8138.	8420.	3.5	593.
R-717-007F	76.85	146.2	145.1	0.0232	76.72	7.00	34.0	24.8	83900.	75.35	75.63	0.22	1.36	3510.	3681.	4.8	2483.
R-717-008F	77.77	148.2	147.4	0.0234	77.65	7.07	17.7	12.9	43859.	75.59	76.03	0.43	1.96	3541.	3815.	7.7	1743.
R-717-009F	79.15	152.2	150.8	0.0238	79.12	7.17	9.8	7.2	24564.	75.92	76.70	0.78	2.84	3580.	3818.	6.6	1215.
R-717-010F	80.94	156.7	155.5	0.0236	80.52	7.08	5.4	3.9	13509.	75.86	77.25	1.38	4.38	3525.	3718.	5.5	775.
R-717-011F	82.55	161.2	159.7	0.0235	81.78	7.04	3.9	2.8	9713.	75.86	77.76	1.89	5.74	3494.	3653.	4.5	587.
R-717-012F	84.69	166.2	165.5	0.1125	84.15	33.62	34.0	24.8	84494.	75.49	76.58	1.02	8.65	16601.	17301.	4.2	1849.
R-717-013F	87.68	174.7	173.9	0.1152	87.03	34.31	17.7	12.9	44267.	75.56	77.51	1.94	11.14	16834.	17139.	1.8	1455.
R-717-014F	92.43	188.7	187.9	0.1152	91.58	34.08	10.0	7.3	25278.	75.63	79.11	3.49	15.06	16554.	17390.	5.1	1059.
R-717-015F	100.63	214.7	214.0	0.1160	98.98	33.92	5.4	4.0	14086.	76.01	82.25	6.23	21.50	16177.	16944.	4.7	725.
R-717-016F	103.66	224.7	224.3	0.1169	102.02	34.02	4.6	3.4	12081.	75.91	83.18	7.26	24.12	16113.	16853.	4.6	644.
R-717-017F	106.64	235.7	234.7	0.1169	104.59	33.89	3.9	2.9	10249.	75.66	84.03	8.36	26.79	15938.	16400.	2.9	573.
R-717-018F	96.40	201.2	200.2	0.1161	95.32	34.13	7.6	5.5	19411.	76.22	80.79	4.57	17.90	16434.	17254.	5.0	885.
R-717-024F	78.47	150.2	149.1	0.0385	78.30	11.61	34.0	24.8	84589.	75.91	76.34	0.36	2.34	5808.	6106.	5.1	2391.
R-717-025F	80.07	154.2	153.2	0.0388	79.59	11.66	17.7	12.9	44392.	76.40	77.11	0.70	3.32	5814.	6181.	6.3	1689.
R-717-026F	81.10	157.2	155.9	0.0388	80.66	11.66	9.8	7.2	24600.	75.81	77.04	1.23	4.68	5798.	6034.	4.1	1194.
R-717-027F	83.69	164.2	162.8	0.0388	82.90	11.63	5.5	4.0	13908.	75.60	77.77	2.16	7.00	5755.	5983.	4.0	792.
R-717-028F	85.03	167.7	166.5	0.0385	83.92	11.50	4.6	3.4	11710.	75.81	78.33	2.52	7.96	5674.	5857.	3.2	687.
R-717-029F	86.47	171.7	170.5	0.0390	85.24	11.64	4.0	2.9	10127.	76.03	78.95	2.92	8.98	5726.	5823.	1.7	615.
R-717-030F	82.24	160.2	158.9	0.0763	81.83	22.88	34.0	24.8	85572.	76.65	77.40	0.68	5.21	11354.	11466.	1.0	2098.
R-717-031F	85.13	167.7	166.7	0.0766	84.43	22.87	17.7	12.9	45198.	77.52	78.82	1.29	6.96	11284.	11417.	1.2	1563.
R-717-032F	87.53	174.2	173.5	0.0767	86.62	22.85	9.8	7.2	25074.	76.75	79.10	2.35	9.60	11219.	11562.	3.1	1125.
R-717-033F	89.38	179.7	178.8	0.0769	88.48	22.83	7.7	5.6	19621.	76.72	79.70	2.97	11.17	11165.	11375.	1.9	963.
R-717-034F	93.20	191.7	190.2	0.0774	91.92	22.88	5.4	3.9	13926.	76.82	81.09	4.28	14.24	11095.	11519.	3.8	751.
R-717-035F	97.36	204.7	203.2	0.0779	95.70	22.98	4.0	2.9	10389.	76.67	82.38	5.71	17.83	10996.	11402.	3.7	594.
R-717-042F	88.04	176.7	175.0	0.0321	87.71	9.56	34.0	24.8	95664.	86.04	86.40	0.29	1.82	4687.	4860.	3.7	2475.
R-717-043F	88.69	178.2	176.8	0.0323	88.24	9.61	17.7	12.9	49724.	85.80	86.38	0.58	2.60	4704.	5122.	8.9	1743.
R-717-044F	89.61	181.2	179.5	0.0321	89.10	9.51	9.8	7.2	27681.	85.48	86.48	1.00	3.63	4649.	4909.	5.6	1233.
R-717-045F	91.89	188.2	186.3	0.0322	90.92	9.53	5.5	4.0	15523.	85.59	87.36	1.75	5.41	4634.	4791.	3.4	825.
R-717-046F	93.23	192.2	190.3	0.0323	92.20	9.53	4.7	3.4	13367.	86.11	88.14	1.98	6.11	4621.	4637.	0.4	729.
R-717-047F	94.72	197.2	194.9	0.0327	93.53	9.63	3.9	2.9	11249.	86.45	88.89	2.42	7.05	4655.	4741.	1.8	636.
R-717-048F	87.36	174.7	173.0	0.0479	86.90	14.25	34.0	24.8	93751.	84.15	84.64	0.42	2.97	6997.	7158.	2.3	2273.
R-717-049F	89.08	179.2	177.9	0.0478	88.38	14.20	17.7	12.9	49243.	84.71	85.57	0.85	3.94	6950.	7514.	8.1	1700.
R-717-050F	90.36	183.2	181.7	0.0480	89.66	14.25	10.1	7.4	28010.	84.15	85.60	1.46	5.49	6951.	7381.	6.2	1220.
R-717-051F	93.44	192.7	191.0	0.0474	92.25	13.99	5.5	4.0	15342.	84.08	86.63	2.57	8.08	6782.	7051.	4.0	808.
R-717-052F	94.85	197.2	195.3	0.0480	93.65	14.16	4.8	3.5	13313.	84.28	87.24	2.98	9.09	6843.	7073.	3.4	725.
R-717-053F	96.60	202.7	200.8	0.0485	95.16	14.27	3.9	2.9	11041.	84.15	87.77	3.66	10.64	6866.	7172.	4.5	621.
R-717-054F	87.36	174.7	173.0	0.0676	86.76	20.14	34.0	24.8	92219.	82.70	83.37	0.59	4.33	9892.	10075.	1.8	2202.
R-717-055F	89.09	179.2	178.0	0.0675	88.42	20.06	17.7	12.9	48145.	82.69	83.85	1.15	5.82	9812.	10163.	3.6	1623.
R-717-056F	91.81	187.2	186.0	0.0675	90.85	19.98	10.0	7.3	27382.	82.80	84.84	2.05	7.99	9721.	10217.	5.1	1172.
R-717-057F	93.70	193.7	191.7	0.0684	92.70	20.18	7.7	5.6	21186.	82.89	85.54	2.67	9.43	9777.	10241.	4.7	993.
R-717-058F	96.83	202.7	201.5	0.0684	95.52	20.11	5.5	4.0	15281.	83.20	86.85	3.69	11.80	9675.	10124.	4.6	790.
R-717-059F	101.44	216.7	216.7	0.0696	99.73	20.33	3.8	2.8	10805.	83.41	88.60	5.21	15.43	9678.	9988.	3.2	604.

Table D-3 (Continued)

Run No.	T_v, °F	P, psia	P_{sat}, psia	F_c, gpm	T_c, °F	$\dot{m}_c$, lb_m/hr	F_w, gpm	v, ft/sec	Re	$T_{w,in}$, °F	$T_{w,out}$, °F	ΔT_w, °F	$\overline{\Delta T}$, °F	Q_c, Btu/hr	Q_w, Btu/hr	$\frac{\Delta Q}{Q}$ X 100	U_o, $\frac{Btu}{hr \cdot ft^2 \cdot °F}$
R-717-060P	86.43	171.2	170.4	0.0882	86.18	26.29	34.0	24.8	89015.	79.73	80.59	0.80	6.26	12934.	13501.	4.4	1989.
R-717-061P	98.77	210.2	207.8	0.0894	97.69	26.20	5.5	4.0	14851.	80.26	85.08	4.84	16.10	12551.	13291.	5.9	751.
R-717-062P	88.50	177.7	176.3	0.0882	88.15	26.20	18.0	13.1	47192.	79.51	81.04	1.53	8.23	12834.	13766.	7.3	1503.
R-717-063P	92.50	189.2	188.1	0.0890	91.86	26.29	9.8	7.2	26139.	79.88	82.62	2.75	11.25	12770.	13513.	5.8	1094.
R-717-064P	94.80	197.2	195.1	0.0894	94.04	26.33	7.7	5.6	20591.	80.14	83.61	3.49	12.92	12722.	13406.	5.4	949.
R-717-065P	104.37	227.7	226.7	0.0906	102.83	26.35	4.0	2.9	10987.	80.78	87.38	6.64	20.29	12459.	13246.	6.3	591.
R-717-066P	84.59	166.7	165.3	0.0422	83.80	12.63	34.0	24.8	91139.	81.85	82.29	0.36	2.52	6236.	6191.	-0.7	2386.
R-717-067P	85.54	169.7	167.9	0.0427	84.75	12.76	17.7	12.9	47428.	81.67	82.41	0.73	3.50	6290.	6463.	2.8	1731.
R-717-068P	87.85	175.7	174.4	0.0436	86.86	12.98	9.9	7.2	26809.	82.24	83.57	1.34	4.94	6366.	6623.	4.0	1241.
R-717-069P	90.57	183.7	182.3	0.0423	89.28	12.56	5.4	4.0	14813.	82.05	84.36	2.33	7.37	6123.	6332.	3.4	801.
R-717-070P	91.82	187.2	186.1	0.0423	90.36	12.54	4.7	3.4	12803.	82.22	84.91	2.71	8.26	6097.	6331.	3.8	711.
R-717-071P	93.18	192.2	190.2	0.0424	91.50	12.53	3.9	2.9	10756.	82.20	85.37	3.21	9.40	6075.	6289.	3.5	623.
R-717-072P	87.86	175.7	174.4	0.1009	87.23	30.02	34.0	24.8	89445.	80.07	81.03	0.89	7.31	14726.	15180.	3.1	1940.
R-717-073P	89.98	181.7	180.6	0.1007	89.14	29.88	17.7	12.9	46487.	79.53	81.30	1.77	9.56	14593.	15602.	6.9	1470.
R-717-074P	94.31	194.7	193.6	0.1015	93.15	29.94	9.8	7.2	26247.	80.06	83.12	3.07	12.73	14486.	15100.	4.2	1097.
R-717-075P	97.59	204.7	204.0	0.1014	96.13	29.77	7.3	5.3	19719.	80.42	84.53	4.13	15.11	14299.	15074.	5.4	912.
R-717-076P	101.69	217.7	217.5	0.1022	99.93	29.84	5.5	4.0	15101.	80.91	86.28	5.41	18.10	14198.	14930.	5.2	756.
R-717-077P	104.04	225.7	225.6	0.1029	102.08	29.95	4.7	3.4	12846.	80.50	86.84	6.36	20.37	14174.	14914.	5.2	670.
R-717-078P	106.71	235.7	235.0	0.1036	104.56	30.04	4.0	2.9	10837.	80.04	87.50	7.47	22.94	14129.	14767.	4.5	593.
R-717-079P	85.81	169.7	168.7	0.0280	84.28	8.37	34.0	24.8	93585.	84.10	84.40	0.24	1.56	4125.	4054.	-1.7	2540.
R-717-080P	86.49	171.7	170.5	0.0278	84.96	8.31	18.2	13.3	50138.	84.07	84.57	0.50	2.17	4089.	4521.	10.6	1819.
R-717-081P	87.47	174.7	173.3	0.0281	85.97	8.38	9.8	7.2	27122.	83.83	84.73	0.90	3.19	4115.	4422.	7.5	1244.
R-717-082P	89.57	180.7	179.4	0.0281	87.76	8.35	5.4	4.0	15096.	84.00	85.55	1.57	4.79	4079.	4279.	4.9	821.
R-717-083P	90.17	182.2	181.1	0.0280	88.27	8.31	4.7	3.4	13081.	83.93	85.71	1.82	5.35	4058.	4290.	5.7	731.
R-717-084P	91.10	184.7	183.9	0.0282	89.12	8.36	3.9	2.9	10893.	83.76	85.90	2.16	6.26	4071.	4227.	3.8	626.
R-717-085P	86.75	172.2	171.3	0.0515	85.75	15.36	34.0	24.8	92862.	83.34	83.88	0.47	3.14	7553.	7921.	4.9	2314.
R-717-086P	87.65	175.2	173.8	0.0520	86.65	15.49	17.7	12.9	48140.	82.80	83.72	0.92	4.39	7602.	8115.	6.7	1669.
R-717-087P	89.72	181.2	179.8	0.0518	88.46	15.40	10.0	7.3	27344.	82.92	84.49	1.57	6.02	7522.	7857.	4.5	1204.
R-717-088P	93.46	192.2	191.0	0.0514	92.73	15.18	5.5	4.0	15206.	83.23	86.00	2.79	8.84	7355.	7658.	4.1	802.
R-717-089P	94.81	196.2	195.2	0.0518	92.90	15.28	4.7	3.4	12926.	83.07	86.35	3.30	10.10	7384.	7697.	4.2	704.
R-717-090P	96.83	202.7	201.5	0.0521	94.68	15.33	3.8	2.8	10708.	83.15	87.08	3.97	11.71	7375.	7621.	3.3	607.
R-717-091P	87.06	173.2	172.2	0.0634	86.19	18.90	34.0	24.8	92233.	82.74	83.35	0.54	4.01	9289.	9159.	-1.4	2229.
R-717-092P	88.86	178.7	177.3	0.0640	87.95	19.02	17.7	12.9	48208.	82.83	83.93	1.10	5.48	9311.	9713.	4.3	1636.
R-717-093P	91.05	185.2	183.7	0.0636	89.86	18.86	9.9	7.2	27027.	82.61	84.53	1.93	7.48	9190.	9512.	3.5	1184.
R-717-094P	93.25	191.7	190.4	0.0640	91.98	18.93	7.8	5.7	21410.	83.34	85.77	2.45	8.69	9177.	9472.	3.2	1017.
R-717-095P	96.23	200.7	199.7	0.0640	94.69	18.83	5.4	4.0	15188.	83.57	86.99	3.46	10.95	9070.	9396.	3.6	798.
R-717-096P	100.14	214.2	212.3	0.0644	98.07	18.85	3.8	2.8	10721.	83.48	88.27	4.82	14.27	9003.	9180.	2.0	608.
R-717-097P	84.25	165.7	164.4	0.0349	84.27	10.42	34.0	24.8	91243.	81.99	82.34	0.29	2.09	5148.	4868.	-5.4	2374.
R-717-098P	84.70	167.2	165.6	0.0353	84.78	10.54	17.7	12.9	47278.	81.48	82.09	0.61	2.92	5207.	5369.	3.1	1718.
R-717-099P	86.38	171.7	170.2	0.0350	86.27	10.44	9.8	7.2	26478.	81.75	82.85	1.11	4.08	5138.	5444.	6.0	1213.
R-717-100P	89.02	179.2	177.8	0.0349	88.41	10.37	5.4	4.0	14765.	81.97	83.90	1.95	6.08	5074.	5299.	4.4	804.
R-717-101P	90.24	182.7	181.3	0.0352	89.64	10.43	4.7	3.4	12802.	82.25	84.52	2.30	6.85	5091.	5402.	6.1	716.
R-717-102P	91.76	187.7	185.8	0.0357	91.06	10.57	3.9	2.8	10640.	82.36	85.10	2.76	8.03	5143.	5352.	4.1	617.

Table D-3 (Continued)

Run No.	T_v, °F	P, psia	P_{sat}, psia	F_c, gpm	T_c, °F	$\dot{m}_c$, lb_m/hr	F_w, gpm	v, ft/sec	Re	$T_{w,in}$, °F	$T_{w,out}$, °F	ΔT_w, °F	$\overline{\Delta T}$, °F	Q_c, Btu/hr	Q_w, Btu/hr	$\frac{\Delta Q}{Q}$ X 100	U_o, $\frac{Btu}{hr \cdot ft^2 \cdot °F}$
R-717-103P	87.69	175.7	174.0	0.0475	97.13	14.15	34.0	24.8	94236.	84.58	85.07	0.41	2.87	6944.	7022.	1.1	2332.
R-717-104P	88.66	178.2	176.7	0.0475	88.05	14.12	17.7	12.9	49005.	84.32	85.15	0.83	3.92	6913.	7311.	5.8	1698.
R-717-105P	90.98	185.2	183.5	0.0477	90.17	14.13	9.8	7.2	27518.	94.77	86.21	1.44	5.43	6885.	7100.	3.1	1207.
R-717-106P	93.67	193.2	191.6	0.0475	92.51	14.03	5.5	4.0	15380.	84.29	86.84	2.57	8.10	6795.	7046.	3.7	808.
R-717-107P	95.37	198.2	196.9	0.0475	93.99	14.00	4.7	3.4	13145.	84.75	87.75	3.04	9.12	6756.	7073.	4.7	714.
R-717-108P	97.00	203.2	202.1	0.0482	95.42	14.17	3.9	2.9	11096.	84.73	88.30	3.60	10.48	6812.	7045.	3.4	626.

Table D-4. Experimental data for ammonia condensing on Tube F-1 (48 corrugations with 1 skirt)

Run No.	T_v, °F	P, psia	P_{sat}, psia	F_c, gpm	T_c, °F	$\dot{m}_c$, lb_m/hr	F_w, gpm	v, ft/sec	Re	$T_{w,in}$, °F	$T_{w,out}$, °F	ΔT_w, °F	$\overline{\Delta T}$, °F	Q_c, Btu/hr	Q_w, Btu/hr	$\frac{\Delta Q}{Q}$ X 100	U_o, $\frac{Btu}{hr \cdot ft^2 \cdot °F}$
R-717-019F1	83.06	162.7	161.1	0.0384	82.84	11.50	34.0	24.8	89619.	80.50	80.91	0.35	2.35	5700.	5920.	3.8	2334.
R-717-020F1	84.09	165.7	163.9	0.0381	83.77	11.41	17.7	12.9	46740.	80.52	81.19	0.65	3.23	5641.	5784.	2.5	1681.
R-717-021F1	85.79	169.7	168.6	0.0386	85.26	11.51	9.8	7.2	26107.	80.55	81.76	1.22	4.63	5669.	5975.	5.4	1179.
R-717-022F1	88.75	178.7	177.0	0.0381	87.78	11.34	5.4	3.9	14367.	80.70	82.82	2.16	6.99	5554.	5803.	4.5	766.
R-717-023F1	89.64	181.2	179.6	0.0380	88.39	11.28	4.6	3.4	12303.	80.65	83.12	2.49	7.76	5511.	5716.	3.7	684.
R-717-024F1	90.72	183.7	182.8	0.0381	89.14	11.29	3.9	2.9	10514.	80.49	83.34	2.87	8.81	5506.	5635.	2.3	602.
R-717-025F1	85.10	167.7	166.7	0.0578	84.44	17.26	34.0	24.8	90524.	81.23	81.81	0.51	3.58	8517.	8735.	2.6	2294.
R-717-026F1	86.05	170.2	169.3	0.0577	85.32	17.23	17.7	12.9	46890.	80.63	81.60	0.97	4.93	8484.	8565.	1.0	1657.
R-717-027F1	88.88	178.7	177.4	0.0574	87.91	17.07	9.7	7.1	25977.	81.13	82.86	1.74	6.88	8356.	8439.	1.0	1170.
R-717-028F1	93.51	192.2	191.2	0.0575	92.06	16.98	5.4	4.0	14843.	81.85	84.90	3.06	10.13	8228.	8322.	1.1	782.
R-717-029F1	94.72	196.2	194.9	0.0570	93.18	16.82	4.6	3.4	12528.	81.59	85.15	3.60	11.35	8131.	8259.	1.6	690.
R-717-030F1	96.57	201.7	200.7	0.0569	94.79	16.74	3.9	2.9	10745.	81.62	85.77	4.17	12.87	8059.	8177.	1.5	603.
R-717-031F1	87.24	174.2	172.7	0.0765	86.69	22.79	34.0	24.8	91148.	81.71	82.45	0.67	5.16	11193.	11347.	1.4	2089.
R-717-032F1	89.14	179.2	178.1	0.0773	88.44	22.96	17.7	12.9	47476.	81.45	82.80	1.34	7.02	11231.	11850.	5.5	1542.
R-717-033F1	92.46	189.2	188.0	0.0774	91.54	22.88	9.8	7.2	26647.	81.65	84.00	2.36	9.64	11113.	11601.	4.4	1111.
R-717-034F1	98.69	208.7	207.6	0.0774	97.13	22.70	5.3	3.9	14602.	82.18	86.47	4.30	14.36	10876.	11382.	4.7	730.
R-717-035F1	100.00	212.7	211.9	0.0775	98.46	22.70	4.6	3.4	12791.	81.67	86.59	4.96	15.87	10842.	11496.	6.0	658.
R-717-036F1	102.45	220.7	220.1	0.0780	100.76	22.76	3.9	2.9	10831.	81.44	87.27	5.85	18.10	10812.	11479.	6.2	576.
R-717-037F1	82.10	159.7	158.5	0.0244	81.95	7.33	34.0	24.8	89569.	80.51	80.81	0.23	1.43	3639.	3952.	3.6	2444.
R-717-038F1	82.78	161.7	160.4	0.0245	82.71	7.35	17.7	12.9	46684.	80.54	80.98	0.44	2.02	3644.	3867.	6.1	1739.
R-717-039F1	83.85	164.7	163.3	0.0243	83.58	7.27	9.8	7.2	26044.	80.57	81.34	0.77	2.89	3596.	3803.	5.8	1197.
R-717-040F1	85.60	169.2	168.1	0.0247	84.93	7.37	5.4	4.0	14444.	80.46	81.84	1.42	4.45	3631.	3853.	6.3	786.
R-717-041F1	86.09	170.7	169.4	0.0246	85.27	7.35	4.7	3.4	12445.	80.27	81.88	1.63	5.02	3618.	3817.	5.5	695.
R-717-042F1	86.71	172.2	171.2	0.0243	85.75	7.26	4.0	2.9	10584.	80.08	81.96	1.90	5.63	3570.	3785.	6.0	605.
R-717-043F1	87.63	175.7	173.8	0.1007	87.27	29.96	34.0	24.8	83311.	79.94	80.91	0.90	7.20	14705.	15333.	4.3	1966.
R-717-044F1	90.48	183.2	182.0	0.1011	89.94	29.95	17.7	12.9	46857.	80.19	81.92	1.72	9.42	14612.	15179.	3.9	1494.
R-717-045F1	94.81	196.7	195.2	0.1020	93.99	30.05	9.8	7.2	26326.	80.29	83.37	3.08	12.98	14523.	15130.	4.2	1078.
R-717-046F1	102.22	220.7	219.3	0.1022	100.62	29.81	5.4	4.0	14879.	80.84	86.31	5.49	18.64	14165.	14915.	5.3	732.
R-717-047F1	104.80	229.7	228.2	0.1020	103.06	29.65	4.6	3.4	12649.	80.40	86.97	6.51	21.16	14005.	15043.	7.4	637.
R-717-048F1	107.56	239.7	238.1	0.1023	105.61	29.62	4.0	2.9	10986.	80.36	87.78	7.47	23.49	13901.	14900.	7.2	570.
R-717-049F1	86.68	172.7	171.1	0.0306	85.96	9.12	34.0	24.8	94300.	84.71	85.05	0.27	1.80	4485.	4630.	3.2	2407.
R-717-050F1	87.42	174.7	173.2	0.0313	86.59	9.32	18.0	13.1	49932.	84.61	85.18	0.56	2.53	4574.	5055.	10.5	1745.
R-717-051F1	88.72	178.2	176.9	0.0310	87.82	9.23	10.0	7.3	27826.	84.68	85.63	0.95	3.57	4520.	4734.	4.7	1221.
R-717-052F1	91.26	185.7	184.4	0.0310	89.93	9.20	5.3	3.9	14997.	84.91	86.63	1.74	5.49	4482.	4652.	3.8	786.
R-717-053F1	92.14	188.7	187.0	0.0308	90.73	9.11	4.7	3.4	13211.	85.16	87.11	1.98	6.01	4429.	4642.	4.8	710.
R-717-054F1	93.47	192.2	191.1	0.0310	91.76	9.15	3.9	2.9	11105.	85.42	87.74	2.36	6.89	4436.	4615.	4.1	620.
R-717-055F1	90.88	184.7	183.2	0.1111	90.35	32.91	34.0	24.8	91971.	82.28	83.35	1.01	9.07	16038.	17080.	6.5	1915.
R-717-056F1	92.91	190.7	189.3	0.1114	92.23	32.91	17.7	12.9	47611.	81.41	83.30	1.88	10.55	15970.	16609.	4.0	1458.
R-717-057F1	98.81	209.7	207.9	0.1113	97.80	32.62	9.8	7.1	27150.	83.10	86.48	3.39	14.02	15625.	16593.	6.2	1074.
R-717-058F1	105.07	228.7	229.2	0.1048	103.16	30.45	5.3	3.9	14862.	82.58	88.38	5.84	19.59	14374.	15491.	7.8	707.
R-717-059F1	107.52	238.7	237.9	0.1071	105.70	31.00	4.7	3.4	13186.	82.50	89.17	6.69	21.68	14551.	15686.	7.8	647.
R-717-060F1	84.56	165.7	165.2	0.0478	84.70	14.27	34.0	24.8	90708.	81.27	82.10	0.44	2.89	7047.	7412.	5.2	2360.
R-717-061F1	85.77	168.7	168.5	0.0480	85.78	14.31	17.7	12.9	47221.	81.27	82.10	0.83	4.09	7052.	7311.	3.7	1663.
R-717-062F1	87.63	174.7	173.8	0.0479	87.46	14.24	9.9	7.2	26523.	81.23	82.66	1.44	5.69	6987.	7109.	1.7	1183.
R-717-063F1	91.44	185.2	184.9	0.0479	90.69	14.17	5.5	4.0	14988.	81.87	84.38	2.55	8.32	6898.	7014.	1.7	799.

Table D-4 (Continued)

Run No.	T_v, °F	P, psia	P_{sat}, psia	F_c, gpm	T_c, °F	$\dot{m}_c$, lb_m/hr	F_w, gpm	v, ft/sec	Re	$T_{w,in}$, °F	$T_{w,out}$, °F	ΔT_w, °F	$\overline{\Delta T}$, °F	Q_c, Btu/hr	Q_w, Btu/hr	$\frac{\Delta Q}{Q}$ X 100	U_o, $\frac{Btu}{hr \cdot ft^2 \cdot °F}$
R-717-064F1	83.98	163.7	163.6	0.0542	84.00	16.20	34.0	24.8	89252.	80.09	80.66	0.50	3.60	8010.	8430.	5.2	2143.
R-717-065F1	85.20	167.7	166.9	0.0551	85.30	16.45	18.3	13.3	48082.	79.97	80.93	0.95	4.75	8114.	8700.	7.2	1646.
R-717-066F1	87.35	173.7	173.0	0.0553	87.37	16.47	10.0	7.3	26351.	79.85	81.51	1.66	6.66	8087.	8286.	2.5	1169.
R-717-067F1	91.82	186.7	186.1	0.0552	91.36	16.33	5.5	4.0	14737.	80.56	83.52	2.99	9.79	7945.	8218.	3.4	782.
R-717-068F1	93.39	191.7	190.8	0.0555	92.80	16.38	4.7	3.4	12645.	80.65	84.10	3.47	11.01	7940.	8127.	2.4	694.
R-717-069F1	95.54	197.7	197.5	0.0557	94.68	16.40	3.9	2.9	10652.	80.95	85.01	4.08	12.56	7911.	8009.	1.2	607.
R-717-070F1	85.66	170.7	168.2	0.0549	85.81	16.38	34.0	24.8	91155.	81.80	82.37	0.50	3.57	8073.	8447.	4.6	2178.
R-717-071F1	87.18	173.2	172.5	0.0545	87.32	16.21	17.7	12.9	47640.	81.95	82.86	0.91	4.78	7964.	8053.	1.1	1606.
R-717-072F1	89.53	180.2	179.3	0.0546	89.45	16.20	9.7	7.1	26252.	82.00	83.71	1.72	6.69	7921.	8304.	4.8	1142.
R-717-073F1	93.77	193.7	192.0	0.0544	93.10	16.06	5.5	4.0	15117.	82.66	85.60	2.97	9.64	7781.	8154.	4.9	778.
R-717-074F1	95.21	197.7	196.4	0.0544	94.50	16.01	4.7	3.4	12963.	82.70	86.13	3.45	10.79	7727.	8084.	4.6	690.
R-717-075F1	97.05	203.7	202.3	0.0548	96.25	16.10	4.0	2.9	10986.	82.68	86.71	4.05	12.36	7739.	8017.	3.6	603.
R-717-076F1	90.64	183.2	182.5	0.0385	90.02	11.41	34.0	24.8	98095.	88.14	88.55	0.34	2.29	5564.	5741.	3.2	2339.
R-717-077F1	91.49	186.2	185.1	0.0390	90.96	11.53	17.7	12.9	51072.	88.02	88.69	0.66	3.14	5611.	5854.	4.3	1724.
R-717-078F1	93.34	193.2	190.6	0.0389	92.73	11.48	9.8	7.1	28289.	88.24	89.43	1.20	4.51	5568.	5813.	4.4	1191.
R-717-079F1	95.92	199.7	198.7	0.0389	94.90	11.45	5.5	4.0	16052.	88.30	90.37	2.11	6.59	5518.	5780.	4.7	807.
R-717-080F1	96.98	203.7	202.0	0.0390	96.05	11.44	4.7	3.4	13653.	88.25	90.71	2.48	7.50	5503.	5761.	4.7	707.
R-717-081F1	98.09	207.2	205.6	0.0387	96.09	11.37	3.9	2.9	11501.	88.11	91.02	2.92	8.52	5457.	5725.	4.9	617.
R-717-082F1	90.35	182.2	181.7	0.0889	90.18	26.35	34.0	24.8	93415.	83.67	84.53	0.79	6.25	12856.	13450.	4.6	1982.
R-717-083F1	92.16	187.7	187.1	0.0894	91.95	26.42	18.3	13.3	50240.	83.29	84.78	1.49	8.12	12844.	13612.	6.0	1523.
R-717-084F1	95.75	199.2	198.1	0.0895	95.36	26.33	9.9	7.3	27534.	83.35	86.03	2.68	11.06	12698.	13313.	4.8	1106.
R-717-085F1	102.39	219.7	219.9	0.0895	101.40	26.08	5.5	4.0	15679.	84.19	88.92	4.77	15.83	12389.	13185.	6.4	754.
R-717-086F1	104.66	227.7	227.8	0.0896	103.58	26.03	4.6	3.4	13142.	83.76	89.43	5.68	19.07	12302.	13157.	7.0	656.
R-717-087F1	107.40	238.7	237.5	0.0893	106.07	25.83	3.9	2.9	11167.	83.75	90.35	6.62	20.35	12127.	12958.	6.9	574.
R-717-088F1	84.38	165.7	164.7	0.0381	84.59	11.39	34.0	24.8	91147.	81.87	82.29	0.35	2.30	5629.	5970.	6.1	2358.
R-717-089F1	85.34	168.2	167.3	0.0382	85.48	11.40	17.7	12.9	47485.	81.80	82.47	0.66	3.20	5624.	5872.	4.4	1692.
R-717-090F1	87.23	173.2	172.6	0.0384	87.26	11.43	10.0	7.3	27013.	82.12	83.29	1.17	4.53	5614.	5842.	4.1	1195.
R-717-091F1	90.20	182.2	181.2	0.0379	89.56	11.23	5.5	4.0	15000.	82.46	84.52	2.09	6.71	5481.	5740.	4.7	787.
R-717-092F1	91.01	184.2	183.6	0.0384	90.50	11.36	4.7	3.4	12858.	82.18	84.60	2.43	7.62	5535.	5734.	3.6	700.
R-717-093F1	92.46	189.7	188.0	0.0380	91.84	11.23	3.9	2.9	10750.	82.29	85.18	2.91	8.73	5456.	5705.	4.6	602.
R-717-094F1	87.39	173.7	173.1	0.0702	87.33	20.90	34.0	24.8	91909.	82.41	83.11	0.63	4.63	10262.	10669.	4.0	2134.
R-717-095F1	88.29	176.2	175.7	0.0699	88.15	20.78	17.7	12.9	47452.	81.48	82.69	1.21	6.21	10184.	10658.	4.7	1581.
R-717-096F1	89.85	181.7	180.2	0.0702	89.69	20.83	9.8	7.1	25806.	79.98	82.10	2.13	8.81	10173.	10346.	1.7	1112.
R-717-097F1	94.62	196.7	194.6	0.0708	93.99	20.87	5.4	4.0	14601.	80.17	83.89	3.76	12.59	10088.	10223.	1.3	772.
R-717-098F1	96.94	204.2	201.9	0.0715	96.20	21.00	4.6	3.4	12405.	80.32	84.81	4.51	14.38	10099.	10352.	2.5	677.
R-717-105F1	89.98	181.2	180.6	0.0622	89.37	18.44	34.0	24.8	95416.	85.69	86.31	0.55	3.98	9004.	9246.	2.7	2181.
R-717-106F1	91.41	185.2	184.8	0.0616	90.77	18.23	18.5	13.5	52018.	85.64	86.69	1.05	5.24	8874.	9656.	8.8	1630.
R-717-107F1	93.84	192.7	192.2	0.0617	92.96	18.21	9.9	7.2	27948.	85.59	87.41	1.82	7.34	8818.	8969.	1.7	1158.
R-717-108F1	98.75	209.2	207.7	0.0621	97.45	18.21	5.5	4.0	15826.	86.32	89.62	3.34	10.78	8721.	9158.	5.0	779.
R-717-109F1	100.28	212.7	212.8	0.0621	98.90	18.17	4.7	3.4	13397.	86.09	90.00	3.93	12.24	8672.	9126.	5.2	682.
R-717-110F1	102.47	219.7	220.2	0.0617	100.73	17.99	3.9	2.8	11285.	86.27	90.92	4.66	13.87	8542.	9061.	6.1	593.
R-717-111F1	87.23	173.2	172.6	0.0427	87.19	12.72	34.0	24.8	93869.	84.28	84.73	0.38	2.73	6246.	6479.	3.7	2207.
R-717-112F1	87.83	175.2	174.3	0.0424	87.87	12.61	17.7	12.9	48724.	83.89	84.63	0.73	3.57	6185.	6481.	4.8	1668.
R-717-113F1	89.63	180.2	179.5	0.0426	89.60	12.64	9.8	7.2	27240.	83.99	85.29	1.32	4.99	6179.	6471.	4.7	1193.
R-717-114F1	92.46	178.7	188.0	0.0424	91.93	12.55	5.5	4.0	15315.	83.93	86.19	2.30	7.40	6094.	6325.	3.8	793.
R-717-115F1	93.84	193.2	192.2	0.0421	93.34	12.43	4.7	3.4	13106.	84.18	86.84	2.68	8.33	6018.	6270.	4.2	696.
R-717-116F1	95.23	197.7	196.5	0.0424	94.64	12.48	4.0	2.9	11123.	84.15	87.30	3.17	9.50	6027.	6278.	4.2	611.

Table D-5. Experimental data for ammonia condensing on Tube G (24 corrugations)

Run No.	T_v, °F	P, psia	P_{sat}, psia	F_c, gpm	T_c, °F	$\dot{m}_c$, lb_m/hr	F_w, gpm	v, ft/sec	Re	$T_{w,in}$, °F	$T_{w,out}$, °F	ΔT_w, °F	$\overline{\Delta T}$, °F	Q_c, Btu/hr	Q_w, Btu/hr	$\frac{\Delta Q}{Q}$ X 100	U_o, $\frac{Btu}{hr \cdot ft^2 \cdot °F}$
R-717-001G	87.42	174.7	173.2	0.0571	86.81	16.99	34.5	18.8	87814.	83.20	83.76	0.49	3.94	8343.	8468.	1.5	1725.
R-717-002G	88.81	178.2	177.2	0.0565	87.85	16.81	17.7	9.6	45005.	82.92	83.88	0.95	5.42	8227.	8388.	2.0	1237.
R-717-003G	92.02	187.7	186.7	0.0572	90.46	16.96	9.7	5.3	24901.	83.35	85.02	1.68	7.84	8243.	8115.	-1.6	857.
R-717-004G	95.92	199.7	198.7	0.0572	93.53	16.85	5.4	3.0	14070.	83.15	86.16	3.03	11.26	8124.	8243.	1.5	587.
R-717-005G	97.36	204.7	203.2	0.0571	94.68	16.80	4.6	2.5	11956.	83.10	86.62	3.56	12.50	8071.	8209.	1.7	526.
R-717-006G	99.08	210.2	208.8	0.0571	96.16	16.77	3.8	2.1	9975.	82.85	87.06	4.21	14.12	8027.	8086.	0.7	463.
R-717-007G	84.50	166.2	165.0	0.0380	84.12	11.36	35.1	19.1	87901.	81.96	82.34	0.31	2.35	5610.	5481.	-2.3	1941.
R-717-008G	87.68	175.2	173.9	0.0384	87.10	11.42	9.8	5.4	24779.	81.93	83.11	1.17	5.16	5602.	5734.	2.4	885.
R-717-009G	90.90	184.7	183.3	0.0383	89.89	11.36	5.4	2.9	13604.	82.05	84.14	2.09	7.80	5535.	5602.	1.2	578.
R-717-010G	93.67	192.7	191.6	0.0380	92.29	11.22	3.7	2.0	9445.	82.24	85.21	2.99	9.94	5437.	5521.	1.5	445.
R-717-011G	85.35	168.2	167.4	0.0247	84.48	7.37	35.0	19.1	89420.	83.65	83.93	0.21	1.56	3636.	3632.	-0.1	1896.
R-717-012G	86.54	171.7	170.7	0.0244	85.47	7.29	17.7	9.6	45506.	84.10	84.53	0.43	2.23	3588.	3762.	4.8	1309.
R-717-013G	88.21	176.7	175.4	0.0246	87.13	7.32	9.8	5.3	25257.	84.56	85.32	0.77	3.27	3587.	3755.	4.7	893.
R-717-014G	90.49	183.2	182.1	0.0244	89.09	7.23	5.0	2.7	13096.	84.64	86.09	1.49	5.13	3526.	3734.	5.9	560.
R-717-015G	90.92	184.7	183.3	0.0246	89.74	7.30	4.6	2.5	12034.	84.61	86.19	1.62	5.51	3559.	3731.	4.8	526.
R-717-016G	91.99	187.7	186.6	0.0244	90.81	7.24	3.9	2.1	10077.	84.88	86.74	1.88	6.18	3519.	3601.	2.3	464.
R-717-017G	90.96	184.7	183.5	0.0782	90.36	23.17	35.0	19.1	91129.	85.01	85.73	0.65	5.60	11291.	11343.	0.5	1643.
R-717-018G	93.34	191.7	190.6	0.0792	92.48	23.38	18.0	9.8	46997.	84.95	86.25	1.29	7.74	11334.	11602.	2.4	1193.
R-717-019G	97.28	204.2	203.0	0.0797	96.17	23.39	9.8	5.4	25946.	85.31	87.65	2.35	10.80	11243.	11514.	2.4	847.
R-717-020G	102.99	222.2	221.9	0.0798	101.27	23.27	5.4	2.9	14294.	85.12	89.28	4.20	15.78	11037.	11260.	2.0	569.
R-717-021G	105.00	229.7	228.9	0.0805	103.25	23.39	4.7	2.6	12530.	85.28	90.08	4.82	17.32	11039.	11257.	2.0	519.
R-717-022G	107.71	239.7	238.6	0.0814	105.80	23.55	3.9	2.1	10565.	85.36	91.05	5.71	19.50	11047.	11171.	1.1	461.
R-717-023G	86.35	170.2	170.2	0.1012	86.23	30.17	35.0	19.1	83871.	78.14	79.06	0.86	7.75	14946.	14981.	0.9	1560.
R-717-024G	90.20	181.7	181.2	0.1015	89.76	30.09	17.7	9.6	42959.	78.74	80.49	1.74	10.58	14689.	15382.	4.7	1130.
R-717-025G	96.08	200.7	199.2	0.1036	95.31	30.46	9.8	5.4	24439.	79.87	82.92	3.06	14.69	14676.	15017.	2.3	813.
R-717-026G	103.38	223.7	223.3	0.1046	102.14	30.44	5.3	2.9	13053.	78.78	84.35	5.61	21.82	14428.	14683.	1.8	539.
R-717-027G	105.78	231.7	231.7	0.1046	104.30	30.36	4.6	2.5	11511.	78.93	85.25	6.35	23.69	14307.	14563.	1.8	492.
R-717-028G	109.35	245.7	244.6	0.1060	107.71	30.58	3.8	2.1	9728.	79.16	86.60	7.46	26.47	14292.	14334.	0.3	440.
R-717-029G	83.38	162.7	162.0	0.0317	83.52	9.49	35.0	19.1	86779.	81.16	81.51	0.28	2.05	4697.	4854.	3.3	1869.
R-717-030G	84.27	165.2	164.4	0.0320	84.36	9.56	17.7	9.6	43857.	81.00	81.58	0.57	2.98	4724.	5068.	7.3	1290.
R-717-031G	85.84	169.7	168.7	0.0321	85.89	9.56	9.8	5.4	24476.	81.02	82.01	0.99	4.33	4711.	4884.	3.7	887.
R-717-032G	88.24	176.7	175.5	0.0315	87.68	9.38	5.4	3.0	13590.	80.95	82.66	1.76	6.44	4596.	4777.	3.9	581.
R-717-033G	89.60	180.7	179.5	0.0319	89.11	9.48	4.6	2.5	11668.	81.29	83.33	2.05	7.29	4632.	4760.	2.8	518.
R-717-034G	90.62	183.7	182.5	0.0319	89.96	9.45	4.0	2.2	10066.	81.37	83.72	2.37	8.09	4610.	4731.	2.6	465.
R-717-035G	86.12	170.2	169.5	0.0488	86.25	14.55	35.0	19.1	98390.	82.60	83.08	0.41	3.28	7163.	7246.	1.2	1778.
R-717-036G	87.77	174.7	174.2	0.0490	87.64	14.58	17.5	9.5	44309.	82.63	83.48	0.85	4.72	7151.	7394.	3.4	1234.
R-717-037G	90.15	181.7	181.1	0.0494	89.89	14.63	9.3	5.1	23722.	82.44	84.00	1.57	6.94	7144.	7318.	2.4	839.
R-717-038G	94.21	194.2	193.3	0.0498	93.44	14.69	5.0	2.7	12831.	82.24	85.10	2.90	10.54	7109.	7269.	2.3	549.
R-717-039G	95.57	198.7	197.6	0.0499	94.66	14.68	4.3	2.4	11090.	82.16	85.45	3.31	11.77	7082.	7175.	1.3	490.
R-717-040G	97.55	205.7	203.9	0.0499	96.31	14.66	3.5	1.9	9880.	81.89	85.96	4.08	13.62	7039.	7070.	0.4	421.
R-717-041G	91.91	186.7	186.3	0.0344	90.55	10.19	35.0	19.1	95831.	89.61	89.95	0.28	2.13	4954.	4811.	-2.9	1894.
R-717-042G	93.40	191.2	190.8	0.0348	91.93	10.27	17.7	9.6	48769.	90.04	90.61	0.57	3.08	4980.	5016.	0.7	1316.
R-717-043G	94.55	195.2	194.4	0.0351	92.88	10.37	9.8	5.4	27063.	89.56	90.59	1.04	4.47	5013.	5112.	2.0	913.
R-717-044G	96.94	202.7	201.9	0.0349	94.67	10.26	5.3	2.9	14718.	89.24	91.13	1.93	6.75	4934.	5140.	4.2	595.
R-717-045G	97.80	206.2	204.7	0.0351	95.48	10.31	4.8	2.6	13098.	89.32	91.46	2.16	7.40	4951.	5112.	3.3	545.
R-717-046G	98.53	208.7	207.0	0.0348	96.06	10.23	4.1	2.2	11296.	89.10	91.53	2.48	8.22	4901.	5064.	3.3	486.

Table D-5 (Continued)

Run No.	T_v, °F	P, psia	P_{sat}, psia	F_c, gpm	T_c, °F	$\dot{m}_c$, lb_m/hr	F_w, gpm	v, ft/sec	Re	$T_{w,in}$, °F	$T_{w,out}$, °F	ΔT_w, °F	$\overline{\Delta T}$, °F	Q_c, Btu/hr	Q_w, Btu/hr	$\frac{\Delta Q}{Q}$ X 100	U_o, $\frac{Btu}{hr \cdot ft^2 \cdot °F}$
R-717-047G	84.10	164.2	163.9	0.1195	84.00	35.71	34.5	18.8	78450.	73.96	75.05	1.02	9.60	17657.	17624.	-0.2	1498.
R-717-048G	89.68	180.2	179.7	0.1207	89.30	35.80	17.7	9.6	41429.	75.76	77.73	1.96	12.93	17494.	17351.	-0.8	1102.
R-717-049G	95.88	199.2	198.5	0.1228	95.21	36.12	10.0	5.4	23834.	76.41	79.94	3.53	17.71	17413.	17600.	1.1	801.
R-717-050G	105.48	230.7	230.6	0.1254	104.17	36.40	5.5	3.0	13274.	76.56	82.95	6.42	25.72	17166.	17495.	1.9	543.
R-717-051G	108.75	242.7	242.4	0.1269	107.38	36.64	4.7	2.6	11552.	76.60	83.99	7.41	28.46	17147.	17445.	1.7	491.
R-717-052G	88.69	177.7	176.8	0.0415	88.06	12.32	35.0	19.1	91673.	85.80	86.21	0.34	2.69	6033.	5979.	-0.9	1828.
R-717-053G	90.20	181.7	181.2	0.0425	89.50	12.61	17.7	9.6	46502.	85.90	86.62	0.71	3.95	6152.	6294.	2.3	1270.
R-717-054G	92.29	188.2	187.5	0.0422	91.40	12.48	9.6	5.3	25478.	86.03	87.32	1.29	5.62	6063.	6224.	2.7	878.
R-717-055G	95.39	198.2	197.0	0.0422	86.12	12.58	5.6	3.0	14841.	86.20	88.38	2.22	8.10	6073.	6167.	1.5	611.
R-717-056G	96.64	202.7	201.0	0.0428	95.27	12.58	4.7	2.6	12596.	86.10	88.71	2.63	9.24	6053.	6186.	2.2	534.
R-717-057G	98.16	207.7	205.8	0.0431	96.88	12.65	4.1	2.2	10968.	86.26	89.32	3.07	10.37	6070.	6279.	3.5	476.
R-717-058G	86.71	171.7	171.2	0.0679	86.40	20.24	35.0	19.1	87339.	81.54	82.18	0.57	4.85	9955.	10005.	0.5	1673.
R-717-059G	89.08	178.2	177.9	0.0688	88.51	20.44	17.7	9.6	44371.	81.65	82.82	1.17	6.84	10000.	10349.	3.5	1190.
R-717-060G	92.19	188.2	187.2	0.0686	91.42	20.30	9.8	5.4	24831.	81.67	83.71	2.04	9.50	9865.	10039.	1.8	845.
R-717-061G	97.45	204.2	203.5	0.0690	96.19	20.26	5.5	3.0	14098.	81.82	85.41	3.63	13.84	9734.	10025.	3.0	573.
R-717-062G	99.50	211.2	210.2	0.0695	98.09	20.35	4.6	2.5	11900.	81.80	86.06	4.28	15.57	9730.	9924.	2.0	509.
R-717-063G	101.73	217.7	217.7	0.0699	100.21	20.41	4.0	2.2	10209.	81.84	86.82	5.00	17.40	9712.	9908.	2.0	455.
R-717-064G	86.37	170.7	170.2	0.0240	85.50	7.16	35.0	19.1	90655.	84.80	85.07	0.20	1.44	3523.	3544.	0.6	1996.
R-717-065G	87.47	173.7	173.3	0.0239	86.58	7.11	17.7	9.6	46061.	85.11	85.54	0.42	2.14	3489.	3753.	7.5	1325.
R-717-066G	88.46	176.7	176.1	0.0238	87.69	7.07	9.8	5.4	25636.	84.97	85.70	0.74	3.12	3463.	3621.	4.6	903.
R-717-067G	90.59	183.2	182.4	0.0237	89.22	7.03	5.5	3.0	14551.	85.31	86.59	1.32	4.64	3426.	3657.	6.8	601.
R-717-068G	91.41	185.7	184.8	0.0239	90.07	7.07	4.7	2.6	12388.	85.42	86.93	1.53	5.23	3443.	3590.	4.3	536.
R-717-069G	92.24	188.2	187.3	0.0239	90.70	7.07	4.0	2.2	10519.	85.46	87.21	1.77	5.90	3433.	3522.	2.6	474.
R-717-070G	86.49	171.2	170.5	0.0890	86.37	26.52	35.0	19.1	85157.	79.41	80.23	0.75	6.67	13047.	13113.	0.5	1593.
R-717-071G	89.72	180.2	179.8	0.0897	89.32	26.62	17.7	9.6	43455.	79.78	81.30	1.52	9.18	13007.	13386.	2.9	1154.
R-717-072G	93.79	193.2	192.0	0.0905	93.10	26.71	10.0	5.4	24710.	79.74	82.38	2.64	12.73	12937.	13190.	2.0	828.
R-717-073G	100.77	214.7	214.4	0.0907	99.54	26.51	5.4	2.9	13533.	79.83	84.59	4.80	18.57	12639.	12920.	2.2	554.
R-717-074G	102.51	220.7	220.3	0.0911	101.16	26.55	4.8	2.6	11894.	79.43	84.85	5.44	20.37	12608.	12898.	2.3	504.
R-717-075G	105.87	232.7	232.0	0.0909	104.26	26.38	3.9	2.1	9862.	79.70	86.19	6.51	22.92	12431.	12660.	1.8	442.

APPENDIX E

SI CONVERSION FACTORS

An attempt has been made to present all key tables and figures in dual units (ACU and SI). The following conversion factors may be used to convert from ACU to SI units:

To convert from	To	Multiply by
Btu/hr	W	0.2929
$Btu/hr \cdot ft^2$	W/m^2	3.152
$Btu/hr \cdot ft \cdot {}^\circ F$	$W/m \cdot K$	1.730
$Btu/hr \cdot ft^2 \cdot {}^\circ F$	$W/m^2 \cdot K$	5.675
Btu/lb_m	J/kg	2.324×10^3
$Btu/lb_m \cdot {}^\circ F$	$J/kg \cdot K$	4.184×10^3
ft	m	0.3048
ft^2	m^2	0.0929
ft/hr^2	m/s^2	2.35×10^{-8}
ft/sec	m/s	0.3048
gpm	m^3/s	6.309×10^{-5}
in.	cm	2.54
lb_f/ft	N/m	14.59
lb_m/ft^3	kg/m^3	16.02
$lb_m/hr \cdot ft$	$Pa \cdot s$	4.134×10^{-4}
$lb_m/hr \cdot ft^2$	$Pa \cdot s/m$	1.356×10^{-3}
psia	Pa	6.895×10^3
$\Delta({}^\circ F)$	$\Delta(K)$ or $\Delta({}^\circ C)$	0.5556

Temperature conversion: $T(K) = 5/9 \times [T({}^\circ F) - 32] + 273.15$

$$T({}^\circ C) = 5/9 \times [T({}^\circ F) - 32]$$

ACKNOWLEDGMENTS

This investigation was performed at the Oak Ridge National Laboratory operated by the Union Carbide Corporation for the Department of Energy (formerly Energy Research and Development Administration). This study was a part of the general program on Low-Temperature Heat Utilization being performed by ORNL for the DOE Division of Solar Energy, Ocean Thermal Energy Conversion Branch. The author wishes to express his appreciation for the assistance of many of the ORNL staff members. The author is particularly grateful for the contributions of the following persons: Dr. H. W. Hoffman who originally suggested this study and who served as Research Committee Chairman; J. W. Michel (Program Manager), Dr. R. W. Murphy (Project Engineer), and Dr. R. N. Lyon (ORNL Consultant) for their helpful suggestions throughout the program; R. L. Linkous and C. V. Hardin (Project Technicians) for operation of the test equipment and collection of data; J. C. Parrott for the graphic arts work; Dolores Eden for her assistance in organizing the materials for the report and for typing the manuscript; and Betty Harmon and Corajane Fields for makeup of the materials for the report.

ORNL-5356
Dist. Category UC-93

INTERNAL DISTRIBUTION

1. S. E. Beall
2. R. H. Chapman
3. F. C. Chen
4-18. S. K. Combs
19. W. B. Cottrell
20. G. G. Fee
21. S. D. Freeman
22. W. Fulkerson
23. M. J. Goglia
24. R. F. Hibbs
25-26. H. W. Hoffman
27. H. W. Hsu, Consultant
28. Hans Landsberg
29. Milton Levenson
30. R. N. Lyon, Consultant
31. R. E. MacPherson
32. G. S. Mailen
33. R. E. Males
34-45. J. W. Michel
46. S. L. Milora
47. J. C. Moyers
48. R. W. Murphy
49. F. R. Mynatt
50. J. J. Perona, Consultant
51. H. Postma
52. R. C. Robertson
53. M. W. Rosenthal
54. M. R. Sheldon
55. V. Kerry Smith
56. I. Spiewak
57. Lester D. Taylor
58. D. G. Thomas
59. H. E. Trammell
60. D. B. Trauger
61. Macauley Whiting
62. G. D. Whitman
63. ORNL Patent Office
64-66. Central Research Library
67. Document Reference Section
68-69. Laboratory Records
70. Laboratory Records, RC

EXTERNAL DISTRIBUTION

71. Director, Research & Technical Support Division, DOE/ORO
72-252. Given distribution as shown in TID-4500-R66 under Energy Conversion
253. J. Hilbert Anderson, Sea Solar Power, Inc., 2422 South Queen Street, York, PA 17402
254. David Aronson, David Aronson Associates, 9 Riverview West, Upper Montclair, NJ 07043
255. Professor Kenneth J. Bell, School of Chemical Engineering, Oklahoma State University, Stillwater, OK 74074
256. Professor A. E. Bergles, Department of Mechanical Engineering, Iowa State University, Ames, IA 50010
257. Dr. R. A. Bonewitz, Aluminum Company of America, Alcoa Labs, 7th Street Road, Route 780, Alcoa Center, PA 15069
258. Robert Douglass, Jr., TRW Systems and Energy Inc., One Space Park, Redondo Beach, CA 90278
259. Dr. Gordon L. Dugger, Applied Physics Laboratory, John Hopkins University, John Hopkins Road, Silver Spring, MD 20810
260. Sigmond Gronich, Division of Solar Energy, Department of Energy, 600 E Street, NW, Washington, DC 20545
261. Dr. R. Philip Hammond, R&D Associates, 4640 Admiralty Way, P.O. Box 9695, Marina del Rey, CA 90291

262. Dr. Matthew Kelleher, Naval Postgraduate School, Department of Mechanical Engineering, Monterey, CA 93940
263. Eugene H. Kinelski, OTEC Branch, Division of Solar Energy, Department of Energy, Washington, DC 20545
264. Professor James G. Knudsen, Engineering Experimental Station, Oregon State University, Covell Hall-219, Corvallis, OR 97331
265-266. Dr. Abrahim Lavi, OTEC Branch, Division of Solar Energy, Department of Energy, Washington, DC 20545
267. Ray I. Lindberg, Reynolds Metals, 4th & Canal Streets, Richmond, VA 32361
268. Dr. A. L. London, 4020 Amaranta Avenue, Palo Alto, CA 94306
269. Dr. Paul Marto, Naval Postgraduate School, Department of Mechanical Engineering, Monterey, CA 93940
270. Professor Jon G. McGowan, Mechanical Engineering Department, University of Massachusetts, Amherst, MA 01002
271. Bernard Messinger, Lockheed Missiles & Space Company, Inc., P. O. Box 504, Sunnyvale, CA 94088
272. W. C. Moore, York Division, Borg Warner Corp., York, PA 17403
273. Frank Notaro, Union Carbide Corp., Linde Division, P.O. Box 44, Tonawanda, NY 14150
274. Robert W. Perkins, Spiral Tubing Corp., 533 John Downey Drive, New Britain, CT 06051
275. Lyle D. Perrigo, Battelle — Pacific Northwest Laboratories, P.O. Box 999, Richland, WA 99352
276. Dr. H. F. Poppendiek, Geoscience, Ltd., 410 South Cedros Avenue, Solona Beach, CA 92075
277. Dr. R. R. Rothfus, Chemical Engineering Department, Carnegie-Mellon University, Schenley Park, Pittsburgh, PA 15213
278. Norman F. Sather, Argonne National Laboratory, 9700 South Cass Avenue, Argonne, IL 60439
279. Joseph F. Sebald, Gilbert Associates, Green Hills, Reading, PA 19603
280. Professor Kenneth E. Starling, School of Chemical Engineering and Materials Science, Room 23, University of Oklahoma, 202 West Boyd, Norman, OK 73069
281. A. Steinbruchel, Aqua-Chem, Inc., P.O. Box 412, Milwaukee, WI 53201
282. William B. Suratt, DDS Engineers, Inc., 7483 Northwest 4th Street, Fort Lauderdale, FL 3317
283. Lloyd C. Trimble, Lockheed Missiles & Space Company, Inc., P.O. Box 504, Sunnyvale, CA 94088
284. C. M. Zener, Chemical Engineering Department, Carnegie-Mellon University, Schenley Park, Pittsburgh, PA 15213

☆ U.S. GOVERNMENT PRINTING OFFICE: 1977-748-189/354